

12-1-2013

## Characterization of Hypothetical Proteins SAS0760 and SAS1738 From "Community Associated Staphylococcus Aureus" MSSA476

Anupama B. Ramalinga  
*Indiana State University*

Follow this and additional works at: <https://scholars.indianastate.edu/etds>

---

### Recommended Citation

Ramalinga, Anupama B., "Characterization of Hypothetical Proteins SAS0760 and SAS1738 From "Community Associated Staphylococcus Aureus" MSSA476" (2013). *Electronic Theses and Dissertations*. 714.

<https://scholars.indianastate.edu/etds/714>

This Dissertation is brought to you for free and open access by Sycamore Scholars. It has been accepted for inclusion in Electronic Theses and Dissertations by an authorized administrator of Sycamore Scholars. For more information, please contact [dana.swinford@indstate.edu](mailto:dana.swinford@indstate.edu).

## **EDUCATION**

Ph.D in Microbiology 2008-2013

Department of Biology, Indiana State University, Indiana 47807, USA

Masters of Science in Microbiology 1999-2001

Bangalore University, Karnataka, India

Bachelor of Science in Chemistry, Microbiology and Zoology 1996-1999

Bangalore University, Karnataka, India

## **PUBLICATIONS**

Ramalinga, AB, Dannelly, HK, Characterization of the invasive nature of a hypothetical protein SAS1738 from community associated *Staphylococcus aureus* MSSA476. (Manuscript in preparation)

Kim, YK, Kaur, H, Ramalinga, A, Dannelly, HK, Kahanov, L (2012) *Staphylococcus aureus* and MRSA in and around a therapeutic whirlpool in a college athletic training room, J Athletic Training. (manuscript submitted)

Biddappa, AC, Sundarrajan, S, Ramalinga, A.B, Sriram, B, and Padmanabhan S, (2012) *Staphylococcus* bacteriophage tails with bactericidal properties: New findings. Biotechnology and Applied Biochemistry, Volume 59, Issue 6, November-December , Pages: 495–502

## **PRESENTATIONS (SELECTED)**

Characterization of the invasive nature of a hypothetical protein SAS1738 from community associated *Staphylococcus aureus* MSSA476. Talk presented in Indiana branch of ASM annual meeting of 2013.

“Hydrolase Activity of a Hypothetical Gene SAS0760 from a Hypervirulent Fucidin-Resistant Methicillin Sensitive *Staphylococcus aureus* Strain MSSA476” Anupama B. Ramalinga and H. Kathleen Dannelly, Poster (# B-145) presented at ASM 109th General Meeting, Philadelphia USA. May 2008

“Lethal *Staphylococcus aureus* phage tails: Their production and properties” Poster (# P25) at XIX Biennial ASM conference on Phage/Virus Assembly, Colorado, USA. Jun 2005

CHARACTERIZATION OF HYPOTHETICAL PROTEINS SAS0760 AND SAS1738  
FROM “COMMUNITY ASSOCIATED *STAPHYLOCOCCUS AUREUS*” MSSA476.

---

A Dissertation

Presented to

The College of Graduate and Professional Studies

Department of Biology

Indiana State University

Terre Haute, Indiana

---

In Partial Fulfillment

of the Requirements for the Degree

Doctor of Philosophy

by

Anupama Byrappa Ramalinga

Dec 2013

©Anupama B. Ramalinga 2013

Keywords: *Staphylococcus aureus*, Virulence factor, Mammalian cells, Apoptosis,

Flow cytometry

COMMITTEE MEMBERS

Committee Chair: H. Kathleen Dannelly, PhD

Associate Professor, Biology: Microbiology

Indiana State University

Committee Member: Gary W. Stuart, PhD

Professor, Biology: Molecular and Developmental Genetics

Indiana State University

Committee Member: Allan Albig, PhD

Assistant Professor, Biological Sciences: Biomolecular Sciences

Boise State University

Committee Member: Margaret M. Moga, PhD

Associate Professor, Anatomy and Cell Biology

Indiana University School of Medicine

Committee Member: James P. Hughes, PhD

Professor, Biology: Molecular Endocrinology

Indiana State University

## ABSTRACT

*Staphylococcus aureus* is known to cause a wide range of infections from simple, curable skin infections like carbuncles, furuncles, and impetigo to deadly infections such as bacteremia, osteomyelitis, endocarditis and post-operative infections. Recently, the emergence of multiple antibiotic resistances has posed a great challenge to therapeutics and infection management. Very early in therapeutics of *Staphylococcus aureus* infections, it acquired resistance to the penicillin, including methicillin [1], that was designed specifically for the penicillin resistant strains. These strains were designated methicillin resistant *Staphylococcus aureus* (MRSA). Originally, MRSA was only seen in hospital-associated infections (HA MRSA) [2-4], but recently, MRSA found in community settings (CA MRSA) are more invasive infections [5, 6] with greater genetic diversity and hence different antibiotic resistance patterns [4, 7]. MSSA476 is a CA MRSA, though evolutionarily, it is closely related to MRSA252, a HA MRSA [2, 8]. Hence we decided to identify hypothetical proteins from MSSA476. Disease management involves understanding the properties of bacteria in order to tackle the infection efficiently and finding new effective drugs to kill the pathogen. Further understanding of such unique, unexplored hypothetical proteins and their characterization with relation to virulence will help understand the increased virulence of CA MRSA.

## PREFACE

This research aims to characterize secreted hypothetical proteins, SAS0760 and SAS1738, from community associated *S.aureus* MSSA476. SAS0760 possessed a COG3863 domain related to cell wall hydrolases. Further structural analysis and protein threading was performed to show the structural similarities of SAS0760 and the NlpC/P60 protein family. Protein threading and modeling showed the conserved catalytic domain of SAS0760. NlpC/P60 family of cysteine proteases had not been explored in *S.aureus*; hence, this is a unique protein to be discovered. Another hypothetical protein, SAS1738, residing in a *Staphylococcus* pathogenicity island was shown to have lethal effects on *Caenorhabditis elegans* by a previous researcher in our lab. My research investigates the lethality of recombinant SAS1738 on various mammalian cell lines using proliferation assay, kinase activation assay and apoptosis analysis by flow cytometry. The recombinant protein rSAS1738 showed varied percentage of reduction in viability of HEK293 cells, HMEC endothelial cells and HaCat keratinocytes. Further, rSAS1738 lead to apoptosis in HEK293 cell line as revealed by Guava Viacount assay and Guava Nexin assay according to flow cytometric analysis. Hence my research investigated the novel invasin proteins of MSSA476, which could be important in the evolution of community associated *S.aureus*.

## ACKNOWLEDGMENTS

My hearty thanks to Dr. H. Kathleen Dannelly for giving me an opportunity to do PhD in her lab and for being my advisor and chairperson of my research committee. She has always been encouraging and helped me overcome my shortcomings.

I am thankful to my committee members, Dr. Gary Stuart, Dr. Allan Albig, Dr. James Hughes and Dr. Margaret Moga for giving me valuable comments and suggestions in all research meetings. I am indebted to Dr. Steve Templeton, Indiana University School of Medicine for allowing me to use flow cytometry which helped a great deal in my project.

I thank my lab mates Deepak Vijayakumar, Haninder Kaur, Yanwen Liu, Toru Matsunobu, Lauren Ford, Arthur Liang, Zach Turner, Amber Wannemacher, Nicholas Gallina who have been my good friends and peers for the past five years. Thanks to Kent Williams, Kristin, Bikram Sharma, Arun Seetharam, Jessy Robbins, Amanda Jamison, Marissa Karody, Joran Scott for the good times spent in the Biology department. Special thanks to my friends Deepak Bala and Dr. Chitra Gowda for all the moral support. I am thankful to Haninder for helping me with formatting my dissertation.

My heartfelt thanks to my parents, Ramalinga Byrappa and Vijayalakshmi Lingappa, For their blessings. And thanks to my brothers and their families, Prashanth Kumar B.R. and Maya, Manjunath B.R. and Poornima, and my niece Samita Prashanth, for their constant encouragement. I am thankful to god for this opportunity and hopes of a bright future.

## TABLE OF CONTENTS

ABSTRACT.....	iii
PREFACE.....	iv
ACKNOWLEDGMENTS .....	v
TABLE OF CONTENTS.....	vi
LIST OF TABLES .....	xi
LIST OF FIGURES .....	xiii
CHAPTER 1 .....	16
INTRODUCTION .....	16
Discovery of <i>Staphylococcus aureus</i> .....	16
<i>Staphylococcus aureus</i> infections and risk factors .....	17
Virulence factors of <i>Staphylococcus aureus</i> .....	18
Cell surface adhesion factors .....	18
Secreted virulence factors .....	20
Gene regulators of <i>S.aureus</i> virulence .....	23
Evolution of <i>Staphylococcus aureus</i> virulence.....	23
Horizontal gene transfer mechanism .....	24
Host specificity and adaptation.....	31
Evolution of antibiotic resistance in <i>Staphylococcus aureus</i> .....	31
Current treatment for <i>Staphylococcus aureus</i> infections.....	33



Clinical lab identification of <i>Staphylococcus aureus</i> .....	34
Community-associated MRSA .....	36
Role of genomics/proteomics or bioinformatics in predicting hypothetical proteins.....	38
Protein secretion system in <i>Staphylococcus aureus</i> .....	38
Predicting hypothetical proteins .....	39
The hypothetical protein - SAS0760 .....	42
The hypothetical protein - SAS1738 .....	43
Specific aims of my research .....	44
CHAPTER 2 .....	45
Partial characterization of a hypothetical protein SAS0760 from community associated <i>Staphylococcus aureus</i> , MSSA476.....	45
Abstract.....	45
Introduction.....	47
Bacterial peptidoglycan hydrolases .....	47
Structural analysis of the SAS0760 using bioinformatics tools.....	48
Methods .....	50
Signal peptide prediction of SAS0760 by Polyphobius.....	50
Secondary structure prediction .....	50
Clustal W multiple sequence alignment .....	50
Tertiary structure analysis by Phyre and Genthreader .....	50
Active site identification .....	51
Expression of SAS0760 Protein in <i>E.coli</i> .....	52

Reverse transcriptase PCR to ensure gene transcription.....	53
Results.....	54
Signal peptide prediction of SAS0760 by Polyphobius.....	54
Secondary structure prediction .....	54
Clustal W multiple sequence alignment .....	54
Tertiary structure analysis of SAS0760 .....	55
Active site identification .....	56
Expression of SAS0760 protein in <i>E.coli</i> .....	57
Reverse transcriptase PCR to ensure gene transcription.....	57
Discussion.....	76
CHAPTER 3 .....	79
Investigating the lethality of the hypothetical protein, SAS1738, from community associated <i>Staphylococcus aureus</i> MSSA476 on mammalian cell lines.....	79
Abstract.....	79
Introduction.....	81
<i>S. aureus</i> interaction with different cell types with respect to human infections.....	81
<i>S.aureus</i> colonization.....	82
<i>S. aureus</i> internalization and invasion .....	83
Host cell death by apoptosis or necrosis .....	85
Methods to analyze mammalian cell death.....	87
Cell signaling pathways in cell death.....	88
MAPK pathway .....	89

Methods .....	91
Over-expression and purification of rSAS1738 protein in <i>E. coli</i> .....	91
Dialysis .....	92
Reverse transcriptase PCR amplication of SAS1738 from MSSA476 cDNA. ....	92
WST-1 cell proliferation or cytotoxicity assay .....	93
Detection of kinase activation by immunoblotting.....	94
Cell death observation by propidium iodide staining .....	95
Phase contrast microscopy .....	96
Guava ViaCount assay by flow cytometry .....	96
Guava Nexin Annexin V binding assay by flow cytometry .....	97
Invasion assay .....	98
Nitrite production by activated macrophages was analyzed by Griess assay .....	99
Results.....	101
Protein over-expression and purification .....	101
WST-1 proliferation assay .....	102
MAPK kinase p38 and erk activation assay .....	103
Propidium Iodide (PI) staining.....	104
Phase contrast light microscopy.....	104
Guava Viacount assay using flow cytometry.....	104
Guava nexin annexin V binding assay by flow cytometry .....	106
Invasion assay .....	106
Griess assay.....	107
Reverse transcriptase PCR amplication of SAS1738 from cDNA of	

MSSA476.....	108
Discussion.....	144
Chapter 4.....	152
Conclusion .....	152
Reference .....	158

## LIST OF TABLES

Table 1: Plasmids of pathogenic <i>S.aureus</i> [72, 73, 75, 76].	29
Table 2: Antibiotic treatment currently used in hospitals for treating <i>S.aureus</i> infections.	34
Table 3: Secreted factors contributing to increased virulence of CA MRSA [49]	37
Table 4: Signal peptide prediction of SAS0760 by Polyphobius	58
Table 5: Tertiary structure analysis by Phyre and Genthreader.	59
Table 6: Phyre analysis of rearranged and trimmed SAS0760 (a+b).	66
Table 7: Phyre analysis of rearranged SAS0760 (b+a).	67
Table 8: Signal peptide prediction of SAS1738 using Polyphobius.	108
Table 9: Cytotoxicity of rSAS1738 on HEK293 cells by WST-1 assay (OD <sub>450</sub> values).	112
Table 10: Cytotoxicity of rSAS1738 on HMEC endothelial cells by WST-1 assay (OD <sub>450</sub> values).	114
Table 11: Cytotoxicity of rSAS1738 on SVEC endothelial cells by WST-1 assay (OD <sub>450</sub> ).	116
Table 12: Cytotoxicity of rSAS1738 on HaCat keratinocyte cells by WST-1 assay (OD <sub>450</sub> values).	118
Table 13: Percentage of cytotoxicity of rSAS1738 on various cell lines by WST-1 assay.	120
Table 14: Guava ViaCount assay: ViaCount viability markers and apoptotic gate markers.	126
Table 15: Percentage of cell death analysis of HEK293 cells treated with 0.2 to 0.6 $\mu$ M rSAS1738 by Guava ViaCount assay.	127
Table 16: Guava nexin assay; Marker position for gate adjustments (trial 1).	133

Table 17: Guava nexin assay; Marker position for gate adjustments(trial 2). .....	135
Table 18: Percent cell death analysis of HEK293 cells with 0.2 to 0.6 $\mu$ M of rSAS1738 by Guava Nexin assay. ....	137
Table 19: Invasion assay of <i>S.aureus</i> in HMEC endothelial cells treated with 0.2 $\mu$ M rSAS1738. ....	140
Table 20: Nitrite production by activated Raw 264.7 macrophages by Griess assay (OD <sub>550</sub> ). ...	141
Table 21: Determination of nitrite ( $\mu$ M) concentration compared to sodium nitrite standard curve by Griess assay. ....	142

## LIST OF FIGURES

Figure 1: SAS0760 sequence data. ....	58
Figure 2: COG3863 domain in SAS0760 hypothetical protein. ....	59
Figure 3: Secondary structure prediction of SAS0760 by Jpred and APSSP. ....	60
Figure 4: Secondary structure analysis of SAS0760 by Psipred.....	61
Figure 5: CLUSTAL 2.0.12 multiple sequence alignment of the SAS0760 (entire sequence) compared with its homologue proteins. ....	62
Figure 6: Threading of SAS0760 (native) with 2evra ( <i>Nosctoc punctiforme</i> ) (6a) and 2k1gA ( <i>Escherichia coli</i> K12) (6b); Top-Ribbon Model. Bottom-Space filling model .....	63
Figure 7: Threading of SAS0760 (native) with 2hbWA from <i>Anabaena variabilis</i> (space filling model). ....	64
Figure 8: Rearrangement of SAS0760 to analyze domain swapping. ....	65
Figure 9: Clustal W 2.0.12 multiple sequence alignment of SAS0760 (a+b) with homologues. ....	67
Figure 10: Clustal W 2.0.12 multiple sequence alignment of SAS0760 (b+a) with a homologue.....	68
Figure 11: SAS0760 threaded with homologue protein, 2if6B. ....	69
Figure 12: SAS0760 (b+a) (permuted form) threaded with homologue protein, 2if6B. ....	70
Figure 13: SAS0760 threaded with homologue protein, 2hbWA.....	71
Figure 14: SAS0760 (a+b) trimmed for conserved domains and threaded with 2hbWA.....	72

Figure 15: SAS0760 (b+a) threaded with 2hbwA. ....	73
Figure 16: PCR amplification of the SAS0760 gene from MSSA476 genomic DNA. ....	74
Figure 17: Reverse transcription of SAS0760 gene from MSSA476 with PCR amplication from cDNA. ....	75
Figure 18: SAS1738 sequence data. (18a) Amino acid sequence of SAS1738; (18b) Signal peptide prediction of SAS1738 by Polyphobius. ....	108
Figure 19: Sequence data of SAS1738 plus His-tag and epitope after expression from Gateway pDEST42 vector. ....	109
Figure 20: SDS analysis of His-tag column purified rSAS1738 expressed in <i>E.coli</i> . ....	110
Figure 21: Western blot of rSAS1738 purified protein. ....	111
Figure 22: Bar graph of cytotoxicity of rSAS1738 on HEK293 cells by WST-1 assay (OD <sub>450</sub> ). ....	113
Figure 23: Bar graph of cytotoxicity of rSAS1738 on HMEC endothelial cells by WST-1 assay (OD <sub>450</sub> ). ....	115
Figure 24: Bar graph of cytotoxicity of rSAS1738 on SVEC endothelial cells by WST-1 assay (OD <sub>450</sub> ). ....	117
Figure 25: Bar graph of cytotoxicity of rSAS1738 on HaCat keratinocyte cells by WST-1 assay (OD <sub>450</sub> ). ....	119
Figure 26: Bar graph of percent of reduction in viability of various cell lines treated with rSAS1738; WST-1 assay. ....	121
Figure 27: Detection of p38 and erk kinase activation by immunoblotting. ....	122
Figure 28: Effect of rSAS1738 on HEK293 cell line by fluorescent microscopy (PI staining). ....	123



Figure 29: Effect of rSAS1738 on HEK293 cells by phase contrast microscopy (unstained). ...	124
Figure 30: Effect of rSAS1738 on HaCat keratinocyte cells by phase contrast microscopy. ....	125
Figure 31: Guava ViaCount assay: positive control (HEK293 cells). .....	128
Figure 32: Guava ViaCount assay: Negative control (HEK293 plus stuarosporine 1µM/2hr). ...	129
Figure 33: Guava ViaCount assay. HEK293 treated with 0.6 µM rSAS1738.....	130
Figure 34: Bar graph of percent cell death analysis by ViaCount assay; HEK293 cells treated with rSAS1738.....	131
Figure 35: Bar graph of percentage apoptotic cells determined by ViaCount assay; HEK293 cells treated with rSAS1738.....	132
Figure 36: Guava Nexin assay (trial 1). .....	134
Figure 37: Guava Nexin assay (trial 2). .....	136
Figure 38: Percent live, dead and apoptotic cells determined by Nexin assay; HEK293 cells treated with 0.2 to 0.6 µM of rSAS1738.....	138
Figure 39: Percent apoptotic cells determined by Nexin assay; HEK293 cells treated with 0.2 to 0.6 µM of SAS1738.....	139
Figure 40: Reverse transcriptase PCR amplification of SAS1738 from cDNA made from MSSA476.....	143

## CHAPTER 1

## INTRODUCTION

**Discovery of *Staphylococcus aureus***

Alexander Ogston, (1844-1929) a Scottish surgeon, was an early supporter of antiseptic techniques that were proposed by Joseph Lister (1827-1912). Alexander Ogston was curious to deeply examine the cause of wound putrefaction by air since Lister proposed that air was the reason for pus formation. Ogston tried to hinder the air exposure to the wound by dressing it with the phenolic dressings and was successful in preventing the putrefaction or suppuration of wounds. But Ogston wanted to find more about the cause of such suppuration in wounds and wondered if there was a new causative germ. Ogston stained the pus sample from a patient wound to find cocci under a microscope. He exclaimed, “My delight may be conceived when there were revealed to me beautiful tangles, tufts and chains of round organisms in great numbers, which stood out clear and distinct among the pus cells and debris...”[9].

Alexander Ogston also injected the pus from the wound into healthy pigs and mice and demonstrated new abscess formation. The heat-killed or phenol-treated pus did not form abscesses. In 1882, these micrococci in grape-like clusters were named as *Staphylococcus* derived from the Greek word staphyle meaning bunch of grapes. Thus, the discovery of the *Staphylococcus* was the contribution of surgeon Alexander Ogston.

Later in 1884, a German scientist named Anton J. Rosenbach named two strains of *Staphylococcus* based on colony pigmentation. The yellow colonies were named as *Staphylococcus aureus* from the Latin word aurum and the white colonies as *Staphylococcus albus*, presently called *Staphylococcus epidermidis* [10].

### ***Staphylococcus aureus* infections and risk factors**

*Staphylococcus aureus* is a ubiquitous organism reported in cattle, pigs, raw meat products, and raw milk due to poor hygiene or handling, but the major reservoir is human beings. *Staphylococcus aureus* colonizes skin or the nasal cavity persistently in 25%-30% of healthy human beings and intermittently in the remaining population [11]. It may also exist as transient flora in areas such as the oropharynx, axilla, vagina, or perineum, leading to opportunistic infections [12]. Recent research data from several groups suggest the nasal carriers are at high risk of skin and soft tissue infections, postoperative complications, bacteremia, and other invasive infections [12-14].

Patients with chronic illness such as cancer, diabetes, and vascular diseases, as well as infants, the elderly and immune-compromised patients have high risk factors for *S. aureus* infections. Other risk factors associated with transmission of infections are those who have close contact with infected individuals, those with skin injuries or disorders, and patients with surgical incisions. Patients with intravenous catheters also show high susceptibility to *S.aureus* infections [14-17]. Hence, *S. aureus* infection is a common cause of nosocomial infections, such as surgical infections and bacteremias [12, 18-21]. Hospital-acquired infections and community-acquired infections such as, skin and soft tissue infections, infective endocarditis, and respiratory infections have increased tremendously due to multidrug resistance in *S.aureus* [22-24].

Most *S.aureus* infections are endogenous, caused by the patient's own normal flora, but the transmission of the bacteria may also occur through person-to-person contact with a pus-filled wound or by the exchange of inanimate objects which serve as transmission agents. *S.aureus* may enter the breached skin or healthy skin by producing hyaluronidase, which damages the extracellular matrix protein and aids the spread of the bacterium in the body [25]. *Staphylococcus aureus* causes a wide range of infections from milder skin infections such as pus-filled boils, furuncles, and abscesses to life-threatening invasive infections like cellulitis, scalded skin syndrome, bacteremia, pneumonia, endocarditis, meningitis, osteomyelitis, toxic shock syndrome, and gastroenteritis [26].

### **Virulence factors of *Staphylococcus aureus***

Bacterial infection involves several stages and begins with colonization of the host by attachment. Attachment is followed by host cell invasion, tissue damage, immune evasion, and dissemination of the bacteria. *Staphylococcus* pathogenicity factors are mainly grouped as cell adhesion factors, invasive secreted proteins, and virulence factors for immune evasion.

#### **Cell surface adhesion factors**

The colonization process is mediated by surface adhesins that aid the bacterium in attachment to the host cells, extracellular matrix (ECM), or plasma proteins. *Staphylococcus* adhesins can be broadly categorized as proteinaceous or non-proteinaceous adhesins. "Microbial surface-components recognizing adhesive matrix molecules" (MSCRAMMs) and "secretable expanded repertoire adhesive molecules" (SERAM) are the two types of proteinaceous adhesins [27]. Non-proteinaceous adhesins include cell wall teichoic acids, lipoteichoic acids, capsular polysaccharide, and polysaccharide intercellular adhesin (PIA) [28-30].

MSCRAMMs are the proteins that attach covalently to the Extra Cellular Matrix (ECM) or to plasma proteins like fibrinogen components. *Staphylococcus aureus* MSCRAMMs includes clumping factors (ClfA and ClfB), fibronectin binding proteins (FnbpA and FnbpB), collagen binding protein (Cna), sialoprotein binding protein (Bbp), and serine aspartate repeat proteins (SdrC, SdrD, SdrE) which bind to fibrinogen [31-33].

Clumping factors, clfA and clfB, specifically bind to fibrinogen but not elastase [31]. FnBPA and FnBPB of *S.aureus* bind to fibrinogen, fibronectin and elastin in host cells. Apart from adhesion, FnBPs also function as invasins and for internalization in epithelial cells, endothelial cells, and fibroblasts. FnBPs are known to bind to the host-cell integrin receptor alpha5beta1, which interacts with fibrinogen. They activate platelet activating factor and promote thrombosis in infective endocarditis [34]. Collagen-binding protein can bind to any collagen substrate (soluble collagen in the ECM) therefore aids bacterial attachment to cartilage, bone and even cornea. Bone sialo-protein binding protein (Bsbp) belongs to the sdr family of MSCRAMMs that bind sialic acid in bone. Bsbp and collagen-binding protein are known to be highly expressed by *S.aureus* from bone and joint infections [30, 32].

SERAMs are non-covalently bound proteins. Examples of SERAMs are autolysins, extracellular adherence protein (Eap), extracellular fibrinogen protein (Efp), and coagulase.

Extracellular adherence protein (Eap) binds to *S.aureus*' cell wall and also to host fibrinogen, fibronectin, or prothrombin, thus serving as an immunomodulatory protein by reducing inflammation. Eap is also known to increase *S.aureus* adherence to fibroblasts, endothelial and epithelial cells [35].

Coagulase (Coa) is a fibrinogen-binding protein. It facilitates fibrin clot formation by activating zymogen which cleaves fibrinogen to fibrin. Eap, Efp and Coa proteins are associated with endovascular diseases and abscess formation [27, 36].

Non-proteinaceous adhesins, mainly cell-wall teichoic acids, lipoteichoic acids, and polysaccharide intercellular adhesin (PIA) are charged and can bind to plastic, polystyrene, or glass surfaces aiding attachment of bacteria to non-living surfaces such as indwelling medical devices. PIA can mediate cell-cell attachment and has an important role in *S.aureus* biofilm formation on medical devices [37]. Capsular polysaccharide is another non-proteinaceous adhesin and immune-evasion surface-virulent determinant. There are eleven known serotypes of capsular polysaccharide but capsular types V and VIII are prominent in clinical isolates and are therefore considered as important antigens for vaccine development [28, 38].

### **Secreted virulence factors**

The secreted virulence factors of *S. aureus* are SERAMs, enzymes, and toxins that play roles in colonization and utilization of host nutrients causing infection and inflammation. *S. aureus* secretes a myriad of enzymes and toxins such as: lipases, hyaluronidase, proteases, collagenase, nucleases, hemolysins, leucocidins, exfoliative toxins (ETA and ETB), and the pyrogenic superantigens including enterotoxins (SEA, SEB, SEC, SED, SEE, SEG, SEH, and SEI), and the toxic-shock-syndrome toxin (TSST-1) [25, 39].

*Enzymes:* Lipases can cleave fatty acids and aid the bacteria survival on the skin-surface. Hyaluronidase and collagenase degrade hyaluronic acids and collagen, respectively, in extracellular matrix and help the bacteria to disseminate. Nucleases can digest host nucleic acids of neutrophil extracellular traps (NET) and protect bacteria from antimicrobial activity of

neutrophils. Researchers have also shown the role of a temperature-stable nuclease, called thermonuclease (Nuc) in CA MRSA biofilms [25, 40, 41].

*Toxins:* Leucocidins and hemolysins are cytolysins with the ability to lyse different types of host cells such as platelets, leucocytes, and various blood cells. They also play roles in host tissue damage and inflammation and can alter the immune response. Four types of hemolysins are known: alpha, beta, delta hemolysins encoded by Hla, Hlb, Hld, respectively, and the gamma hemolysins encoded by hlgA, hlgB, hlgC. Alpha hemolysins are pore-forming toxins known to lyse blood cells and platelets. Beta hemolysins, also called sphingomyelinase C, cause damage the erythrocytes by hydrolysis of the cell membrane. Delta hemolysins disrupt the cell membrane by surfactant-like activity. Gamma hemolysins and leucocidins are two-component toxins with subunits for binding the cell and pore formation. Pantone valentine leucocidin (PVL) is more prevalent in CA MRSA strains [25].

Pyrogenic toxin superantigens (PTSAgs), toxic shock syndrome toxin (TSST-1), exfoliative toxins, and enterotoxins bind to the MHC II and T cells leading to excessive T cell activation and amplified cytokine release ultimately resulting in inflammation, shock, and multiple organ failure. Toxic shock syndrome can be caused both by TSST-1 and some types of enterotoxins. Menstruation-associated toxic shock syndrome associated with tampon usage is caused by TSST-1, whereas non-menstrual TSS is caused by enterotoxins namely SEB and SEC. Enterotoxins are thermo-resistant toxins known to cause food poisoning from meat or milk products. There are ~20 different types of enterotoxins known currently that have different roles in causing gastrointestinal inflammation, emetic activity, and ultimately, dehydration. Overall, PTSAgs are known to exert cytotoxic effects on endothelial cells, increase endotoxin sensitivity of endothelial cells, and increase cytokine and TNF- $\alpha$  release from leucocytes [25, 42].

*S.aureus* extracellular proteases cleave their own cell wall proteins and hence can be referred to as autolysins. They are known to have roles in dispersal of biofilms and host tissue damage. These proteases exist as inactive zymogens unless activated by proteolytic cleavage. Currently known proteases include staphopain A and B (sspB and sspC) that belong to the cysteine protease family, aureolysin (Aur) that belongs to the metallo-protease family, and the V8 protease (sspA) that is a serine protease. Staphopain is activated autolytically or by proteolytic cleavage aided by V8 protease. Staphopain can cleave host fibrinogen, elastin, kininogen and fibronectin. Some studies show that one role of staphopain in immune evasion is suppression of neutrophil activation [43]. Exfoliative toxins, which also belong to the serine protease family, hydrolyze desmosomal skin proteins and can cause scalded skin syndrome, dehydration and secondary infections [39, 44].

V8 protease, a glutamyl endopeptidase serine protease, is activated proteolytically by aureolysin. It has a role in bacterial growth and survival, degrades fibronectin-binding protein, and cleaves clumping factor. These actions detach the bacterial mass and help in dissemination. Aureolysin, a thermolysin, is known to play a role in immune evasion by cleaving LL-37 antimicrobial peptide and hindering complement activation. Aureolysin activates V8 protease (sspA) and activated sspA further activates sspB, but the mechanism of activation of aureolysin is not clear. Thus, a cascade of protease activations contribute to bacterial growth, survival, immune evasion and dissemination in systems such as biofilms [43, 45, 46].

Phenol soluble modulins (PSMs, also known as  $\delta$ -toxin, PSM $\gamma$ ) are cytotoxic to white and red blood cells. They also have a role in pro-inflammatory activity leading to priming of neutrophils and cytokine induction. PSMs are amphipathic in nature and their surfactant-like property has role in biofilm organization of channel-like structures. PSMs may play a role in



colonization where they function as virulence factors [47]. PSMs are also secreted by *S.epidermidis* where they are utilized for antimicrobial activity against other bacteria including *Streptococcus* sp. [48]. PVL,  $\alpha$ -toxin, and  $\gamma$ -toxin are heptameric pore-forming toxins that lyse human cells such as epithelial cells and polymorphonuclear leukocytes (PMNs). Phenol soluble modulins are small molecular weight cytolysins found in CA MRSA and known to ameliorate cytolysin activity and hence contribute to invasive virulence of CA MRSA. CA MRSA produces a novel superantigen called SE-I Q, in addition to TSST-1, in some strains [49].

### **Gene regulators of *S.aureus* virulence**

There are primarily two types of gene regulator in *S.aureus*: a) Two component systems such as: agr, saeRS, srrAB, arlSR and lytRS systems, and b) DNA-binding proteins: SarA homologues (SarR, Rot, SarS, SarT, SarU). Two-component regulatory systems consist of a sensor kinase and response regulators. Accessory gene regulator (agr) and staphylococcal accessory regulator (sar) are the two major regulators of virulence in *S.aureus*. Virulence determinants are expressed in a growth phase dependent manner. Initially, the growth phase cell wall associated proteins are synthesized and in post-exponential phase only, extracellular secretory proteins like hemolysins, lipases and proteases are expressed. Such growth phase dependent protein expression and further virulence expression are under the control of the agr regulator, whereas sar regulator controls virulence determinants by controlling the agr regulator [50-52].

### **Evolution of *Staphylococcus aureus* virulence**

Bacterial pathogenicity can be defined as the ability to cause diseases in the host. The infection process starts from bacterial attachment followed by invasion of cells and tissues causing the damage to the host. Bacteria must also tackle the host immune response efficiently in

order to succeed as a pathogen. Most bacteria share common virulence mechanisms and spread of virulence can be mainly attributed to acquiring new virulence determinants from a common bacterial ancestor. A new pathogenic bacterial strain evolves by gene mutation and gene rearrangement or recombination primarily by horizontal gene transfer (HGT), also termed Lateral Gene Transfer (LGT), mechanisms [53, 54].

### **Horizontal gene transfer mechanism**

HGT refers to transfer of genetic elements from any donor bacteria to recipient bacteria by any of the gene transfer mechanisms: transformation, conjugation, and transduction. Such genetic elements that form the genomic islands are also called pathogenicity islands since they carry virulence determinants such as toxins, enzymes, adhesins, antibiotic resistant cassettes, and other such factors. Pathogenicity islands (PAI), typically 10-200 kb in size, are predicted to be acquired by HGT since they vary in their G+C content compared to the genome of the host bacteria. PAIs are unique to pathogenic bacterial strains compared to non-pathogenic bacteria in the same species but some virulence factors, such as adhesins, can also exist in non-pathogenic bacteria. PAIs are flanked by inverted repeats and carry mobility loci and integrase determinants, all of which aid in mobility or deletion from the genome; they are, therefore, considered genetically unstable. PAIs can be transferred by conjugative transposons, plasmids or bacteriophages and play major role in the evolution of virulence and multi-drug resistance in bacteria. Understanding bacterial evolutionary mechanisms and the acquisition of new virulence factors are very important for infection management and therapeutics [55, 56].

Comparative analysis of whole genome sequences of pathogenic and non-pathogenic species aids the understanding of acquired virulence determinants and sheds light on the genetics and evolution of virulence. The *Staphylococcus* genome is highly conserved compared to those

of many other pathogenic species such as *Listeria* and *Bacillus* indicating that large-scale recombination plays a lesser role in speciation [57]. About 78% of the genome is conserved between any two *Staphylococcus aureus* species, whereas 50% of the genome is conserved across genera [58, 59]. Based on its conserved nature, the entire genome can be categorized as: core genome, core variable region (CV), and accessory genome. The core genome is 75% conserved and consists of genes essential for cell growth, maintenance, and survival. The CV region is 10% conserved in species with evolutionary relatedness. The genes are related to the factors of species-specific infection processes such as adhesion proteins and virulence regulatory factors [60]. *S. aureus* adhesion proteins, such as the MSCRAMMs, are involved in colonization. MSCRAMMs show low sequence homology between species. Ligand-binding specificity has evolved as an adaptation to environmental habitat. For example, the MSCRAMM, ClfB, is differentially expressed in response to the nasal environment by *S. aureus* but not by other species [29, 61, 62].

The downstream region of the Ori C environ, 300-540 kb, is considered as the main determinant of staphylococcal speciation. It encodes a major portion of the virulence proteins involved in niche-bacterium interactions. Protein A is one example. Several gene rearrangements occur in the OriC environ. Chromosomal inversion is the major type of rearrangement observed in *S. hemolyticus*, *S. epidermidis* and *S. saprophyticus* [59]. Correlating genetic changes in the variable genomic regions with the phenotypic characteristics of habitat and the environmental niche of bacteria would shed light on pathogenic evolution as a result of niche adaptation.

#### Mobile genetic elements

The accessory genome consists of many types of mobile genetic elements (MGEs). MGEs include the staphylococcal cassette chromosome element (SCC element), prophages,

Staphylococcal pathogenicity island (SaPI), plasmids, transposons, and insertion sequences. The accessory genome undergoes high-frequency genetic exchange and is largely responsible for the rapid rate of adaptation and evolution of pathogenicity [60]. Differences in pathogenicity and virulence in different strains can be attributed to the variation in genes encoding virulence proteins involved in host-pathogen interaction existing in the accessory genome.

Bacteriophages are bacterial viruses with two life cycles: the lytic phage and the temperate phages (prophage). The temperate phage can lysogenize the host and exist in the genome for long periods of time until induced by external stresses or mutagens. Exposure to antibiotics used to treat *Staphylococcus* infections is one such stress factor, inducing prophages and HGT [63]. Bacteriophage integration and mobilization have been reported in several cases of *Staphylococcus* colonization and infection [64-67]. Many virulence determinants are conferred by bacteriophages. In CA MSSA476, prophages encode the following virulence determinants: *Staphylococcus* complement inhibitor (*scn*), staphylokinase (*sak*), enterotoxin G (*seg*), enterotoxin A (*sea*), and enterotoxin K (*sek*). Prophages in MRSA252 encode the genes for chemotaxis inhibitory factor (*chp*), *scn*, *sek*, and *sea* [67].

Prophage transduction leads to a high probability of HGT and can aid in the spread of virulence determinants because the prophages in *S. aureus* exist in mobile genetic elements rather than in the chromosome [56]. Phage particles are known to be functional even after being induced from clinical isolates [65, 68].

Available genome sequence data of seventy-eight strains of *S. aureus* in the Genbank database categorizes the strains into twenty different clonal complexes (CCs) or lineages and twenty-eight sequence types (ST). Whole genome sequencing and annotation are available for twenty-eight *S. aureus* strains [69]. Eight bacteriophage families have been identified based on

the integrase (int) genes in seventy-four of the sequenced *Staphylococcus* genomes. They are named as follows:  $\phi 1$ ,  $\phi 2$ ,  $\phi 3$ ,  $\phi 4$ ,  $\phi 5$ ,  $\phi 6$ ,  $\phi 7$  or  $\phi 8$ . The major prophage of human *S. aureus* isolates is  $\phi 3$  [70]. The prophage  $\phi 2$  carries PVL and is found in CA MRSA populations [71]. The putative secreted proteins of  $\phi 1$ ,  $\phi 4$ ,  $\phi 5$ ,  $\phi 6$ ,  $\phi 7$ , and  $\phi 8$  prophage have not been characterized, so it is unclear at this time whether these prophages carry significant virulence factors.

SaPI, a 15-20 kb genetic element that is conserved across many toxigenic strains, is known to encode superantigens (SAGs) and toxins such as TSST-1 and enterotoxins. SaPI1 codes for TSST1 and superantigens SEK and SEL, SaPI3 encodes the enterotoxin-B, and SaPI4 encodes enterotoxin-C. SaPIs can exist in the host genome unless mobilized by induction or by a helper temperate bacteriophage which excises and packages it into capsid particles. Hence, they are also called phage inducible chromosomal islands. These phage particles carry SaPI genetic elements and spread at a high frequency of  $10^8$ /ml phage particles to other bacteria by phage infection [72-74].

#### Role of plasmids in evolution

Plasmids are extrachromosomal, self-replicating genetic material in bacteria, and they are laterally transferred either by conjugation or phage transduction [75, 76]. *Staphylococcus* plasmids are known to have genes for virulence determinants, antibiotic resistance, and heavy-metal resistance. *S.aureus* plasmid pETB carries the exfoliative toxin B (ETB), cadmium resistance operon, and lantibiotic producing gene [76, 77]. *S. aureus* plasmids of <5 kb that replicate by the rolling circle (RC) method carry only a single antibiotic-resistance determinant whereas larger plasmids of 15-40 kb carry multiple resistance determinants and replicate by the theta model. The latter plasmids usually harbor insertion sequences (IS) or transposons (Tn) [78,

79]. For example, pSK41 plasmid carries the *aacA-aphD* gene on Tn4001-IS257, which confers multidrug resistance to tobramycin, gentamycin, aminoglycosides and kanamycin. pSK41 also has integrated plasmids pUB110 on IS257 conferring neomycin resistance [80].

Table 1: Plasmids of pathogenic *S.aureus* [72, 73, 75, 76].

Strain	Plasmid (Size)	Gene
MSSA476	pSAS1	blaZ and cadD blaZ encodes penicillinase cadD encodes cadmium resistance
MW2	pMW2 (20.6kbp)	blaZ and cadD
N315	pN315 (24.6kbp)	cadDX - cadmium resistance determinant arsRBC - arsenate-resistant determinant aTn552- harbors blaZ
Mu50	pUB110	Bleomycin and kanamycin-resistant genes
	pMu50 (25.1kbp) and pUB110	Tn 4001 carries aacaphD (aminoglycoside resistance). qacA genes- resistance to quaternary ammonium compounds Bleomycin and kanamycin-resistant genes
MRSA252	Integrated plasmid	Heavy metal resistance - arsenic ( arsBC) and cadmium ( cad AC)
	pUB110	Bleomycin and kanamycin-resistant genes
COL	(pT181)	Tetracycline resistance

### Transposon (Tn)

Smaller transposons (<2kb) exist in multiple copies in bacterial genomes and integrate at specific sites into plasmids, MGE, or the chromosome. Larger transposons (~18kb) usually exist as a single copy and confer resistance to tetracycline (Tn6009), vancomycin, trimethoprim (Tn4003), or aminoglycosides (Tn4001). The site-specific transposon, Tn554, confers resistance to macrolide-lincosamide-streptogramin B and spectinomycin antibiotics in the N315, Mu50, and MRSA252 genomes. A conjugative transposon, Tn5801, found in strain Mu50 carries tetracycline and minocycline resistance [81-83].

### Insertion sequence (IS)

ISs generally do not encode any virulence determinants but are involved in mobilization by integrating into transposons, plasmids, or bacteriophages. ISs have terminal inverted repeats and a transposase that aids in integration and mobilization [84]. *S. aureus* IS256 in transposon Tn4001 confers resistance to aminoglycosides and IS257 in transposon Tn4003 confers resistance to trimethoprim [83].

### SCC element

Staphylococcal cassette chromosome (SCC), is one of the genetic elements in the accessory genome that confers resistance to many antibiotics and has diversified into eight types characterized by different types of recombinase, *mecA* gene complex, and *ccr* genes [85]. Community associated methicillin resistant *S.aureus* (CA MRSA) is known to harbor the smaller SCC*mec* IV, V, or VII elements. The larger elements, SCC*mec* I, II, III, VI, or VIII, prevail in hospital associated methicillin resistant *S.aureus* (HA MRSA) strains along with other antibiotic-resistance determinants.

SCC usually harbors the *mec* determinant but sometimes variants can be present in *mec* cassette. One such variant is the *mec*-like element (SCC<sub>476</sub>) seen in methicillin-sensitive *S.aureus*, MSSA476, which confers fusidic acid resistance. Clonal expansion of HA MRSA CC22 SCC*mec*IV clones with increased antibiotic resistance has been reported to be the result of gene shuffling. Such variations in MGE contribute to rapid clonal adaptation to the antibiotic pressure and to the stability of the clone [67]. The role of the SCC element is not limited to antibiotic resistance; researchers have shown that capsular polysaccharide genes that help in immune evasion by phagocytosis are present in SCC element [86-88].

The arginine catabolic mobile element (ACME) *arcA* genes also exist as MGEs. These genes are known to be acquired by HGT from *S. epidermidis* and other coagulase-negative *Staphylococcus*, such as *S.capitis* and *S.hemolyticus*. The genes are later propagated by vertical gene transfer to the progenies. The *arc* gene cluster allows the bacteria to survive in low pH by metabolizing L-arginine to carbon dioxide, ammonia, and ATP. These actions increase the pH to a basic environment. *Arc* genes allow the bacteria to survive on skin at low pH and also evade the immune response [89, 90].



Horizontal gene transfer (HGT) is not only limited to MGEs but is observed in chromosomal genes also. HGT plays an important role in the creation of a new clonal complex in *S.aureus*. Multiple-copy gene sets show a higher frequency of HGT compared to single copy gene sets. Gene duplication, lineage sorting, or gene conversion give rise to new clones and thus play a role in evolutionary clonal expansions and diversity [91].

Some genetic events such as single nucleotide polymorphisms, insertion/ deletion mutations, and protein-truncating mutations are found in some of the new virulent strains. Comparative genomics among *S. aureus* nasal colonized strains and *S.aureus* bacteremia invasive strains revealed such small genetic variations. Some loss-of-function mutations in transcriptional regulators can bring major functional differences in the bacterial strain. This indicates that increased virulence is multifactorial and not just conferred by emergence of antimicrobial resistance [92].

### **Host specificity and adaptation**

Historically *S.aureus* has primarily colonized human beings, but recently has adapted efficiently to colonize and infect other hosts such as cow, pig, horse, goat, sheep, and dog. Highly specific genetic adaptation for certain animals has been observed and, in fact, some lineages have adapted to infect only animals. Other human strains are known to cause bovine mastitis and infect horses. Bovine *S.aureus* strains of distinct clonality are mainly due to genetic divergence although studies have shown that bovine *S.aureus* clones arose from human *S.aureus* clones [70, 93].

### **Evolution of antibiotic resistance in *Staphylococcus aureus***

Penicillin has been the “Cinderella of drugs” for microbial therapeutics since its discovery in 1928. Bacteria have developed resistance by inactivating the antibiotic or by

blocking its site of action. Trans-peptidases and carboxy-peptidases are the cell-wall peptidoglycan-synthesizing enzymes susceptible to penicillin. Penicillin acts as an analogue of the cell-wall d-alanine-d-alanine peptide and binds strongly to cell-wall synthesizing enzymes, hindering cell wall synthesis. Penicillin-resistant *Staphylococcus* evolved to produce a  $\beta$ -lactamase that is induced in the presence of penicillin.  $\beta$ -lactamase is encoded by a single gene found on plasmids, which spreads by HGT through phage transduction [22, 63].

Semi-synthetic penicillin-based  $\beta$ -lactamase stable antibiotics named cloxacillin and methicillin were produced in 1959. Within 2 years, *S. aureus* evolved methicillin resistance by acquiring the modified penicillin-binding protein PBP2a encoded by the *mecA* gene from *Staphylococcus scuri*. Further, *mecA* was incorporated into the staphylococcal chromosome cassette (SCC) and was capable of blocking antibiotic action [94, 95]. By the late 1990s, multidrug resistant strains developed in hospital and community settings. MRSA associated with hospital staff and hospitalized individuals is called hospital associated MRSA, whereas community-associated *S. aureus* strains are found on individuals in community with no prior history of hospitalization in the prior six months.

Later, vancomycin was used for treating MRSA but strains developed resistance to vancomycin by the year 2000. These strains were called VRSA strains. Vancomycin resistance was achieved by a change in bacterial cell-wall d-alanine-d-alanine moiety to d-alanine-d-lactate. Vancomycin resistance is transposon (Tn1546) mediated and confers multidrug resistance to aminoglycosides, trimethoprim/sulfamethoxazole, clindamycin, rifampicin, and fluoroquinolones. Because of its high rate of evolution, *S.aureus* also poses a challenge to the currently available treatments involving daptomycin and linezolid [96, 97].

### **Current treatment for *Staphylococcus aureus* infections**

*Staphylococcus aureus* infections are generally treated with cephalosporin, nafcillin or related antibiotics. Currently, *Staphylococcus aureus* is rarely (~10%) susceptible to penicillin. Vancomycin (an intravenous drug) is used to treat serious infections since the traditional regimen may not work on antibiotic resistant strains such as HA MRSA [22, 64].

In most cases, methicillin-sensitive *Staphylococcus aureus* strains are resistant to penicillin since they produce beta-lactamase. They are often treated using one of the penicillins plus a beta-lactamase inhibitor such as ampicillin/sulbactam, amoxicillin/clavulanate, or with one of the modified forms of penicillin, such as oxacillin or nafcillin (Table 2). MRSA is resistant to methicillin, oxacillin, and the cephalosporins. MRSA carries the *mecA* gene, which encodes PBP-2a, and penicillin binding protein 2a [98].

CA MRSA strains like USA300, USA500, or USA1000 isolates are often susceptible to the tetracyclines such as, minocycline, doxycycline, and tigecycline. In some cases, strains are erythromycin resistant and they are subjected to a clindamycin susceptibility test called the D-test. Vancomycin-resistant MRSA infections are often treated with daptomycin [23, 71, 99].

Table 2: Antibiotic treatment currently used in hospitals for treating *S.aureus* infections.

Johns\_Hopkins\_ABX\_Guide; MayoClinic [100-102]

<b>Infection</b>	<b>MSSA treatment</b>	<b>MRSA treatment</b>
Bacteriemia	Oxacillin/nafcillin- 2gms- IV (4hrs)	Vancomycin/Daptomycin- FDA approved Linezolid, Quinupristin/dalfopristin/ ceftaroline, telavancin – Not approved by FDA
Endocarditis	Cefazolin for hemodialysis patients. Gentamycin and Oxacillin/nafcillin, 2gms-IV Ciprofloxacin + rifampicin oral regime Vancomycin in case of penicillin allergy	Vancomycin or daptomycin
Soft tissue infections	Vancomycin/daptomycin IV Oral	Clindamycin/ doxycycline/ minocycline/linezolid For CARMSA Trimethoprim+Sulfamethoxazole (TMP+ SMX) and tetracycline's
Recurrent soft tissue infection	Mupirocin 2% ointment +/- chlorhexidine washes	Any one of the above oral drugs along with rifampin
Pneumonia	Select from susceptibilities list	Vancomycin/linezolid/clindamycin IV, Daptomycin cannot be used
Meningitis/ Brain abscess	Oxacillin/nafcillin IV	Vancomycin, Linezolid /TMP+ SMX
Toxic shock syndrome	Oxacillin/nafcillin + clindamycin IV	Vancomycin+clindamycin/ Linezolid IV

### **Clinical lab identification of *Staphylococcus aureus***

*S.aureus* is a non-spore forming, non-motile, facultatively anaerobic, and gram-positive coccus that occurs in clusters. *S.aureus* is characterized by yellow pigmentation, mannitol fermentation,  $\beta$ -hemolysis of sheep red blood cells, and is deoxyribonuclease and coagulase positive. The bacterium also can be identified by several advanced techniques involving enterotoxins, phage typing, and serotyping. Routine identification of *S.aureus* in a clinical lab is performed by Gram staining, plating on mannitol salt agar, a catalase positive reaction, the lysostaphin sensitivity test, protein A positive reaction, and tests for clumping factor (clumping of tube coagulase or StaphaueX-latex agglutination test) [103]. Recently, strains with varied

reactions for the standard identification tests have been isolated such as coagulase-negative *Staphylococcus* sp., catalase negative *S.aureus*, or mannitol-negative *S.aureus* [104-106]. Hence, additional tests like the DNase test and rapid genotypic tests (e.g., 16SrRNA detection) [107, 108] should also be considered for confirming *S. aureus* infections in critical care.

Once the antibiotic susceptibility profile indicates methicillin resistance, MRSA analysis begins by DNA extraction and PCR analysis of the 16S rRNA, *mecA* gene, and PVL genes. SCC*mec* typing is performed by multiplex PCR using primers for 11 different SCC types, including subtypes based on different *mec* complexes. Pulsed-field gel electrophoresis, multi-locus sequence typing, *spa* typing, and SCC*mec* typing have been used to characterize MRSA and MSSA strains

Pulsed-field gel electrophoresis (PFGE) was introduced to replace bacteriophage typing of *S.aureus* strains. PFGE techniques involve digesting bacterial DNA with restriction endonucleases and electrophoresis using different electric voltages and different time intervals. The restriction pattern of DNA fragments separated in the range of 10 kb to 800 kb is compared with those of well-characterized outbreak strains. The strains are interpreted as unrelated if there are more than six differences in the gel pattern comparison. Small differences in the gel pattern are considered different genetic events in the newer pathogenic strains. However, there are reproducibility problems with PFGE since different labs have variable results of gel pattern analysis [109].

Multi-locus sequence typing (MLST) was introduced by Enright et al., [1, 110] to analyze MRSA and MSSA strains. Internal variable fragments of seven housekeeping genes of *S.aureus* are amplified, purified, and sequenced in MLST. The housekeeping genes analyzed in MLST are: *aroE* encoding shikimate dehydrogenase; *glpF* encoding glycerol kinase; *arc* encoding

carbamate kinase; *gmk* encoding guanylate kinase; *pts* encoding phosphate acetyltransferase; *tpi* encoding triose phosphate isomerase; and *yquiL* encoding acetyl coenzyme A acetyl transferase. Each housekeeping gene represents an allele and the combination of alleles can be grouped as allelic profiles or sequence types (ST). Further, the typing groups are assigned to the bacterial strain based on allele quantification and sequence groups. The availability of sequencing facilities is the primary limitation of this technique. Analysis of MRSA and MSSA strains by MLST and *SCCmec* typing reveals five prominent clonal complexes (CC) of MRSA: CC8, CC5, CC30, CC45, and CC20. These studies also indicate that MRSA arose from a common MSSA ancestor [1, 110].

*spa* typing is performed by analyzing the variable repeat regions of the protein A gene. *spa* typing can detect any micro-variation in *S.aureus* strains and it works better than other typing methods like MLST, coagulase typing, or PFGE [111].

*SCC* typing: *Staphylococcus* chromosomal cassette (SCC) typing is performed by analyzing the *ccr* gene complex and the *mec* cassette. Further subtypes are determined by analyzing the junkyard regions (J region) of the DNA. Three *ccr* gene complexes (*ccrA*, *ccrB*, *ccrC*) have been classified based on <50% sequence similarity. Eight types of *ccr* cassette combinations have been observed consisting of the *mecA* gene with regulatory genes and accompanied by insertion sequences. Six classes of *mecA* gene complex variations exist and are grouped as A, B, C1, C2, D and E [85, 88].

### **Community-associated MRSA**

CA MRSA is known to be more invasive than HA MRSA due to genomic and phenotypic variations. Recent comparisons of MRSA and MSSA do not show differences in the levels of any virulence factors or host immune response, thus, these comparisons do not explain

why infection with MRSA is associated with higher mortality than infection with MSSA [3, 112, 113]. Mechanisms of increased invasiveness of CA MRSA are also still not clear. Hence, our research group aims to characterize hypothetical exported proteins of community strains. Understanding new virulence factors may help to manage community-associated infections and pave the way to new therapeutics.

Evolutionarily, CA MRSA and HA MRSA are genetically distinct and clonally unrelated. Rather, CA MRSA has evolved from CA MSSA and expanded further into many diverse clonal types. Most of the CA MSSA and CA MRSA are known to produce Pantone Valentine leucocidin (PVL), a pore forming cytolysin encoded by the *lukS-PV* and *lukF-PV* genes. However, some PVL-negative CA MRSA strains have been isolated from infections similar to PVL-positive CA MRSA infections. Another virulence factor, ACME, has also been shown to be unique to CA MRSA USA300 strain [49].

Table 3: Secreted factors contributing to increased virulence of CA MRSA [49]

PSM- phenol-soluble modulins, Enterotoxin (ET)

<b>Strain</b>	<b>Cytolysins/toxins</b>	<b>Superantigen</b>	<b>PSM</b>
USA400	$\alpha$ -toxin+, $\gamma$ -toxin+, PVL+	Enterotoxin (SE) B+ or C+	PSMs+
USA300	$\alpha$ -toxin+, $\gamma$ -toxin+, PVL+	ET like (SE-1) Q+ Some strains TSST-1+	PSMs+
USA100/200	$\alpha$ -toxin+/-, $\gamma$ -toxin+/-, PVL+/-	TSST-1+	PSMs+
New evolved strains	$\alpha$ -toxin-, $\gamma$ -toxin-, PVL-	TSST-1+	PSMs+

### **Role of genomics/proteomics or bioinformatics in predicting hypothetical proteins**

Understanding the entire genome of pathogenic bacteria would aid in understanding the evolution of new virulence factors and antibiotic resistance. Pathogenic bacteria have evolved to adapt to their host by nurturing the genes for pathogenicity and silencing unwanted gene functions. Modern day technologies related to whole-genome sequencing analysis, comparative genomics, and microarrays make it possible to predict the functions of hypothetical genes, 25% of which are of unknown function [3, 60, 70].

Secretory proteins of *Staphylococcus* are grouped as peptidoglycan hydrolases, enzymes, toxins, and superantigens. These proteins are known to play important roles in all stages of pathogenesis from colonization and immune evasion to host invasion [114]. Secretory proteins are studied by various research groups for use as vaccines or toxoids for therapeutics. Several toxins are known to elicit humoral responses involving elevated IgG responses. Immunization with major secretory proteins of USA200 superantigens, TSST-1, SEC, and the cytolytins ( $\alpha$ -toxin,  $\beta$ -toxin and  $\gamma$ -toxin) conferred protection in rabbits. USA200 strains with these virulence factors are known to play roles in pneumonia, sepsis, and endocarditis. Elucidation of gene functions will help us to control CA MRSA and develop new antimicrobial therapeutics [44, 115].

### **Protein secretion system in *Staphylococcus aureus***

Protein secretion by *S. aureus* requires transport of proteins across the plasma membrane and the cell wall. The exported proteome is referred to as the secretome. Extracellular protein transport in *S. aureus* occurs mainly by the general secretory pathway (Sec) in which the protein is transported across the plasma membrane via the translocation complex *secAYEG*. The proteins to be exported have signal peptides consisting of hydrophobic amino acids at the N-



terminus. During transport the signal peptide is cleaved by a type I signal peptidase. In the case of membrane proteins the signal peptide is not cleaved and the protein remains attached to the membrane. The Sec pathway is known to transport only unfolded proteins and is involved in the secretion of virulence factors [116, 117].

The roles of other protein translocation pathways in pathogenesis are not well characterized. Such pathways include: the twin-arginine translocation (Tat) pathway, pseudopilin export com pathway, ABC transporters, holins, and the early secreted antigen targets 6 kDa (ESAT-6) pathway. The Tat pathway, named after the twin arginines in the signal peptide, translocates folded proteins across the membrane via the TatA-TatC translocase. Pseudopilin export com pathway homologues are suggested to have a role in the solute uptake process [116, 117].

Bacteriocins and lantibiotics are short peptides with antimicrobial activity effective against other *S.aureus* or *Micrococcus luteus* strains. ABC transporters are known to be involved in bacteriocin and lantibiotic export. The holin system involves a protein export system with murein hydrolase activity similar to the bacteriophage holin/anti-holin system. *S.aureus* has two operons related to the holin family, the *lrg* and *cid* operons, that exhibit murein hydrolase activity and reduced penicillin tolerance. However, their roles in extracellular protein secretion are not clear. The ESAT-6 pathway, discovered in *Mycobacteria*, is not as well understood in terms of pathogenesis however, *EsxA* and *EsxB*, related to the ESAT-6 pathway, have been identified in *S. aureus* [116, 117].

### **Predicting hypothetical proteins**

Studying bacterial genomics and proteomics related to secretomics is important since most of the therapeutic strategies are aimed at extracellular or secreted proteins. Comparative

secretomics refers to comparing proteomics of any two bacterial strains which helps to predict the hypothetical proteins. Microarrays can be used to compare the entire transcriptional profile of the stationary phase with the profile of any of the pathogenic conditions. Such comparisons will help researchers to predict new proteins involved in pathogenicity. Changes in whole gene expression and proteomics in various growth conditions are analyzed further by 2-dimensional gel electrophoresis, LC-mass spec analysis, or MALDI-TOF analysis [8, 73, 99, 113, 116, 118].

Another approach for predicting hypothetical genes or proteins is based on whole genome sequence analysis which is used to annotate functional genes based on gene ontology. Gene ontology is computationally analyzed on the basis of molecular function, cellular location, and biological process. Then several function-prediction tools are used to further analyze. BLAST is one of the primary tools used to check the sequence similarity or identity at the gene and protein levels. BLAST compares all of the available gene sequences and gives an output of all similar sequences. Genes with the highest sequence similarities are most likely have similar functions since high similarity also indicates evolution from a common ancestor. This is also called homology-based annotation transfer. Other software programs such as, prosite, dali, and jpred are used to predict hypothetical genes or proteins based on sequence similarity, protein similarity, chromosomal proximity, structural alignment, and patterns. Further, gene expression microarrays can be compared between bacterial strains and common gene expression data is clustered. The data generated is compared to predict unknown gene function [119-121].

Once the hypothetical proteins have been identified, the individual protein sequences are analyzed for a signal peptide using bioinformatics tools such as signal P or hydrophobicity plot. Signal-peptide analysis gathers evidence that the predicted protein is a secreted protein. We can further check for any known conserved motifs or domains, protein structural features, and

interactions with other proteins to predict function [119-121]. In addition, the hypothetical gene can be studied in vitro by expressing the hypothetical secretory protein. The predicted hypothetical gene can be cloned in suitable vectors to express the recombinant protein in heterologous systems such as *E. coli* or a mammalian cell line. The expressed protein can be purified and used to perform lethality or functionality assays using *C.elegans* models, mammalian cell culture, or animal models [119, 122-124].

Our research group aimed to identify hypothetical secreted proteins with a predicted role in CA MRSA virulence. We explored hypothetical proteins from *S. aureus* MSSA476. MSSA476 is a CA MSSA although it is evolutionarily closely related to MRSA252, a HA MRSA [8]. MSSA476 is reported to have a unique SCCmec type with a fusidic acid resistance gene whereas MRSA252 has SCCmec IV with methicillin resistance. Other strains of CA MRSA have Panton Valentine leucocidin (PVL) toxin but MSSA476 lacks this toxin. MSSA476 is sensitive to many antibiotics (methicillin, erythromycin, gentamycin, amikacin, tetracycline, rifampicin, ciprofloxacin, and trimethoprim) while MRSA252 is resistant to all of these and potentially others. MSSA476 is resistant to penicillin and fusidic acid [8]. Because of the close relationship to the MRSA, exploring hypothetical proteins from MSSA476 will afford information about the invasiveness of most CA MRSA strains [5, 8, 98].

We followed two approaches, gene ontology and subtractive genomics from microarray data, to identify hypothetical proteins. The hypothetical proteins identified by subtractive genomics were from the microarray data published by Holden, M.T. et al., [8] and from our bioinformatics analysis using search engines. We found some of the hypothetical proteins to be unique to CA MRSA, and thus, were suspected to have role in increased

invasiveness and overall virulence.

This research involves characterization of two such hypothetical proteins: SAS0760 and SAS1738.

### **The hypothetical protein - SAS0760**

Bacterial secreted proteins are often enzymes or toxins required for virulence, hence, we were interested in exploring hypothetical exported proteins secreted by the bacteria. Initial research began with screening hypothetical proteins using bioinformatics features of the proteins. Exported proteins are known to have signal sequences and absence of any transmembrane domains. Seventy-three such putative exported proteins were listed by the NCBI website. After analysis, one of the identified hypothetical proteins, SAS0760, was seen to have the COG3863 domain and was a distant relative of cell wall hydrolases as annotated by NCBI. Further bioinformatics studies revealed that the COG3863 domain was related to cysteine proteases NlpC/P60 family of enzymes. The SAS0760 sequence and folds were analyzed to check the structural similarities with the known homologues of NlpC/P60 family proteins.

Peptidoglycan hydrolases are grouped as three types (serine proteases, metallo-proteases and cysteine proteases) based on their catalytic sites. Cysteine proteases are cysteine-based catalytically-active enzymes consisting of “LD transferases” and “NlpC/P60” family of proteins [125]. Hydrolases are implicated in diverse roles such as cell division, virulence, and antibiotic resistance. The NlpC/P60 family hydrolases have been shown to play a role in bacterial virulence [126], but have not been explored thus far in *S. aureus* virulence. Some of the important hydrolases in *S.aureus* are aureolysin, staphopain and V8 protease. So far, there is no known NlpC/P60 family cysteine proteases characterized in *Staphylococcus aureus*.

SAS0760 showed structural similarities with other cysteine proteases, but overlapping domains were found in several of the proteins. Such overlapping domains were called permuted version proteins [125]. This research involved the structural analysis of SAS0760 by threading to its homologue proteins found in BLAST. The analysis was aimed at analyzing the active site of the enzyme and determining if it retained conserved catalytic residues (Discussed in Chapter-2).

### **The hypothetical protein - SAS1738**

Another of the hypothetical proteins, SAS1738, selected for our research is unique to community associated *S.aureus* MSSA476 strain, as compared to MRSA252 [8]. SAS1738 was found to be a 20.38 kDa hypothetical protein and predicted to be similar to a pathogenicity island protein using the bioinformatics search engines NCBI and GeneDB. The recombinant SAS1738 protein expressed in *E.coli* BL21-AI strain by a previous lab researcher showed lethal effects on *Caenorhabditis elegans*, a eukaryotic nematode, causing the animals to exhibit a known stress behavior called bordering. It was observed that rSAS1738 significantly reduced the viability of *C. elegans* in an average of 8 min (unpublished data). SAS1738 has a diphtheria toxin C motif in its gene structure (as predicted by NCBI website annotation). The diphtheria toxin C motif is the N-terminal catalytic domain involved in blocking protein synthesis by transfer of ADP-ribose from NAD to a diphthamide residue of EF-2 [127]. Hence this domain is known to contribute to toxicity in eukaryotic cells in a similar manner to the diphtheria toxin [128]. This research project aimed to further characterize the hypothetical protein, SAS1738, by determining its effect on various mammalian cell lines and to elucidate the mechanism of cell death.

**Specific aims of my research**

- Partial characterization of hypothetical protein, SAS0760, from community associated *Staphylococcus aureus* strain MSSA476.
- Investigation of the lethality of the hypothetical protein, SAS1738, from community associated *Staphylococcus aureus* strain MSSA476 on mammalian cell lines.

## CHAPTER 2

PARTIAL CHARACTERIZATION OF A HYPOTHETICAL PROTEIN SAS0760 FROM  
COMMUNITY ASSOCIATED *STAPHYLOCOCCUS AUREUS*, MSSA476**Abstract**

The virulence of a pathogen is determined by the combined effect of all its properties such as secreted toxins and enzymes that allows the bacterium to colonize in the host or have a damaging effect on the host cells [3, 121]. Our research group is focused on understanding the unexplored virulence properties of CA MRSA. Most of the bacterial toxins or enzymes are known to be secreted proteins hence we were interested in exploring hypothetical exported proteins secreted by community associated MSSA476 [114, 115]. One of the hypothetical proteins identified by analyzing seventy-three proteins available from NCBI data was SAS0760. The hypothetical protein, SAS0760, was analyzed by bioinformatics tools to check for any domains or conserved catalytic sites to predict the possible function [129]. COG3863 domain was found in SAS0760 protein with predicted cell wall hydrolytic enzyme properties. Further protein fold recognition was done by structural analysis using protein threading with its homologue proteins as mentioned by researchers Anantharaman and et al., [125] and protein data bank [130, 131]. Overall analysis revealed that SAS0760 belonged to NlpC/P60 family of cysteine proteases. Structural analysis showed the interaction of the catalytic triad cysteine, glycine and histidine. Hydrolases have an important role in bacterial cell division, cell wall

recycling, non-classical protein secretion by forming pores and also in some of the stages of biofilm dissemination [132-135]. The role of the NlpC/P60 family cyteine protease in terms of *Staphylococcus* virulence is still not clear. Thus exploring the hypothetical protein SAS0760 would be interesting.



## Introduction

### Bacterial peptidoglycan hydrolases

The bacterial cell wall is a polymer, peptidoglycan, consisting of N-acetyl glucosamine and N-acetyl muramic acid connected by  $\beta$  - (1,4) glycosidic linkages. Peptidoglycan hydrolases can be either glycosylases or amidases [130]. Amidases are very specific in their activity of cleaving specific amide linkages and it is known that the bacterial amidases exceeds the number of amide linkages. Enzyme families are categorized based on the sequence and structure of these amidases. Peptidoglycan amidases are grouped into nine classes [130]. The three main catalytic classes are metallopeptidases, serine peptidases and cysteine peptidases. The hypothetical roles of NlpC/P60 related to cell division in *Corynebacterium* [136], *Bacillus* [137-139] and the role of NlpC/P60 protein contributing to the virulence of vaccinia viruses in mice has been shown by some researchers [140]. Cysteine peptidases of NlpC/P60 protein family has not yet explored in *Staphylococcus aureus*, though the role of other cysteine hydrolases belonging to LD-transferases (CHAP) are already known to play role in *Staphylococcus aureus* pathogenesis Eg., biofilm maturation [141].

The NlpC/P60 family is related to cysteine peptidases and other cysteine peptidases are 'Ldt' type [125]. Though Ldt types are not related to NlpC/P60 peptidases, both use the same cysteine catalytic mechanism. These comprise 2 pfam families- NlpC/P60 and CHAP. Some authors use these terms interchangeably, but there are some clear structural differences [125]. The sequence similarity is unclear but it is predicted to have common papain-like folds.

The unique arrangement of catalytically active cysteine, glycine, and histidine served as a good marker of the NlpC/P60 family of proteins [125]. Cysteine acts as nucleophile, attacks the peptide bond, while histidine acts as the base and then acid catalyst for the proton transfer. The third polar residue may indicate the orientation of the catalytic histidine. Proteins belonging to NlpC/P60 family contain a characteristic amino terminal conserved region with C-terminal histidine and N-terminal cysteine and conserved glycine in between followed by aspartate [125]. The C-H pair in the NlpC/P60 along with the central glycine, defines the unique constellation of residues serving as a marker for NlpC/P60 family of peptidases [125].

Conserved domains were searched using Gibbs sampling procedure. Some structural variations are observed in NlpC/P60 family proteins and this new group of distant relatives of NlpC/P60 family included the proteins like LRAT forms, eukaryotic versions, viral homologs, and *E. coli* YaeF. These relatives had signature conserved residues but in the reversed order of amino terminal glycine followed by histidine and then cysteine [125]. This was suggested as a circular permutation compared to the classical forms C-H-G arrangement. However permuted and classical versions were >90% similar. The classical, permuted, and divergent amidase-domain proteins indicates a different type of biochemical activity [125]. Comparison of classical and permuted forms of NlpC/P60 would reveal catalytic cysteine and histidine in close proximity.

### **Structural analysis of the SAS0760 using bioinformatics tools**

Secondary structure of a protein is comprised of alpha and beta strands, which interact in three-dimensional structure also referred to as tertiary structure [142]. The three-dimensional structure is comprised of folds, motifs and domains, which are the functional units and which can function as independent units [142, 143]. Hence, folding is critical in the activity of the protein

[130]. Domains are stable but can rearrange to form new proteins with different functions during evolution. Domain identification and analysis of structure will help us to predict the function of the hypothetical protein [129, 144]. Structures of Nlpc/p60 representatives are already known but the structure of CHAP representatives are not well known. Some known CHAP amidases are SleI, Phage phi11, and *Streptococcus agalactiae* phage B30 lysin. Some known Nlpc/p60 representatives are *Anabaena variabilis* protein Q3M7N3 and an unknown protein of *cyanobacteria* [130].

My project aims to characterize the protein folds in SAS0760 using comparative modeling and structural fold recognition. Conserved domains of SAS0760 are studied by comparing it with the closest homologues and protein threading to identify the active sites in SAS0760.

## **Methods**

### **Signal peptide prediction of SAS0760 by Polyphobius**

Polyphobius prediction was performed to check for transmembrane helix and signal peptide. Based on hydrophobicity plot and polyphobius software plots, the presence of a signal peptide can be predicted [145]. The transport of the protein is directed by the signal peptide, hence, presence of signal peptide is indicative of a secretory protein.

### **Secondary structure prediction**

Secondary structure prediction was done by the software JPRED [146] and APSSP [147] analysis. These software programs predict alpha and beta strands. By comparing several software tools, the expected probability of the prediction will be increase.

### **Clustal W multiple sequence alignment**

Multiple sequence alignment by Clustal W is used to compare sequences of many related proteins [148]. Protein sequences were aligned in Clustal W software tool and each amino acid position was inspected to compare domains or conserved active sites. This analysis aids in recognition of domain swapping, which is known to occur for some proteins.

### **Tertiary structure analysis by Phyre and Genthreader**

Tertiary structure analysis involves protein fold recognition using Phyre [149, 150] and Genthreader [150, 151] software tools. This analysis functions by comparing the features of identical proteins such as sequence, class, and percent identity to the folds. Threading of the

unknown SAS0760 protein with the nearest identical protein as the template was performed to predict the probable structure.

### **Active site identification**

The active site in the hypothetical protein, SAS0760, was identified by comparing it with the closest protein homologs found in the protein data bank [131] using Genthreader and Phyre software analysis. Using the protein homologues, NlpC/P60 distant relatives and conserved residues were searched [125]. The sequence analysis was used to locate the conserved catalytic residues: cysteine, histidine and glycine. The protein data bank was used to search the structure files of the protein templates and the sequence of each template containing COG3863 domain was examined carefully by alignment using multiple sequence alignment (Clustal W). One of the templates was analyzed to look for the catalytically active site in SAS0760 protein. Analysis of the SAS0760 protein backbone for active sites cysteine and histidine was performed in Protein Workshop using both the ribbon and the space-filling model. All templates predicting the protein backbone of SAS0760 were saved from the jmol file, and further analysis images in Protein Workshop were also saved.

The active site of SAS0760 was identified by threading with permuted versions of the NlpC/P60 protein family. The sequence of SAS0760 was rearranged by comparing it with other permuted proteins of NlpC/P60 family selected based on studies by Anantharaman, et al., [125]. The rearranged or permuted sequence of SAS0760 was again submitted to Phyre and Genthreader and permuted versions of NlpC/p60 proteins were threaded with SAS0760 protein to analyze the active site residues.

### **Expression of SAS0760 Protein in *E.coli***

The SAS0760 gene was amplified using MSSA476 genomic DNA as template and cloned into the Gateway entry vector (Invitrogen), then sub-cloned into the pDEST42 expression vector (Invitrogen).

Cloning the gene and sequencing the entry clone was performed using gateway cloning technology (Invitrogen), which uses phage recombination strategy to clone the gene. Phage lysogenization into the bacterial genome and prophage excision by induction involves site-specific recombination. This unique site is called the attachment site. The phage genome has the sequence called the *attP* site and bacterial genome, the *attB* site. This is a phage lambda-based site-specific recombination system. Primers are designed with *attB* sites while maintaining the reading frame of our gene. The gene is amplified with intact *attB*, using *Staphylococcus aureus* MSSA476 genomic DNA as template, and further cloned into the vector containing the *attP* site. This reaction is called the BP reaction and the result is called the entry clone.

The entry clone with *attL* sites was allowed to recombine with the expression vector called pDEST42 with *attR* via the LR reaction between the *attL* and *attR* sites. The vectors were transformed into *E. coli* DH5 $\alpha$  cells and expression positive clones were transformed into BL21-AI™ chemically-competent cells. BL21-AI cells serve as a good expression strain since it can tolerate toxic proteins because of the tight regulation under the T7 promoter. T7 polymerase is regulated under the control of arabinose-inducible *araBAD* promoter which tightly regulates our gene of interest in this gene expression system. Expression level can be controlled to improve protein folding and solubility. The expression clones were sequenced to confirm the absence of any mutations. BL21-AI induction and protein expression was carried out at 37°C using 1mM

IPTG and 0.2% arabinose. Protein analysis was performed by SDS polyacrylamide gel electrophoresis (SDS-PAGE) and Western blot.

### **Reverse transcriptase PCR to ensure gene transcription**

Transcription was analyzed using MSSA476 genomic DNA since the expression of SAS0760 was unsuccessful. RNA was extracted from overnight culture of MSSA476 bacteria using RNA extraction ribozol reagent following the kit protocol with slight modifications (Amresco). The bacterial culture was pelleted and treated with phenol:ethanol (5%:95%) to maintain RNA stability [152]. The pellet was washed with fresh media and treated with 20 µg of lysozyme for 20 mins at 37°C. Then, the Ambresco Ribozol RNA extraction from bacterial cells protocol was followed to extract RNA. The extracted RNA was checked using OD<sub>550</sub> to determine the concentration and used for preparing cDNA by reverse transcriptase PCR.

cDNA was synthesized using MSSA476 RNA as the template following the iScript cDNAkit (Bio-rad). The cDNA was used to amplify the SAS0760 gene by PCR. RNA was used as the PCR template for the negative control to ensure no DNA contamination. Genomic DNA of MSSA476 was used as the template for positive control in the PCR.

## Results

### Signal peptide prediction of SAS0760 by Polyphobius

The sequence of the hypothetical protein, SAS0760, has 189 amino acids (Fig 1a). The signal peptide spans from 1 to 27 amino acids. The signal peptide sequence is as follows: MNYIKRTIILLILFVVVSPINSPKTIA. There were no transmembrane domains found and the topology of the domain was non-cytoplasmic. Presence of a signal peptide with no transmembrane domain indicates that this is a secretory protein (Fig 1b).

### Secondary structure prediction

JPRED analysis of SAS0760 predicted the presence of three  $\alpha$ -helices; APSSP predicted four  $\alpha$ -helices. Out of those four helices, three were predicted in almost the same regions, whereas fourth helix predicted by APSSP showed 7 residues were not predicted by JPRED (Fig 3). Global alignment prediction from JPRED predicted eight  $\beta$ -strands but three of these consisted of only three residues (Fig 4). APSSP predicted seven  $\beta$ -strands but three of the seven  $\beta$ -strands consisted of just three residues, which is doubtful  $\beta$  strands (Fig 3).

### Clustal W multiple sequence alignment

Domain analysis of SAS0760 indicated the presence of COG3863 (Fig 2). Clustal W analysis used for aligning SAS0760 and CAC0029, its nearest homolog. Before analyzing the structure files of each template, multiple sequence alignment of the nearest members of the COG3863 and one of the templates was used to align and identify the catalytically active site in



SAS0760 protein. The domain in SAS0760 belongs to a cluster of orthologous genes, COG3863, which has three closely related proteins: CAC0029, AF1513, and BS\_ycy0 (Fig5).

SCOP lineage showed SAS0760 belonged to family of alpha and beta proteins; folding consisted of one alpha-helix and 4 strands of antiparallel beta-sheet and contained the catalytic triad, Cys-His-Asn. This analysis revealed that SAS0760 belongs to a superfamily of cysteine proteinases.

### **Tertiary structure analysis of SAS0760**

Phyre selected best templates analysis showed 100% precision score homology with cysteine proteases, as follows: NlpC/P60 family in *Nostoc punctiforme* (protein data bank ID- 2evra), lipoprotein *Escherichia coli* K12 (PDB ID- 2k1gA), NlpC/P60 protein of *Anabaena variabilis* (PDB ID- 2hbwA), and metalloprotein yiix of *Escherichia coli* 0157:h7, duf1105 (PDB ID- 2if6B) of unknown function. All pairwise identities of the templates were only 8% to 12% (Table 5b). Genthreader software analysis showed only metalloprotein yiix of *Escherichia coli* 0157:h7, duf1105 (PDB ID - 2if6B) as the best template with 9.3% sequence identity (Table 5a).

The structural analysis was performed using Phyre and Genthreader which showed the tertiary structure of SAS0760 on the basis of the templates. It also showed the catalytically conserved domains (cysteine, histidine and glycine) by Clustal W. However, some of the templates did not show similarity to COG3863 domain or the catalytically active triad of the SAS0760 (Fig 5). This may be because of its permuted structural form as explained by Anantharaman et al. [125]. Therefore, the primary sequence was manually aligned and analyzed for the catalytic site. The permuted sequence of SAS0760 was then submitted to Phyre and

Genthrader for threading structural models compared to its nearest homologues of the COG3863 domain.

### **Active site identification**

The active site identification in SAS0760 was determined by threading both native and domain-swapped versions of SAS0760 (Fig 8) with their closest homologues. The manually rearranged SAS0760 conserved amino acid sequence were denoted by fragments a and b, first and second part of the sequence, respectively. The conserved sequences in SAS0760 trimmed in the native form of SAS0760 was labeled as SAS0760 (a+b) (Fig 8a), whereas the SAS0760 rearranged to indicate domain swapping was labeled as SAS0760 (b+a) (Fig 8b).

These modified sequences were further compared with the homologue proteins of NlpC/P60 family. The closest homologues found in Phyre and Genthrader were 2if6B, 2evra, hbwA, 2k1gA proteins (Table 5 and 6) [125]. The protein structure was observed both in the ribbon model and the space filling model. The native form of SAS0760 did not show the interaction of catalytically active residues. But only Gly-His was noticed in 2hbwA (Fig 7), 2evra (Fig 6a), and 2k1gA (Fig 6b).

Neither the native SAS0760 nor the trimmed SAS0760(a+b) showed the catalytically active sites when threaded with the permuted forms of NlpC/P60 proteins as shown in 2if6B (Fig 11). Phyre analysis of SAS0760 (b+a) indicated that 2if6B had higher sequence identity (13%) compared to other proteins (Table 6). Threading of SAS0760 (b+a) with 2if6B protein from *E.coli*0157, a metalloprotein yiix, indicated the active site triad to be Gly-His-Cys. The image (Fig 11). also indicated the interaction of three conserved catalytic amino acids and supports the hypothesis of an active role in catalysis (Fig 12).

Phyre analysis of the conserved residues of the native form of SAS0760 did not show the interaction of the conserved catalytic triad, Cys-Gly-His. Only Gly-His was seen in 2hbwA (Fig 7), 2evra, and 2k1gA (Fig 6). Phyre analysis of the trimmed SAS0760(a+b) indicated that 2evra, hbwA, and 2k1gA showed higher sequence identity compared to 2if6B (Table 5). Native (untrimmed) SAS0760 (Fig 15) and trimmed SAS0760(b+a) (Fig 15) sequences threaded with 2hbwA showed only cys-his, however, threading 2hbwA with trimmed SAS0760(a+b) revealed the permuted catalytic triad, Gly-His-Cys (Fig 14). As per Ananthraman et al, [125]. Proteins 2evra, hbwA, and 2k1gA had the native cysteine protease catalytic triad, Cys-His-Gly, whereas 2if6B had the permuted catalytic domain, Gly-His-Cys.

Thus, we can conclude that the hypothetical protein, SAS0760, exists in the permuted version of NlpC/P60 family. The interaction of catalytically active amino acids indicated functionality of the cysteine protease even in the permuted identical proteins.

### **Expression of SAS0760 protein in *E.coli***

The SAS0760 gene, cloned in the entry and expression clones, showed the expected sized band at 560 bp using PCR to amplify the DNA (Fig 16). However, induction and protein purification of SAS0760 did not produce significant protein as analyzed by SDS and Western blot. Multiple attempts to express SAS0760 in pRSETa, pET28a, as well as mammalian expression systems, also were not successful.

### **Reverse transcriptase PCR to ensure gene transcription**

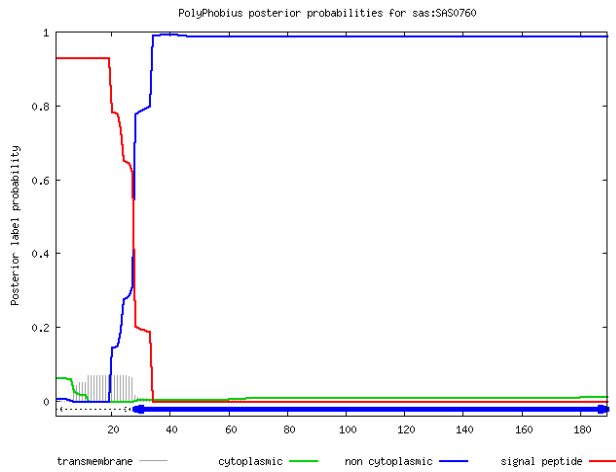
SAS0760 mRNA transcripts were amplified by reverse transcriptase PCR using cDNA of MSSA476, indicating efficient transcription of the gene in MSSA476 stationary bacterial culture (Fig 17).

---

MNYIKRTIILLILFVVVSPINSPKTIADNKYSEIQDDKFQLQPGDIIVTKGPVMWGFFGHCSIAIDDKTILQIEG  
 PGDKPTTQSFESFKYNYASGKNDWMKVYRCSYPGAGKKAAEWVKKNYENTNHRYLVTNLNLSKKFTYC  
 TKIYQAYKFGVSEKSVKSYGLHIISPYAIKDNFIDPYKLRLVKAY

---

(1a)



(1b)

Figure 1: SAS0760 sequence data.

SAS0760 amino acid sequence data (1a); Polyphobius prediction of SAS0760 (1b)

Table 4: Signal peptide prediction of SAS0760 by Polyphobius

ID sas:SAS0760					
FT	SIGNAL	1	.....	27	
FT	REGION	1	.....	7	N-REGION.
FT	REGION	8	.....	18	H-REGION.
FT	REGION	19	.....	27	C-REGION.
FT	TOPO_DOM	28	.....	189	NON CYTOPLASMIC.

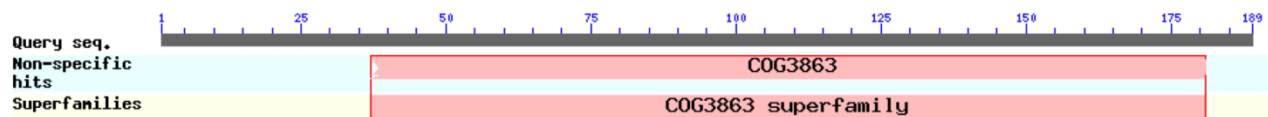


Figure 2: COG3863 domain in SAS0760 hypothetical protein.

Table 5: Tertiary structure analysis by Phyre and Gentreader.

Gentreader templates (5a); Phyre templates (5b)

(5a)

PDB ID	Name of the protein	Species/organism	% Sequence identity
2if6B	Unknown function metalloprotein yiix	<i>Escherichia coli</i> 0157:H7, duf1105	9.3

(5b)

Phyre selected best templates (estimated precisions >90%)			
PDB ID (est. prec)	Name of the protein	Species/organism	% Sequence identity
2evra (100%)	NlpC/p60	<i>Nostoc punctiforme</i>	8
2k1gA (100%)	Lipoprotein	<i>Escherichia coli</i> K12	8
2hbwA (100%)	NlpC/p60	<i>Anabaena variabilis</i> ATCC 29413	8
2if6B (95%)	unknown function metalloprotein yiix	<i>Escherichia coli</i> 0157:H7 duf1105	12

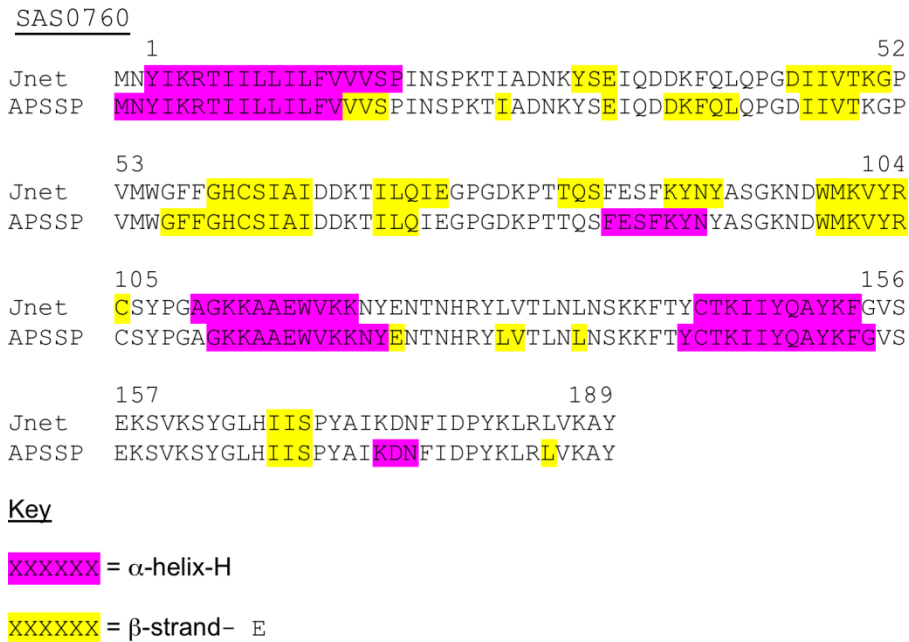


Figure 3: Secondary structure prediction of SAS0760 by Jpred and APSSP.



```

CAC0029  MVNIKKNTALVAAFIITATTLTNVKAYAVTNGMTGNERNVLKQYQSNIDNTYNSFGDKKK 60
SAS0760  MNYIKRTIILLILFVVVSP-----INSPKTIADNKYSEIQDDK- 38
          *:   :::  .                               :.  .:  .:  ..

CAC0029  TKVVNDYKNKVKKAQRFISRDTDENYGDYPTRSGVILVTRDSNTMGIHYGHAG-IIWDAS 119
SAS0760  -----FQLQPGDIIIVTKGP-VMWGFFGHCS-IAIDDK 68
                              *  ::  .             :.*  . :  .

CAC0029  TTVESPSGVERYPNWKS-RYNTIKG-----ITVNSTTAEQDKEAADWCNNOVGKPYN- 172
SAS0760  TILQIEGPGDKPPTQSFESFKYNYASGKNDWMKVYRCSYPGAGKKAAEWVKKNYENTNHR 128
          *  *  .   :.  :  .*  .   .             ::  *:  :.  :.  .

CAC0029  -WNEFNINTRDKFYCSQLVWAAWKDLYGMDIDPKKTIPSVIIP-----VDLP 218
SAS0760  YLVTLNLNSKKFTYCTKIIYQAYK--FGVSEKSVKSYGLHIIS-----PYAI 173
          .  **:::  .*:  *:  :.  :.

CAC0029          KQNTVDTIYAQWQAN----- 233
SAS0760          KDNFIDPYKLRLVKAY----- 189

```

Figure 5: CLUSTAL 2.0.12 multiple sequence alignment of the SAS0760 (entire sequence) compared with its homologue proteins.

Color: Red highlighted aminoacids are catalytically active residues. Yellow highlighted is the hydrophobic residues.



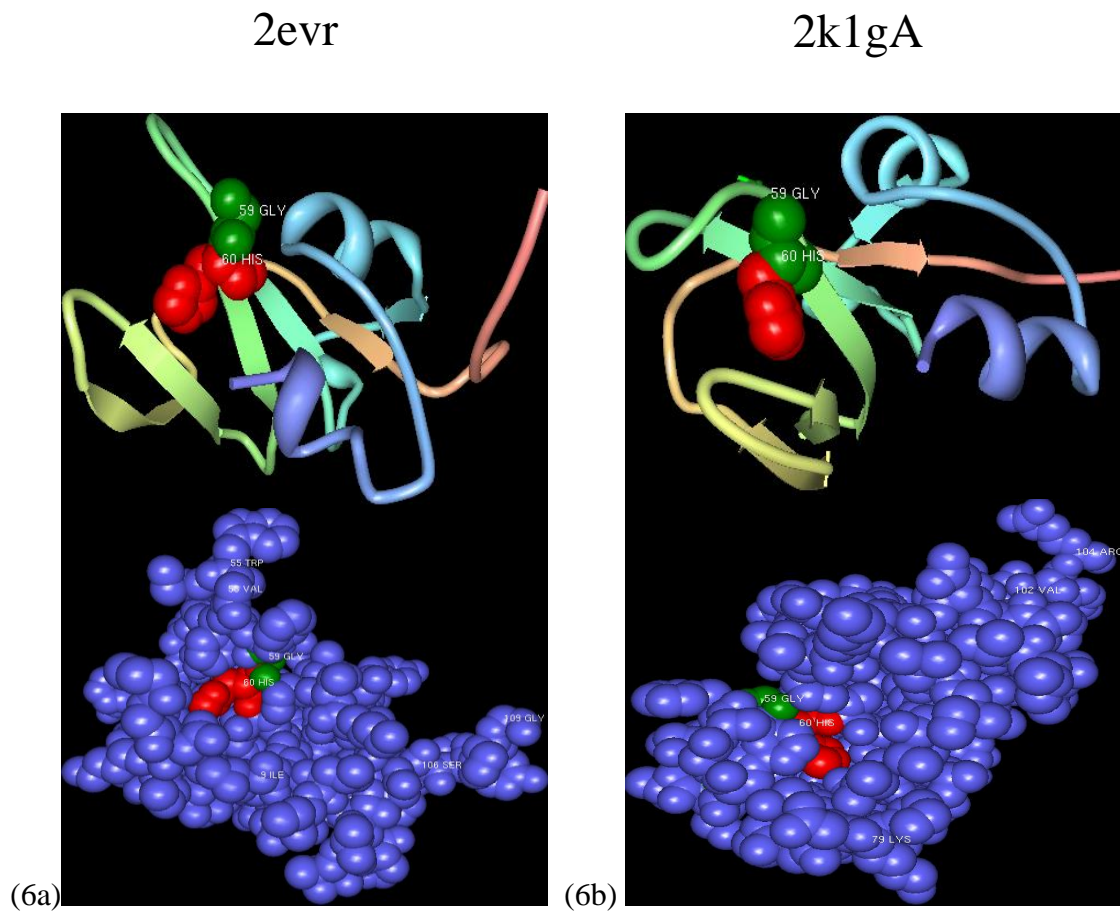


Figure 6: Threading of SAS0760 (native) with 2evr (*Nosctoc punctiforme*) (6a) and 2k1gA (*Escherichia coli* K12) (6b); Top-Ribbon Model. Bottom-Space filling model

## 2hbwA

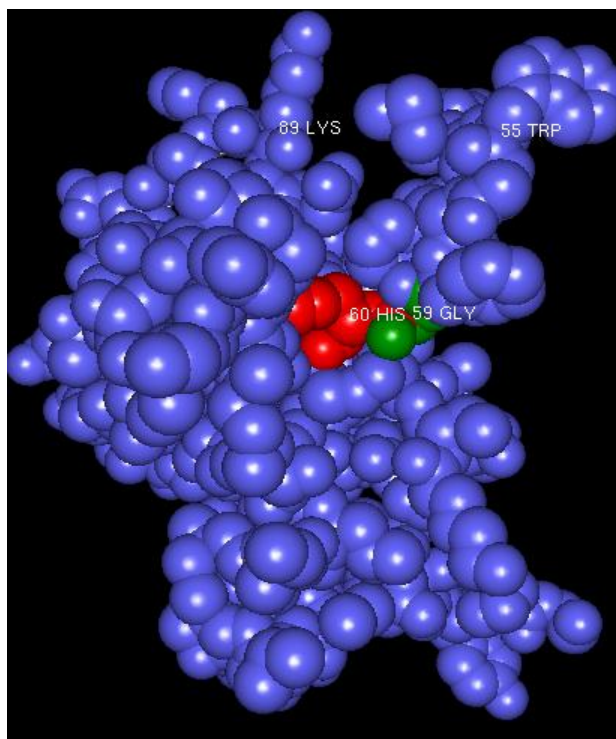


Figure 7: Threading of SAS0760 (native) with 2hbWA from *Anabaena variabilis* (space filling model).

Fig 8a

MNYIKRTIILLILFVVVSPINSPKTIADNKYSEIQDDKFQLQPGDIIVTKGPVMWGF  
FGHCSIAIDDKTILQIEGPGDKPTTQSFESFKYNYASGKNDWMKVYRCSYPGAGKKAEE  
WVKKNYENTNHRYLVTLNLNSKKFTYCTKIIYQAYKFGVSEKSVKSYGLHIISPYAIKD  
NFIDPYKLRLVKAY

Fig 8b

GKKAEEWVKKNYENTNHRYLVTLNLNSKKFTYCTKIIYQAYKFGVSEKSVKSY  
GLHIISPYAIKDNFIDPYKLRLVKAYMNYIKRTIILLILFVVVSPINSPKTIADNKYSEIQDD  
KFQLQPGDIIVTKGPVMWGGFGHCSIAIDDKTILQIEGPGDKPTTQSFESFKYNYASGKN  
DWMKVYRCSYPGA

Figure 8: Rearrangement of SAS0760 to analyze domain swapping.

SAS0760: Native Amino acid sequence; (8a) Domain swapped or permuted sequence of SAS0760; (8b) Blue highlighted sequence is the rearranged sequence.

Table 6: Phyre analysis of rearranged and trimmed SAS0760 (a+b).

<b>PDB ID (est. prec)</b>	<b>Name of the protein</b>	<b>Species/organism</b>	<b>% Sequence identity</b>
2k1gA (100%)	Lipoprotein	<i>Escherichia coli</i> K12	10
2evra (100%)	NlpC/p60	<i>Nostoc punctiforme</i>	10
2hbwA (100%)	NlpC/p60	<i>Anabaena variabilis</i> ATCC 29413	12
2if6B (95%)	unknown function	<i>Escherichia coli</i> 0157:h7	8
	metalloprotein yiix	duf1105	

```

SAS0760      GKKAAEWVKKNYENTNHRYLVTLNLSKFTYCTKIIYQAYKFGVSEKSVKSYGLHIISP 60
CAC0029      DKEAADWCNNQV GKPYNWNFFNINRDK---FYCSQLVWAA YKD-----LYGMDIDPK 49
YaeF_Ec      ATDITAFANKIKDSGYNYRGIVEFKKS---WFCSEFVTDAFAKAG-----HPLTLAQS 50
yiiX_Ec      QOKLAQTAKRYL GKPYPDFSFWSDDRQ---YCSSEVVWKVYQN-----ALGMRVGEQ 48
.            . : :. . . . . :*::: . : : :

SAS0760      YAIKDNFIDPYKLRRLVKAYMNYIKRTIILLILFVVVSPINSPKTIADNKYSEIQDDKFQL 120
CAC0029_     KTIN-----YGDYPTR----- 60
YaeF_Ec_16128186  GWIS-----PEITAP-----DL 62
yiiX_Ec_15804534  QCLK-----EFDPAFAWQP----- 62
.            :.

SAS0760      QPGDII VTKGPVMWGFFC HCSIAIDDKTILQIEGPGDKPTTQSFESFKYNYASGKNDWMK 180
CAC0029      -SGVILVTR-DSNGIHYG HAGI IWDASTTVESEPSGVERYPNTWKS-RYNTIKG----IT 113
YaeF_Ec      KPGDLLFSS-SLGTSSVSHVAIFLGDNNVAEATGAGVQIVSLKKAMKHSKDLFV----LR 117
yiiX_Ec      QTGDII FQI---SHSDYSHTGMLVMRNKKPYVFEAVGVPKYTPLKQWIAHGEK GK---- 116
.            :. . . *

SAS0760      VYRCSYPGA 189
CAC0029_Cac_15893327  VNSTT---- 118
YaeF_Ec_16128186  VPDLTP--- 123
yiiX_Ec_15804534  YVV---RRV 120
.            *

```

Figure 9: Clustal W 2.0.12 multiple sequence alignment of SAS0760 (a+b) with homologues.

Conserved domains of SAS0760 amino acids were rearranged based on comparisons of classical and permuted versions of homologue proteins. The rearranged SAS0760 is named as SAS0760 (a+b). Color: Red-highlighted amino acids are catalytically active residues. Yellow-highlighted are the hydrophobic residues.

Table 7: Phyre analysis of rearranged SAS0760 (b+a).

PDB ID (est. prec)	Name of the protein	Species/organism	% Sequence identity
2if6B (95%)	unknown function metalloprotein yix	<i>Escherichia coli</i> 0157:H7 duf1105	13
2k1gA (100%)	Lipoprotein	<i>Escherichia coli</i> K12	7
2evra (100%)	NlpC/p60	<i>Nostoc punctiforme</i>	6
2hbwA (100%)	NlpC/p60	<i>Anabaena variabilis</i> ATCC 29413	7

```

CAC0029  MVNIKKNTALVAAFIIITATTLTNVKAYAVTNGMTGNERNVLKQYQSNIDNTYNSFGDKKK 60
SAS0760  MNYIKRTIILLILFVVVSP-----INSPKTIADNKYSEIQDDK- 38
          *:   :::  .                               ::  ::  ::  ..

CAC0029  TKVVNDYKNKVKKAQRFISRDTDENYGDYPTRSGLVTRDSNTMGIHYGHAG-IIWDAS 119
SAS0760  -----FQLQPGDIIVTKGP-VMWGFFGHCS-IAIDDK 68
                               *  ::  .           :.*  .  :  .

CAC0029  TTVESEPSGVERYPNTWKS-RYNTIKG-----ITVNSTTAEQDKEAADWCNNOVGKPYN- 172
SAS0760  TILQIEGPGDKPTTQSFESFKYNYASGKNDWMKVYRCSYPGAGKKAAEWVKKNYENTNHR 128
          *  *  .  :.  :  .*  .  :  :  *  :  :  :  :  .

CAC0029  -WNFFNINTRDKFYSQLVWAAYKDLYGMDIDPKKTIPSVIIP-----VDLP 218
SAS0760  YLVTLNLNSKKFTYTKIIYQAYK--FGVSEKSVKSYGLHIIS-----PYAI 173
          .  **:::  :.  .*  *  :  :  :  :  :

CAC0029          KQNTVDTIYAQWQAN----- 233
SAS0760          KDNFIDPYKLRLVKAY----- 189

```

Figure 10: Clustal W 2.0.12 multiple sequence alignment of SAS0760 (b+a) with a homologue.

The catalytic triad observed as gly-his-cys indicates the permuted version of the NlpC/P60 protein. Color: Red highlighted amino acids are catalytically active residues. Yellow highlighted are the hydrophobic residues.

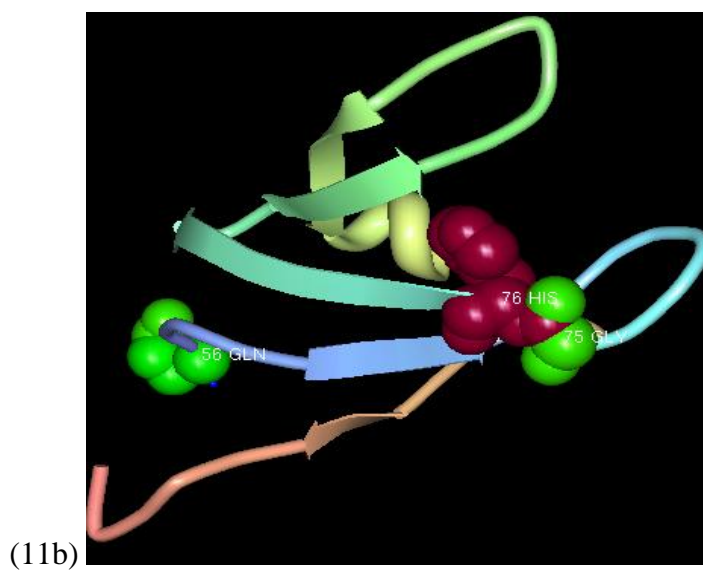
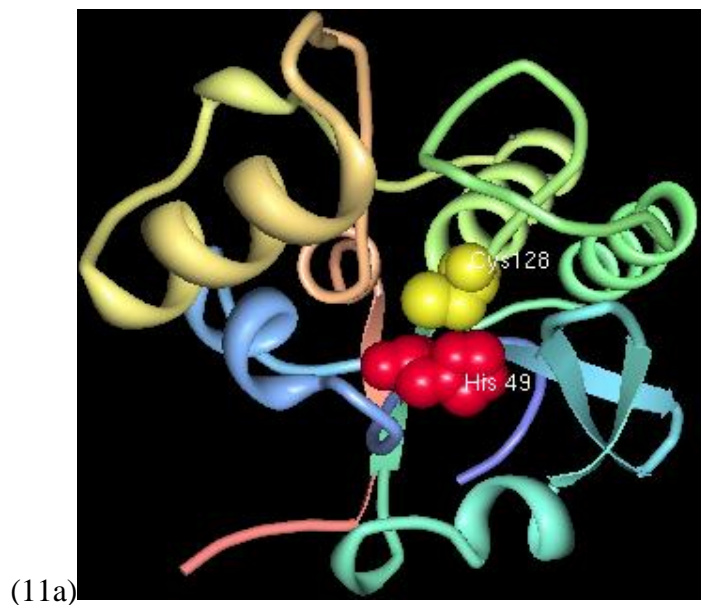
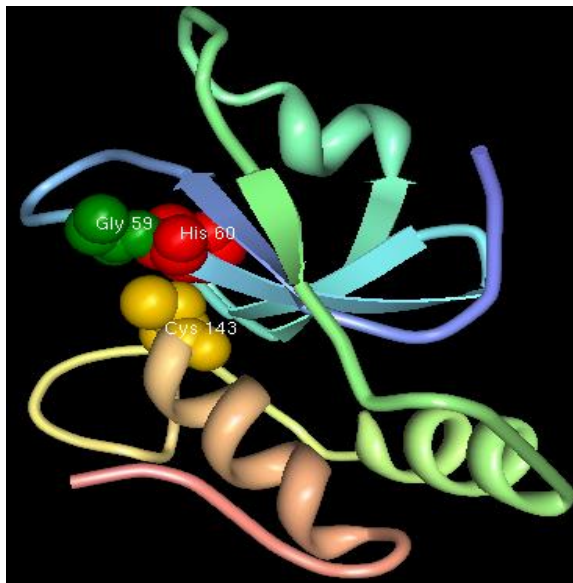
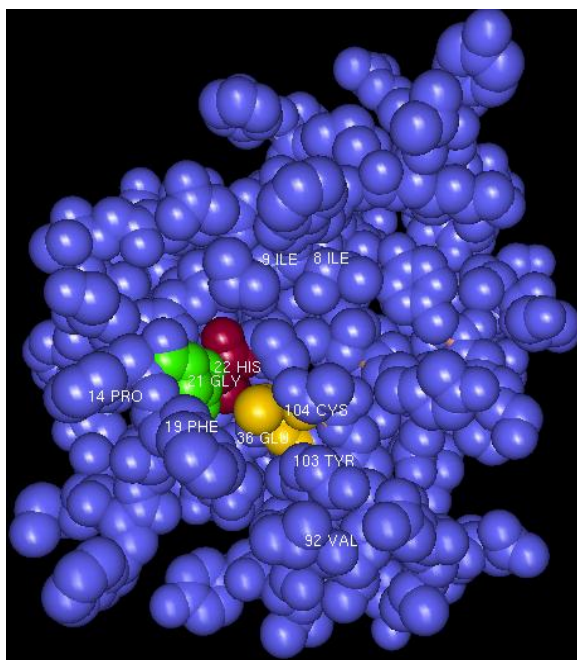


Figure 11: SAS0760 threaded with homologue protein, 2if6B.

Fig 11a: 2if6B (permuted NlpC/P60 version) threaded with SAS0760; Fig 11b: 2if6B threaded with SAS0760 (a+b).



(12a)

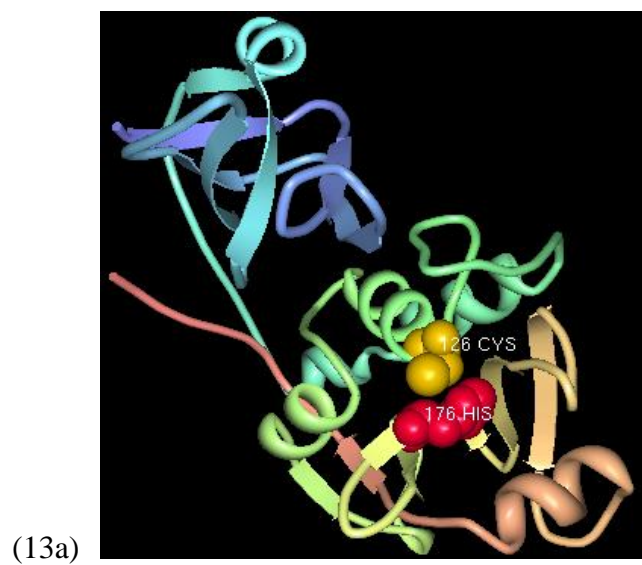


(12b)

Figure 12: SAS0760 (b+a) (permuted form) threaded with homologue protein, 2if6B.

(12a) Ribbon model; (12b) space filling model.





## 2hbwA

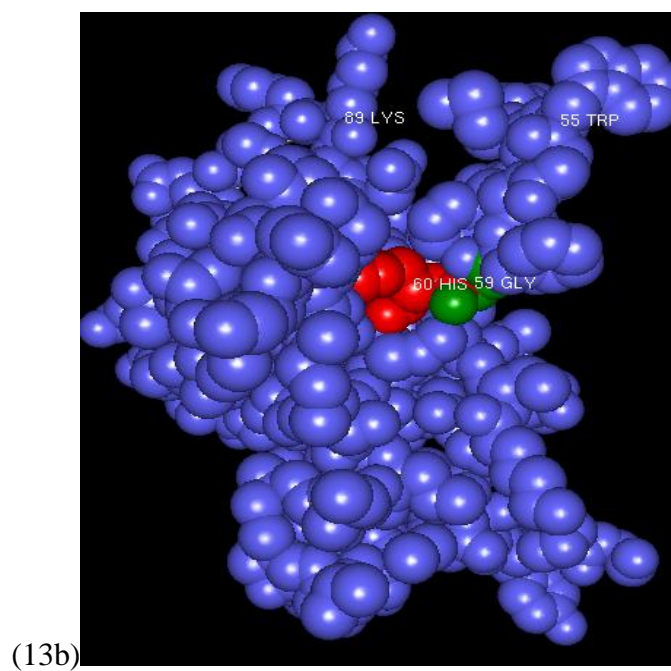


Figure 13: SAS0760 threaded with homologue protein, 2hbwA.

(13a) Ribbon model; (13b) space filling model.

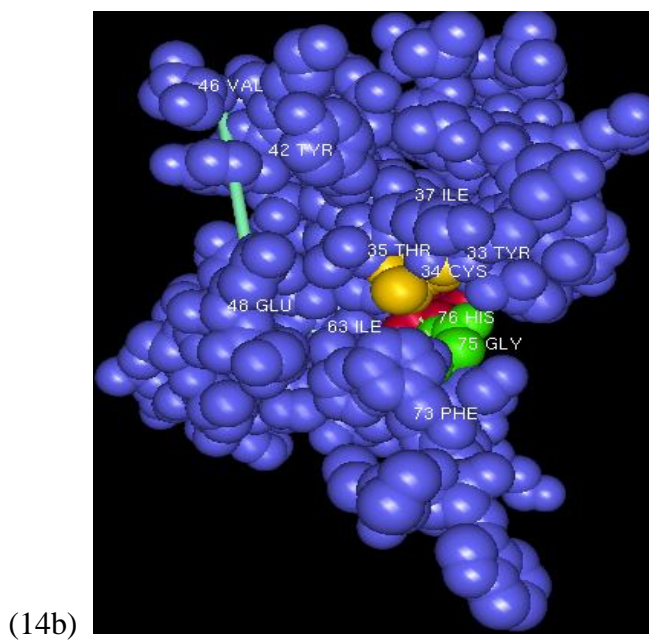
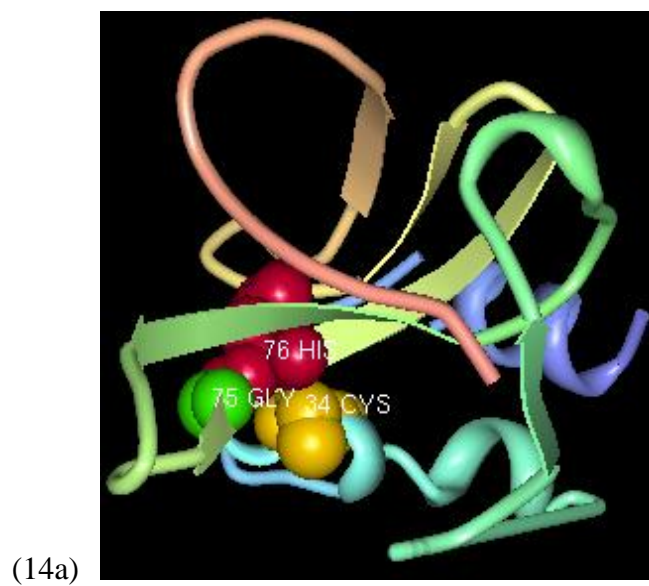


Figure 14: SAS0760 (a+b) trimmed for conserved domains and threaded with 2hbwA.

(14a) Ribbon model; (14b) space filling model.

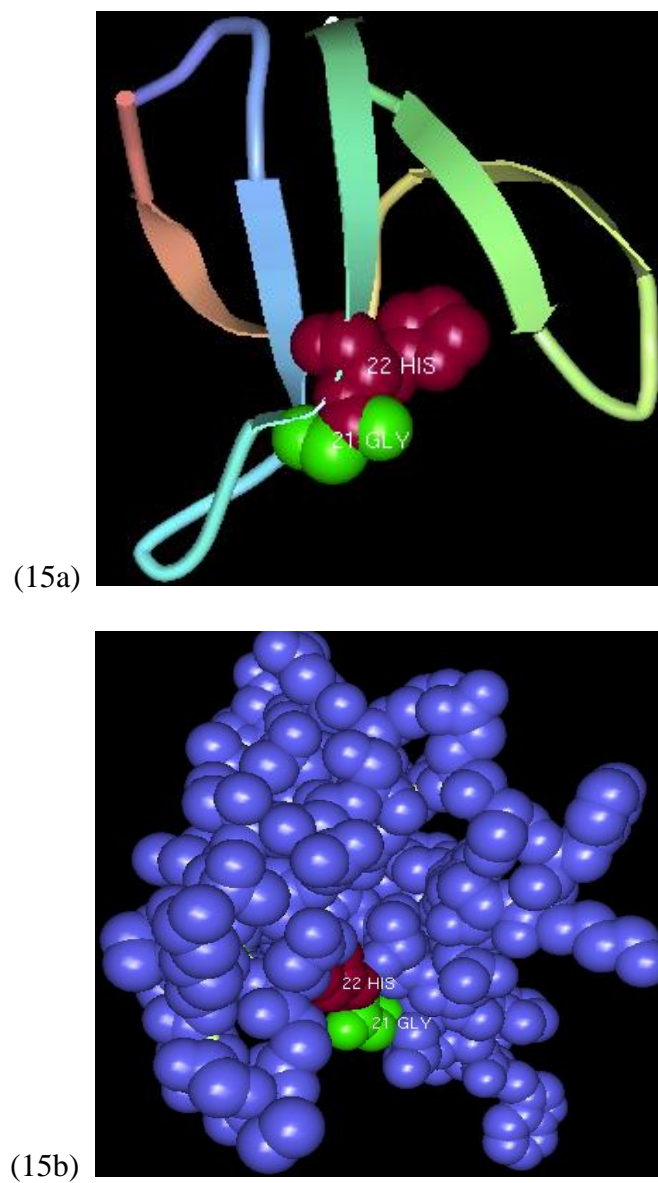


Figure 15: SAS0760 (b+a) threaded with 2hbwA.

(15a) Ribbon model; (15b) space filling model.

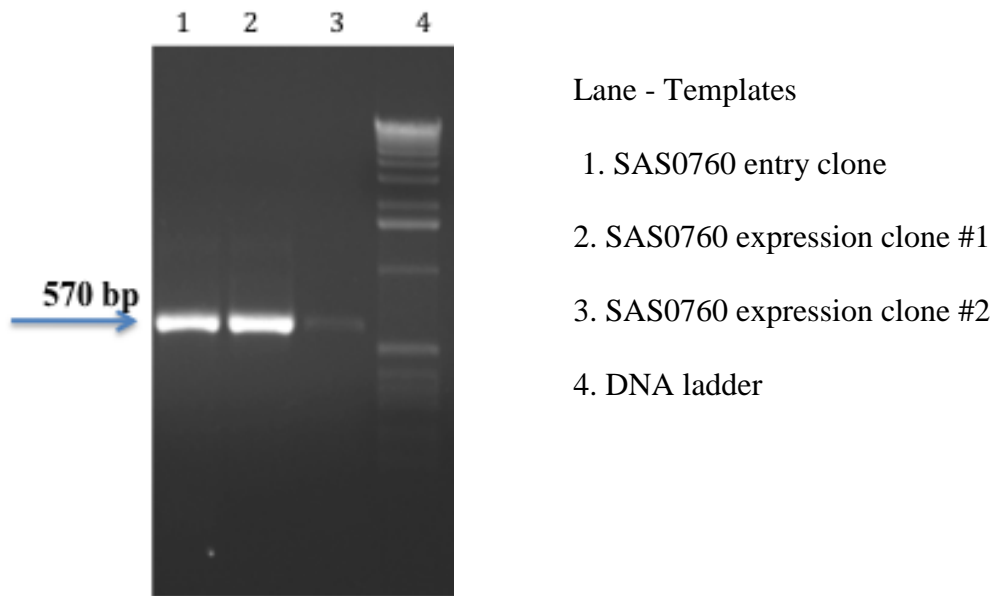


Figure 16: PCR amplification of the SAS0760 gene from MSSA476 genomic DNA.

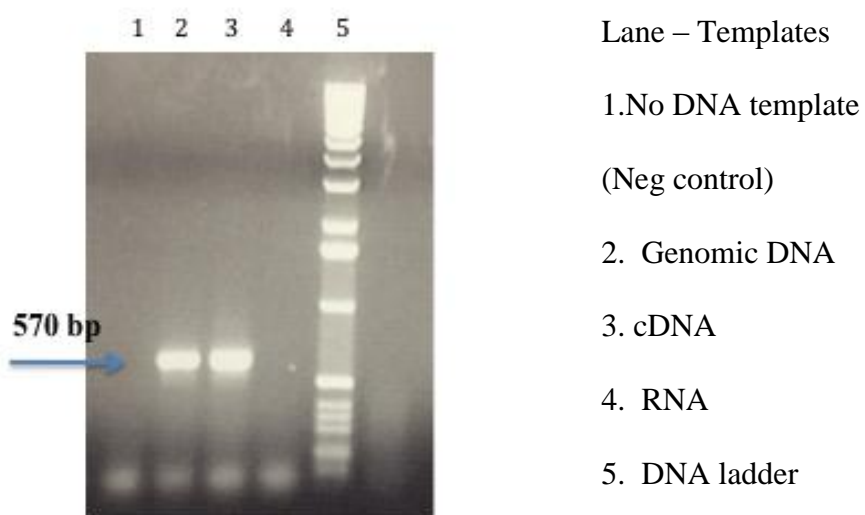


Figure 17: Reverse transcription of SAS0760 gene from MSSA476 with PCR amplification from cDNA.

## Discussion

Bioinformatics tools were used to analyze the structural similarities of SAS0760 protein with the known NlpC/P60 family proteins. Bioinformatics prediction data annotated the hypothetical protein, SAS0760, as a distant relative of the cell wall hydrolases with COG3863 domain (Fig 2). SAS0760 had a signal peptide and, hence, is a secreted protein (Fig 1). Protein structural threading was performed based on comparison with the other identical templates of NlpC/P60 family proteins, Hbwa and 2if6B, as found by protein data bank and Clustal W alignment (Table 5). Upon comparing with nearest permuted identical protein, 2if6B, it indicated that SAS0760 exists in permuted versions of NlpC/p60 family. The catalytically active cysteine-histidine-glycine triad was identified in the permuted version of the SAS0760 by the Clustal W and protein threading. Ribbon model images show catalytically active residues more clearly compared to space filling models. Space filling models help to analyze the other properties such as hydrophobic amino acids and folding (Fig 12).

According to the threading results observed in Fig 12, the catalytic triad interaction was observed, indicating that the activity of the catalytic domain should be retained even with the permuted rearrangement, as explained by Anantharaman et al., [125]. However, there can be many possible expression problems with hydrolases. Each protein has a very specific pH, temperature and iso-electric point at which it can be expressed or secreted. It is known that peptidoglycan hydrolases have high isoelectric points and clump to the cell wall or resin components due to positive charges, making the purification process difficult. Even if we

achieve expression at a lower level, the protein may be lost during the purification process or the purified protein may not be stable [153]. On the other hand, some cysteine proteases may not directly lyse the cell wall but are involved in activating other hydrolases by cleaving the propeptide [154].

The hypothetical gene *sas0760* was cloned in the *E.coli* gateway expression system, PET28a, or in a mammalian expression system, but the stable expression of protein was not successful. SAS0760 gene transcription was analyzed using the RNA from stationary phase cells of MSSA476 strain. Amplification of SAS0760 from mRNA indicated efficient transcription in MSSA476 (Fig 17). However, we cannot predict if there is any hindrance in translation of SAS0760 protein.

There may be other drawbacks in SAS0760 expression such as the requirement of the homologous or native host systems. SAS0760 protein expression may need specific conditions as in the native MSSA476 strain and, therefore, could not be expressed in the heterologous host systems like *E.coli* or mammalian culture. Sometimes protein expression levels may be very low or may aggregate to form insoluble bodies due to the differences in codon usage between the natural host and the expression host [155]. The heterologous protein may be degraded by *E.coli* proteases. However, we have expressed the SAS0760 in BL21-AI strain which is OmpT and Lon protease deficient. We should still consider using protease inhibitors to reduce any proteolytic damage and thus aim to achieve stable protein expression in the future.

SAS0760 protein expression must be explored further in different vectors or using different promoters to aid the expression of this unique hydrolase. SAS0760 could be cloned after removing the signal peptide to increase the chances of protein expression. Cloning SAS0760 in codon optimized *E.coli* strains or gram positive bacterial expression systems such as

*Lactobacillus* could minimize the expression errors due to the differences in GC content or codon usage errors between species [156].

Cysteine proteases, like staphopain and autolysins, are known in *S. aureus*, but there are no NlpC/P60 family cysteine proteases characterized in *S. aureus* to date. SAS0760 analysis is unique and has led to the discovery of a new class of hydrolases and the indication that this class is related to virulence in *S. aureus*.



## CHAPTER 3

INVESTIGATING THE LETHALITY OF THE HYPOTHETICAL PROTEIN, SAS1738,  
FROM COMMUNITY ASSOCIATED *STAPHYLOCOCCUS AUREUS* MSSA476 ON  
MAMMALIAN CELL LINES.**Abstract**

MSSA476 and other CA MRSA strains are known to be more invasive than HA MRSA. CA MRSA is more genetically diverse than HA MRSA from sharing the gene pool of diverse bacteria from different communities [2, 4, 157]. Lateral gene transfer led to the variation in the conserved, mobile and pathogenicity islands of various MRSA strains. It is important to understand all the hypothetical genes that may contribute to increased virulence and varied antibiotic resistance patterns. MSSA476 is a community associated *Staphylococcus aureus* and, evolutionarily, closely related to MRSA252, a HA MRSA [5, 8, 98, 158, 159]. Further understanding of such unique, unexplored hypothetical proteins and characterization of their role in virulence will aid the understanding of the increased virulence of CA MRSA.

Based on the microarray data of Holden, M.T. et al. (2004), genes from HA MRSA and CA MRSA were compared, and subtractive genomics of these data gave us a list of genes coding for hypothetical proteins from CA MRSA [8]. One such hypothetical protein named SAS1738 from MSSA476, residing in a *Staphylococcus* pathogenicity island, was shown to have lethal effects on *Caenorhabditis elegans* by a previous researcher from our lab. Lethality of purified

SAS1738 was determined by WST-1 proliferation assay on the following mammalian cell lines: NIH3T3 cells, CHO 1 fibroblast cells, Raw 264.7 mouse macrophage cell line, human embryonic kidney cell line (HEK293), human microvascular endothelial cells (HMEC-1) and human keratinocytes (HaCat). Viability of HEK293, HMEC and HaCat cell lines was reduced by SAS1738. Kinase (p38 and erk kinase) activation studies were performed by immunoblotting. Erk kinase was activated at 60 mins time point. Host cell death by apoptosis or necrosis was analyzed by Viacount assay and Nexin assay using flow cytometry. Flow cytometry analysis confirmed HEK293 cell death occurred by apoptosis due to SAS1738 protein.

## Introduction

### ***S. aureus* interaction with different cell types with respect to human infections**

Skin plays a major role in protection against microbial entry and invasion. Human skin constitutes the major organ covering the entire body and composed of epidermis, dermis, and hypodermis layers. Epidermis is composed of keratinocytes and melanocytes. The keratinocyte layer is composed of stratified squamous epithelium; outermost is a layer of dead cells covering in stratum corneum that exfoliates periodically and is replaced by new keratinocytes made in the basal layer. The pigmentation cells are melanocytes in the basal layer protecting the keratinocytes from UV mutation due to sun exposure. The second layer, dermis, consists of hair follicles, oil glands, sweat glands, blood vessels and connective tissue made up of fibroblasts, collagen and elastin. The hypodermis is the deeper layer of tissue composed of fat cells called adipocytes and connective tissue composed of blood cells, osteocytes in bone, and blood vessels lined with endothelial cells [160].

Skin acts as the first barrier for bacterial invasion into the human body. Normal microbial flora of skin includes *Propionibacterium acnes*, *Staphylococcus epidermidis*, *S. aureus*, *Corynebacterium*, *Streptococcus* species, and *Enterococcus* species. All are known to be involved in protection against the pathogenic species by niche specific competition and antimicrobial substances on the skin. These bacteria colonize the skin mainly in the stratum corneum and hair follicles, occasionally breaking the barrier and invading superficially or deeper layers leading to skin and soft tissue infections (SSTIs) [161, 162]. Most hospital acquired STTIs

are caused by *Staphylococcus aureus*, known to be the major cause of SSTI (~45%), followed by *Pseudomonas aeruginosa* (~11%) and *Enterococcus* sp. (~9%). The widespread recent emergence of community associated *S.aureus* (CA MRSA) involvement in STTIs is alarming [7, 163].

Infections in superficial layers of skin are called erysipelas. Further, infections of epidermis and deeper layers can be pyogenic types: carbuncles, folliculitis, furuncles or epidermal necroses. Scalded skin syndrome and bullous impetigo is characterized by peeling of the skin. Deeper tissue infections can lead to fasciitis, myositis or cellulitis. Skin and soft tissue infections can affect all the layers of skin and disseminate to other organs through the bloodstream causing secondary infections like abscesses in organs, endocarditis, and osteomyelitis [102, 161].

*S.aureus* is known to enter the human body mainly through the skin barrier or through respiratory passages. Nasal carriers are known to have higher risk of bacteremia and other infections [164]. The bacterium enters the skin through follicle or gland pores, injuries, cuts, wounds, burns, surgeries, and indwelling medical devices such as urinary or intravenous catheters. Upon entry *S.aureus* encounters basal layer keratinocytes leading to deeper tissue invasion. Keratinocytes are activated by Fc receptors, complement receptors or by bacterial toll-like receptors. The activated keratinocytes secrete inflammatory molecules such as defensins, reactive oxygen intermediates, cathelicidins and also activate the host immune system by recruiting neutrophils and macrophages [165].

### ***S.aureus* colonization**

The bacterial colonization and infection process begins with the attachment of the bacteria to keratinized epithelial lining. *S. aureus* attachment is known to vary with age of the

keratinized epithelial cells; attachment is enhanced in fully matured keratinocytes compared to granular keratinocytes. Staphylococcal protein A (spa), coagulase (coa), clumping factor (clfA), and the fibronectin binding proteins A and B (fnbA/B) are shown to be involved in HaCat keratinocyte attachment. Cell wall teichoic acids and lipoteichoic acids were known to be involved in attachment to nasal epithelium and fibronectin. Recent studies demonstrate the role of many other *S.aureus* adhesins in adherence to the nasal squamous epithelial cells:

MSCRAMMs, surface protein (SasG), clumping factor (ClfB), IsdA , SdrC, SdrD. Elastin binding protein and sialo binding protein showed involvement in osteocyte attachment [166-169].

The other secretory exotoxins, lipases, serine proteases, and PVL are known to be involved in damaging the skin barrier and skin cell death. Skin desmosomes are lysed by serine protease leading to bullous diseases and scalded skin syndrome. Lipases are known to aid bacterial entry through skin by digesting fatty acid depositions on skin. PVL, a pore forming protein, is known to damage skin tissue and neutrophils [39, 42, 170].

### ***S. aureus* internalization and invasion**

Pathogenic bacterial invasion occurs either by extracellular or intracellular modes, or both. The pathogen gains access to the inside of cells and can further disseminate, leading to the spread of infection to other organs. Heparinase, hyaluronidase and collagenase lyse components of extracellular matrix and aid in increasing invasiveness. *S. aureus* secretes hyaluronidase to damage connective tissue, staphylokinase to break the fibrin clots, lipase to digest host lipids and nuclease to cleave DNA and RNA from the host cell. Hemolysins help in spread of infection by lysing erythrocytes and their neighboring cells. Thus, the bacteria can proliferate intracellularly

in tissues, disseminate through the body and, during this process, cause inflammatory reactions [171, 172].

Phagocytes such as polymorphonuclear (PMN) leukocytes, dendritic cells and macrophages are the first line of host immune system cells to recognize and kill the intracellular bacterial invader. Macrophages act on the bacterium by secreting proinflammatory cytokines, lowering the pH inside the vacuole containing the bacteria, producing degradative proteases, tumor necrosis factor (TNF- $\alpha$ ), and by producing reactive oxygen species (ROS) or reactive nitrogen species (RNS). Researchers have shown the production of nitrite from Raw 264.7 macrophages when activated with lipopolysaccharides, interferon gamma or lipoteichoic acids. Nitrite and nitrate production are known to be bactericidal and tumoricidal, thus aid in killing the pathogen [173, 174].

An intracellular bacterium survives inside the phagocytes by overcoming the phagocytic killing mechanisms. *S. aureus* can survive intracellularly for a few days or weeks. This persistence is aided by virulence factors like aureolysin, alpha toxin, and MSCRAMMs [175]. Intracellular *S.aureus* did not lead to apoptosis of macrophages nor did it hinder macrophage bactericidal activity like reactive oxygen species [176-178].

The *S. aureus* intracellular mode helps the actual survival of the pathogen inside the host environment protecting it from antibiotics and the host immune response. Bacteria can be internalized either by receptor mediated endocytosis (RME) or phagocytosis. *S. aureus* has been known to be internalized by both non-phagocytic cells like keratinocytes, epithelial, fibroblasts, endothelial cells, osteoblasts and also phagocytic cells like macrophages and neutrophils. In osteocytes, *S.aureus* is known to internalize by RME mediated by host actin filaments [179, 180]. *S.aureus* invasion into the host epithelial, endothelial and fibroblasts is aided mostly by

adhesin and fibronectin binding protein (Fnbp) attachment to the host  $\alpha_5\beta_1$  integrin of fibronectin. The role of FnBP in attachment to keratinocytes is not evident but it is involved in internalization and invasion of keratinocytes. *S.aureus* invasion into keratinocytes is slower and to a lesser extent when compared to the endothelial cells; this is due to the presence of low expression levels of  $\alpha_5\beta_1$  integrin in keratinocytes. Slower invasion may allow the bacteria efficient colonization before it invades further [33, 181]. Internalization of *S.aureus* into the host endothelium from the bloodstream plays an important role in the pathogenesis of endocarditis. FnbPs are also known to induce the actin remodeling and integrin mediated cell signaling in endothelium [182].

*S.aureus* can remain internalized in host cells ranging from 7 to 28 days as observed by different research groups. The intracellular bacteria exhibit varied phenotypic changes and are called small colony variants (SCV) because they are smaller than the normal wild type *S.aureus* on culture plates. SCV are the temporary phenotypic modification to evade host immune response or antibiotic treatment and can revert to normal morphology upon further subcultures. Such intracellular persistence can lead to chronic infections [177, 178, 183].

### **Host cell death by apoptosis or necrosis**

Internalized bacteria will be released into cytoplasm by killing the host cell either by necrosis or apoptosis. Necrosis is uncontrolled cell damage due to any type of mechanical stress such as temperature change or pathological stress of toxins, infections or trauma. Necrosis can lead to cell swelling or pores, and bursting the internal contents of the cell resulting in inflammation. Apoptosis, also known as programmed cell death, is a natural process to renew old cells due to the aging process triggered by various factors such as pathological conditions, agents like hormones, cancer treatment or any physiological stimuli.

The apoptotic mechanism does not involve cell lysis, swelling or pore formation but is characterized by membrane blebbing, caspase cascade activation and cell death without inflammation. Hence, apoptosis can be considered as beneficial clearing of unwanted damaged cells. Some stimuli may lead to both apoptosis and necrosis depending on the dose and time of exposure. Cells that die due to apoptosis can exhibit some of the features of necrosis and, hence, can be referred to as secondary necrosis or secondary apoptosis, and such cells cannot be clearly categorized as apoptotic or necrotic [184-186].

*S.aureus* toxins can damage the host cell either by apoptosis or necrosis, as observed in the case of alpha toxin and PVL. Alpha toxin can induce apoptosis, whereas PVL is known to induce necrosis or apoptosis based on the concentration and time of exposure. Genestier et al. observed the effect of rPVL on human neutrophils. rPVL at low concentration of 5 nM for 6 hrs induced apoptosis, whereas 200 nM for 1 hr led to necrosis [170, 187, 188].

Apoptosis occurs by either an intrinsic or extrinsic pathway. The intrinsic pathway, also called the mitochondrial pathway, is triggered by stimuli such as radiation, toxins or hypoxia. In this case, the mitochondrial changes and apoptosome formation will activate caspase 9 and caspase 3. In the extrinsic pathway, receptor-mediated cell lysis occurs by activating caspase 8. Such caspase cascade activation leads to degradation of chromosomal DNA, followed by protease activation. Then, nuclear degradation and cytoskeletal reorganization occurs, leading to morphological changes such as nuclear fragmentation, chromatin condensation and formation of apoptotic bodies. *S. aureus* is known to induce apoptosis in epithelial cells, endothelial cells, neutrophils and keratinocytes [170, 176, 187, 188].

Pyroptosis is another type of cell death with shared features of both necrosis and apoptosis. Pyroptosis is characterized by cell swelling, pore formation, cell lysis and



inflammation similar to necrosis, but pyroptosis is programmed cell death and involves caspase-1 mediated cell lysis. *S.aureus* USA300 has been shown to induce pyroptosis in HaCat keratinocytes [189, 190].

Morphological changes in apoptotic cells can be observed as cell shrinkage and chromatin condensation under light microscopy but necrotic cells appear swollen. Morphological changes do not clearly differentiate apoptotic and necrotic cells since energy depletion occurs in both cases. Necrotic damage occurs more by direct cell damage and can be observed as cytoplasmic vacuoles, loss of cell membrane integrity and release of cytoplasmic contents from disrupted cells. Electron microscopic observation helps to reveal morphological differences [191].

#### **Methods to analyze mammalian cell death**

Cytotoxicity assays, also called proliferation assays, are aimed at checking cell viability and percentage of cell death. Cell viability analysis can be performed using LDH, MTT or WST-1 assay based on detection of the mitochondrial dehydrogenase enzymes released from the live cells. MTT and WST-1 assays are tetrazolium-based, which are cleaved by mitochondrial dehydrogenases that are released from live cells to form the purple colored formazan dye in a positive test. More cell proliferation leads to more color development due to increased mitochondrial dehydrogenases [192].

Apoptotic cells are marked by caspase activation and DNA laddering. Internal cellular lipid molecules like phosphatidyl serine, annexins, and calreticulin are exposed to the external surface. Various antibody kits are available to detect the particular caspases. DNA fragmentation or damage can be detected by assays such as the TUNEL assay and comet assay. DNA damage can also be detected by apoptosis response proteins like phosphorylation and activation of p53

kinase, check point kinase 2, or histone H2AX. The DNA laddering analysis is performed by preparing the whole genomic DNA and running it on an agarose gel. TUNEL assay (terminal deoxynucleotidyl transferase-mediated dUTP biotin nick end-labeling of the DNA fragments) detects damaged DNA under fluorescent microscope by treating the apoptotic samples with dUTP-FITC conjugates which bind to the damaged 3'OH ends of DNA. The comet assay is most commonly used to analyze apoptosis from individual cells. The DNA from individual cells are subjected to electrophoresis to observe comet-like spreading [191-193].

Cellular molecules like phosphatidyl serine exposed in apoptotic cells can also be detected by using a binding protein like Annexin V conjugated with a fluorescent tag (FITC). Further, Annexin V conjugates are used along with other live/dead dyes like 7-amino-actinomycin (7-AAD) or propidium iodide (PI). Dead or damaged cells are permeable to the PI stain. Early apoptotic cells will be positive to Annexin V but not PI/7-AAD, whereas late apoptotic or dead cells will be positive for both Annexin V and 7-AAD/PI. Annexin V assay kits are commercially available to test various methods like ELISA, fluorescence microscopy and flow cytometry [194, 195].

### **Cell signaling pathways in cell death**

Eukaryotic cell receptors are activated in response to the external stimuli to bring some physiological response. Such stimulus signals are amplified through the cascade of signal messenger molecules to bring internal changes in the cells, and later, communicated to external physiological changes; these systems are called signal transduction systems. The most important extracellular receptors are integrins, receptor tyrosine kinases (RTK) and G protein-coupled-receptors.

Kinases are phosphotransferases that transfer phosphate groups from ATP to substrates like serine, tyrosine or threonine. Phosphorylation of proteins can activate signaling pathways involved in growth, differentiation, inflammation and apoptosis [196]. Integrins cannot mediate signaling pathways by themselves since they lack kinase activity, but integrin mediated kinases coordinate with other RTK pathways. RTK transmembrane proteins have extracellular ligand binding domains and intracellular kinase domains. Signal transduction occurs by dimerization of the RTKs in plasma membrane leading to autophosphorylation and conformational changes. Autophosphorylation activates the kinase domain and signaling is further transduced through a series of other effector molecules in the cytoplasm, activating different cellular metabolism. Important pathways are the cAMP pathway, MAPK/erk pathway and diacylglycerol pathway. Defective pathways lead to disorders like diabetes, tumors, schizophrenia, and heart disease.

### **MAPK pathway**

The MAPK pathway consists of serine/threonine kinases such as p38, extracellular signal regulated kinases (Erk1/2) and cJNK pathways. p38 kinase pathway is activated by a variety of cellular stresses such as osmotic shock, UV light and lipopolysaccharide, proinflammatory cytokines, and growth factors and can be expressed prior to caspase activation [197]. Apoptosis induced by various factors like environmental stress, shock or bacteria can be activated via p38 kinase. *S. aureus* induced apoptosis in neutrophils is shown to be involved with p38 kinase activation. Blocking p38 kinase using a chemical called SB203580 in these studies hindered apoptosis [198]. *S.aureus* induced apoptosis in human monocytic U937 cell lines were also shown to be involved with P38 kinase activation in a time dependent manner. P38 kinase activation peaked at 30 min, whereas Erk and JNK kinase activation peaked at 90 min in U937 cell apoptosis [199].

Erk-MAP kinase is phosphorylated or activated during cell differentiation and proliferation. However, some virulence factors from *S. aureus* supernatants and hemolysins have been shown to activate the erk pathway in airway epithelial cells [200]. Some studies have shown that erk1/2 kinases were activated during *S. aureus* invasion into osteoblast cells, whereas the p38 pathway was not activated in the same studies [201]. Hence, p38 and erk kinase seem to be activated inversely in response to *S. aureus* infection in most of the studies reported thus far [200, 202].

## Methods

### Over-expression and purification of rSAS1738 protein in *E. coli*

The following materials were used for this experiment. *E. coli* BL21-AI + *sas1738* clone, terrific broth, ampicillin (100mg/ml), 1M Isopropyl  $\beta$ -D-1-thiogalactopyranoside(IPTG), 20% arabinose, Novagen His-bind protein purification kit (TB054) Rev E0405, TB234, and Novagen chromatography column (catalog no.69673).

Recombinant SAS1738 (rSAS1738) was purified using the His-bind purification kit. The procedure was followed as per the manufacturer's instructions for the inclusion body purification method. Overnight culture of *E. coli* expression clone (BL21-AI+*sas1738*) was prepared in Luria Bertani (LB) broth with ampicillin (100 $\mu$ g/ml). Terrific broth (1 L), supplemented with ampicillin (100 $\mu$ g/ml), was inoculated with 5% overnight culture of the expression clone. The culture was incubated for 5 hours at 37°C to reach OD<sub>600</sub> of 0.8. The protein was induced at 30°C with 1mM IPTG and 0.2% arabinose overnight in a shaker incubator. After 12 to 14 hours of induction, the culture was centrifuged to pellet the cells, and the supernatant discarded. The pellet was resuspended in 1x column binding buffer. The induced cells of the clone were pelleted, resuspended in binding buffer and subjected to sonication for 6 min; this procedure was repeated three times with 5 min intervals in an ice bath. Solubilization of the pellet containing inclusion bodies was performed in 6M urea dissolved binding buffer. Complete solubilization was aided by incubation on ice for 1 hour. Cells were centrifuged to separate insoluble material from the supernatant. The supernatant, containing inclusion bodies, was separated from the pellet

and filtered using a 0.45micron filter before passing through the His-bind column. The filtered supernatant was passed through the column to allow the protein to bind to the nickel-charged column. The column was then washed with binding buffer and wash buffer, and the protein was eluted in 1 ml fractions using the elute buffer. After elution, all buffers contain 6M urea to retain the denatured condition. SDS PAGE was performed to visualize the purified protein.

### **Dialysis**

The eluted protein samples were subjected to dialysis (as per Novagen protocol TB234, with slight modifications). Dialysis was performed in Tris-NaCl buffer with reducing concentrations of urea to remove salts and imidazole and to refold the protein. Protein refolding was aided by dialysis in sequential treatment of Tris-NaCl buffer containing 4M urea and Tris-NaCl buffer with 2M urea. Each treatment was performed for at least 3 to 4 hrs. The last round of dialysis was in Tris-NaCl buffer without urea for 4 hrs and then again, overnight with change of buffer. Dialysis was carried out in the cold with a slow stirrer to preserve any protein stability problems. Purified protein samples were analyzed by SDS PAGE, and protein specificity confirmed by western blot using the His-tag antibodies (Invitrogen).

### **Reverse transcriptase PCR amplication of SAS1738 from MSSA476 cDNA.**

RNA from MSSA476 was extracted using the Ambresco RNA extraction kit and following the manufacturer's protocol with slight modifications to treat the bacterial culture with phenol:ethanol (5%:95%) [152] and continued with RNA extraction protocol as outlined by Ambresco. This experiment was also explained in Chapter 2 of this document. cDNA was extracted using the iScript cDNAsynthesis kit (Bio-Rad) and used as a template to check SAS1738 mRNA amplication by reverse transcriptase PCR.

**WST-1 cell proliferation or cytotoxicity assay**

The cell lines used were as follows: HEK293, human embryonic kidney cell lines; monocytes; CHO1, Chinese hamster (epithelial-like) cells; SVEC, simian virus 40-transformed mouse endothelial cell line; NIH3T3, mouse embryo fibroblast cell line; HMEC, human microvascular endothelial cell line; and HaCat, human keratinocytes. All cell lines were cultured in DMEM complete media supplemented with penicillin-streptomycin and 10% fetal bovine serum (FBS). Reagents and equipment used were as follows: 0.05% trypsin-EDTA, DMEM complete media, FBS, penicillin-streptomycin mix (Sigma), WST-1 reagent from Clontech (catalog #630118), hemocytometer, 96-well microtitre plates, and an ELISA plate reader.

A cytotoxicity assay using WST-1 reagent was used to detect the cytotoxic effect of the rSAS1738 on cell lines. WST-1 is a formazan-based water soluble tetrazolium salt. WST1 detects the mitochondrial dehydrogenases released in live cells and therefore reduction in this enzyme can detect the extent of cell death or proliferation. WST1 is comparable to a mono-tetrazolium (MTT) dye reduction assay but is known to be a more rapid and efficient method to check cell viability [203].

WST-1 assay protocol was performed as per the manufacturer's instructions (Clontech). Mammalian cell lines were grown in DMEM complete media in a humidified atmosphere at 37°C with 5% CO<sub>2</sub>. Semi-confluent cells were detached by trypsinization and counted using a hemocytometer via the trypan blue exclusion assay. Trypan blue stains only live cells. The cell concentration was adjusted to  $2 \times 10^4$ /ml. Cells (100 µl) were seeded per well into flat bottom 96-well plates. Varying concentrations of rSAS1738 purified protein were added to the well. Cells with Tris-NaCl buffer were maintained as positive control. BSA protein was added to the cells to check the effect of non-specific protein activity. Total volume was increased to 200 µl in each

well using Tris-NaCl buffer. All samples (cell control, cells with BSA control, and cells with rSAS1738 purified test protein) were incubated in a humidified atmosphere at 37°C with 5% CO<sub>2</sub> for 24 hrs. WST-1 cell proliferation reagent (10 µl) was added to the samples in the microtitre plate and incubated for 4 hrs in the humidified incubator. The developed color was proportional to cell viability. The absorbance was read in an ELISA plate reader at OD<sub>450</sub> and the values were plotted graphically to compare the cell viability in each sample. All samples were maintained in triplicate. Experiments have been repeated with different lots of purified rSAS1738 protein.

### **Detection of kinase activation by immunoblotting**

The HEK293 cell line was grown in DMEM complete media supplemented with penicillin-streptomycin mixture and 10% FBS. Other materials that were used include 0.05% trypsin-EDTA, a hemocytometer, SDS gel reagents and apparatus and western blot reagents. The primary antibodies used were p44/42 erk rabbit Mab or p38 rabbit ab. The secondary antibody used was anti-rabbit IgG-HRP conjugate plus whole ab (donkey). Antibodies were purchased from Cell Signal. Six-well plates (tissue culture treated) were purchased from CytoOne.

Activation of p38 and erk kinase in HEK293 in response to rSAS1738 was studied following the standard immunoblotting protocol with slight modifications [198, 199]. HEK293 cells were adjusted to 10<sup>5</sup> cells/2 ml/well inoculated into the 6-well tissue culture plate and incubated overnight in a humidified incubator (final cell concentration was approximately 5x10<sup>4</sup>/ml). The following day, the spent media was aspirated and discarded; the cells were washed with 2 ml PBS/well and 2 ml serum free media was added to each well to turn off any kinases since growth factors in serum can activate kinases. Cells were incubated overnight in serum free media. The next day, rSAS1738 (400 µl) (final concentration 0.4 µM) was added to



each well for 60 min, 45 min, 30 min, 15 min and 0 min (one time point/well). At the end of the time period, the media was aspirated and the well washed with PBS, followed by the addition of 120  $\mu$ l of SDS PAGE lysis buffer to lyse the cells. Cells were collected into labeled vials, boiled for 5 min, and electrophoresed on SDS 12% PAGE to separate protein bands. The separated proteins were then transferred to a nitrocellulose membrane using the standard western blot procedure.

The nitrocellulose membrane was developed by first blocking with 5% casein for 1 hr and treating with primary antibodies specific to p38 or Erk (anti p38/anti-erk) overnight at 4°C. The blot was washed with TBS-T, treated with secondary antibody in 0.5% casein milk for 1 hr and thrice washed with TBS-T and TBS for 15 min. The development was continued using the electro-chemiluminescent detection method. Kinase activation was indicated by the appropriate sized band appearing on x-ray film. The same nitrocellulose membrane was reused again for different kinase detection by stripping in a buffer containing  $\beta$ -mercaptoethanol and treating at 50°C for 30 min. The blot was washed thoroughly and reused for detection of other MAP kinases by repeating the above steps. The blot was stripped and probed for actin or unphosphorylated erk/p38 antibodies as the control.

### **Cell death observation by propidium iodide staining**

The following materials and chemicals used in these experiments were HEK293 cell lines, rSAS1738 test protein, propidium iodide (PI) stain (Genscript), Vecta shield H-1200 mounting media, fluorescent microscope, Guava Viacount reagent (EMD Millipore) and Guava Nexin assay kit (EMD Millipore).

Propidium iodide (PI) stain binds to nucleic acids by penetrating cell membranes of dead or dying cells and fluorescence (pink) at excitation spectrum of 535 nm. The Genscript protocol

was followed for staining cell lines with the following modifications. HEK293 cells ( $10^5/\text{ml}$ ) were seeded in 12-well plates on cover slips. rSAS1738 protein ( $0.5 \mu\text{M}$ ) was added to the well overnight and incubated in a humidified incubator to observe cell morphological changes or cell death by microscopy. The following day, the spent media was aspirated and the cells washed with 1 ml PBS buffer. Fixation was performed by treating the cells with 3.7% formaldehyde for 1 hr and washed with PBS buffer. Cells were stained by adding 1X binding buffer diluted in water with  $4 \mu\text{l}$  of PI. Samples were kept away from light for 10 min while staining and washed with PBS before fixing the cover slips for microscopy. The cover slips were inverted gently using a needle, making sure not to form air bubbles, onto a drop of Vecta shield H-1200 to mount on microscope slides. Microscopic observation was performed using red excitation (535 nm) filters.

### **Phase contrast microscopy**

The  $0.5 \mu\text{M}$  rSAS1738-treated HEK293 cells were observed using phase contrast microscopy at 400X magnification without staining to observe for morphological changes.

### **Guava ViaCount assay by flow cytometry**

We performed the Guava ViaCount assay using the kit protocol provided by Guava Technologies. Guava ViaCount Flex reagent is primarily used to assess cell health and viable cell count.

ViaCount assay is based on two dyes: a nuclear dye stains all nucleic acids in live, dead or apoptotic cell types, whereas the viability dye stains only the dying or dead cells. Cells are categorized as apoptotic, if they are moderately stained by the viability stain. Hence, live or apoptotic cell differentiation is based on efficiency of uptake of the viability stain and may not give clear-cut differentiation. However, ViaCount was a good assay for preliminary analysis of

cell health due to rSAS1738 treatment. Later, the Nexin kit was used to analyze the apoptotic index as a confirmatory test for apoptosis.

The ViaCount assay was set up with HEK293 cell lines ( $10^5$  cells/well) in a 6-well tissue culture plate and treated with rSAS1738 test protein. After overnight incubation in a humidified incubator at  $37^{\circ}\text{C}$ , the cell lines were detached with non-enzymatic EZ strip reagent. The cell count was adjusted to 50 cells/ $\mu\text{l}$  and the ViaCount sample preparation performed as per manufacturer's instructions by mixing 50  $\mu\text{l}$  of the sample cells with 450  $\mu\text{l}$  of ViaCount reagent. After staining for 5 minutes, the samples were acquired on Guava 2.2.2 system using Guava ViaCount software.

#### **Guava Nexin Annexin V binding assay by flow cytometry**

Guava Nexin assay kit consists of reagents with two dyes, Annexin V and 7AAD. The 7AAD binds to dead cells; Annexin V binds to apoptotic cells. Live cells stain negative for both AnnexinV and 7AAD. The materials used in this assay were as follows: stuarosporine (1 mM), HEK293 cells, purified rSAS1738, 6-well tissue culture plates, DMEM complete medium, EZ strip reagent (Zenbio), and the Guava Nexin kit (EMD Millipore).

The assay was followed based on the protocol from Guava Nexin kit (EMD Millipore). The assay was started by seeding HEK293 ( $2 \times 10^6/\text{ml}$ ) cells into 6-well plates and allowing them to attach for 4 to 6 hours. Purified rSAS1738 was added to each well, working in triplicate, and incubated overnight in a humidified incubator at  $37^{\circ}\text{C}$ . Untreated cells were maintained as positive controls. Cells treated with stuarosporine ( $1\mu\text{M}$ ) for 2 hrs were used as a negative control. After treatment, cells were washed twice with PBS and detached by adding 1 ml of EZ strip/well for 10 min. Cells were collected into vials for sample preparation to perform the Nexin assay. Cells were pelleted by centrifugation at 2000 rpm for 5 min with PBS and the cell

concentration was adjusted  $10^5$  cells/ml. Cells (100  $\mu$ l) were mixed with 100  $\mu$ l of Nexin reagent and incubated for 20 min in the dark. Samples were acquired on Guava 2.2.2 system using the Nexin software.

### **Invasion assay**

The invasion assay was performed using the following bacteria, cell lines and chemicals: *S. aureus* MSSA476, *S. aureus* MRSA252, *S. epidermidis*(lab strain), human dermal microvascular endothelial cells (HMEC) cell lines, DMEM complete media with 10% fetal bovine serum (FBS) plus antibiotics (penicillin and streptomycin), trypsin/EDTA (Invitrogen), gentamycin, 24-well tissue culture plates (Cell one), Thermanox coverslips, and lysis buffer containing 0.05% trypsin/EDTA plus 0.5% triton X-100.

The invasion assay was performed as per Massey R.C. et al. with modifications [204]. HMEC cells ( $10^4$ /ml per well) were seeded into 24-well tissue culture plates with cover slips. Cells were incubated for 48 hrs in a humidified incubator and spent media was replaced with fresh DMEM complete media. HMEC cells were treated with 0.4  $\mu$ M rSAS1738 for 1 hr. Untreated cells were kept as a control. Bacterial attachment and internalization studies were performed by adding fresh log phase bacterial cells ( $10^7$  cfu) to each well and incubating for 90 mins in a humidified incubator. Cover slips containing the bacteria were dip-washed thrice in PBS. Cell lysis was performed using buffer containing trypsin/EDTA plus 0.5% triton X 100 for 30 mins at 37°C and agitated pipetting to release the internalized bacteria. The detached and lysed cells were pelleted and serial diluted. The dilutions were plated on mannitol salt agar plates to count the attached and internalized bacterial cells.

For the bacterial invasion assay, the above protocol was followed except that we removed the attached and unattached bacterial cells to check for internalized bacteria. Bacteria ( $10^7$  cfu)

were added to the HMEC cells and incubated for 90 mins to internalize. Spent media was removed from each well, and the cells washed with PBS thrice to remove any unattached bacteria. Fresh DMEM complete media (1 ml) supplemented with gentamycin (100 µg/ml) was added to each well and incubated in humidified incubator for 1 hr to kill any attached bacteria that were not internalized into the endothelial cells. Gentamycin media was removed after 1 hr and washed with PBS thrice to remove any gentamycin on the HMEC cells. This step is crucial since gentamycin can kill the internalized bacteria after cell lysis. Cells were then lysed with trypsin/EDTA plus 0.5% Triton X-100 to release internalized bacteria. The sample was centrifuged and the pellet washed with PBS before serial dilution. The serially diluted sample was plated on mannitol salt agar to enumerate the internalized bacteria.

#### **Nitrite production by activated macrophages was analyzed by Griess assay**

Materials used to determine nitrite production were: mouse macrophage cell line (Raw 264.7), Griess reagent (Invitrogen, catalog # G-7921), 24-well tissue culture plate, DMEM complete media plus antibiotics and 10% FBS, DMEM serum free media, 0.05% trypsin/EDTA, lipopolysaccharide (LPS), interferon gamma (IFN), and bovine serum albumin (BSA).

Nitrite production by activated macrophages was analyzed by Griess assay as per Invitrogen [205]. Raw macrophages ( $10^6$ /ml/well) were seeded into 24-well tissue culture plates and allowed to attach overnight in a humidified incubator with 5% CO<sub>2</sub> at 37°C. Later, cells were treated with LPS (10 µg) or LPS (10 µg) + IFN (5 units) to activate the macrophages. Activated macrophages were treated with test protein, rSAS1738 (400 nM), or 10 µg BSA as a negative control. After incubation time points, spent media was collected and mixed with equal volumes of Griess reagent as per the manufacturer's instructions. The absorbance was read at OD<sub>550</sub> nm and plotted graphically to analyze the nitrite level compared to a sodium nitrite standard curve.

The same was repeated at various time intervals from 8 to 28 hrs. The standard curve was prepared using 0.1 M sodium nitrite solution.

## Results

### Protein over-expression and purification

SAS1738 protein was cloned in the *E.coli* expression vector pET<sup>TM</sup>-DEST42 (Invitrogen). pDEST42 has a polylinker region sequence attached to the C terminal region of the cloning site. Hence, the cloned gene would express along with the polylinker region that includes C-terminal 6X-histidine affinity tag and C-terminal V5 epitope (Fig19). The molecular weight of polylinker region is 4.16 kDa. Therefore, SAS1738 (~21 kDa) plus the polylinker (4.16 kDa) region equals ~25 kDa when expressed in pDEST42 vector (Fig 19).

When SAS1738 inductions were performed in Luria Bertani broth at 37°C by a previous researcher in our laboratory, it resulted in two bands at ~21 and 25 kDa on SDS PAGE (Fig 20a). To optimize the protein expression conditions, protein induction was performed in terrific broth at a lower temperature to prevent proteolysis during the protein purification. Protein purification was performed following the modified induction condition and a single protein band was observed at ~25 kDa on SDS-PAGE (Fig 20b). Western blot analysis using His-tag antibodies confirmed the band to be rSAS1738 (Fig 21). The column purified protein elutants were analysed by SDS PAGE and the purified elutant fractions were pooled for dialysis. The dialyzed protein was again checked by SDS-PAGE and Western blot specificity to ensure no loss of specific protein. This protein was used for all the lethality assays. The concentration of purified rSAS1738 protein was determined by the Bradford assay. The concentration of protein was

found to be ~100 µg/ml. The protein yield for most purifications was in the range of ~350 µg/L indicating rSAS1738 expression in gateway system was low.

### **WST-1 proliferation assay**

Cell death checked by the WST-1 assay was indicated by reduction in color compared to the cell control as read by the ELISA reader at OD<sub>450</sub> nm. The OD<sub>450</sub> was further converted to percentage of cell viability, and results were plotted graphically with customized error bars. All assays were performed with triplicate samples and repeated at least three times for reproducibility. The data and graphs mentioned here are representative of several trials.

WST-1 assay of rSAS1738 on the HEK293 cell line showed the reduced OD<sub>450</sub> indicating reduced viability at different concentrations of rSAS1738 protein (Table 8). rSAS1738 (0.45 µM) reduced the percentage to 80%, 0.9 µM reduced the cell viability to 68% and 1.8 µM reduced the cell viability to 43% (Fig 22). This demonstrated the lethal effect rSAS1738 on HEK293 human cell lines reducing the OD<sub>450</sub> from 1 to 0.4. HEK293 cells treated with BSA did not show any significant cell death. This indicated the null effect of other protein (20 µg/ml) on HEK293 cells (Fig 22).

OD<sub>450</sub> values of WST-1 assay of different concentrations of rSAS1738 on HMEC cells and HaCat cells is represented in Table 9 and Table 11, respectively. The OD<sub>450</sub> values plotted graphically indicated 0.45 µM rSAS1738 reduced the viability of HMEC endothelial cell line to 92% (Fig 23) and HaCat keratinocytes cell viability was reduced to 86% (Fig 25). 0.9 µM rSAS1738 reduced the viability of HMEC cell line to 79% and HaCat cell viability to 72%. 1.8 µM rSAS1738 reduced the viability of HMEC cell line to 57% and HaCat cell viability to 65% (Table 8-10) (Fig 22, 25, 26).



Overall lethality of purified rSAS1738 indicates that 0.9  $\mu\text{M}$  reduced the cell viability of HEK293 cells to 68%; hence, concentration ranges from 0.2  $\mu\text{M}$  to 0.8  $\mu\text{M}$  rSAS1738 are used for all other assays on HEK293 cells (Fig 22). This concentration of rSAS1738 would not kill >50% of the cells during any of the other assays and aids us to observe effects on the cells. Similarly, the effective lethal concentration of rSAS1738 on the HaCat cell line would be higher than 1.8  $\mu\text{M}$  since 1.8  $\mu\text{M}$  killed only ~30% of HaCat (Fig 26).

The highest concentration of rSAS1738 (1.8  $\mu\text{M}$ ) reduced the SVEC endothelial cells to 90% (Table 10). rSAS1738 showed negligible reduction of SVEC endothelial cells (Fig 24). Similarly, viability of other non-human cell lines, NIH3T3 mouse embryonic fibroblasts, and Raw 264.7 mouse macrophages were not reduced by rSAS1738 protein (Data not shown)

WST-1 assay, performed with all cell lines, was performed at least three times, and in triplicate at each trial. WST-1 on HEK293 was performed after every batch of protein purification to ensure the functionality of every batch of protein purification. Present data analysis is the representative average results of the triplicates in one experiment.

### **MAPK kinase p38 and erk activation assay**

Kinase activation was detected by immunoblotting using phosphokinase specific antibodies. Erk kinase, a serine threonine kinase, was detected as two protein bands, 42 and 44 kDa, upon activation (Fig 27b). Erk kinase was not activated in HEK293 cells when treated with rSAS1738 for 60 min (Fig 27a). However, p38 kinase, a 38 kDa protein, was activated in HEK293 cells at 60 min rSAS1738 treatment but was not activated in 15, 30 or 45 min treatments (Fig 27c). The 38 kDa band appeared at 60 min when immunoblotted with phospho-p38-antibody. Total Erk (phosphorylated and dephosphorylated) was detected on the same blot to ensure uniformity of sample loading control (Fig 27b).

**Propidium Iodide (PI) staining**

PI enters only the dead cells and binds to nucleic acids. PI is observed as red fluorescence at 535 nm using fluorescent microscopy. The dead cells can be further grouped as apoptotic if the intensity of fluorescence is lower than the dead cells. The test samples, HEK293 cells treated with 0.4  $\mu\text{M}$  rSAS1738, showed fluorescence with PI staining indicating cell death (Fig 28e, 28f). Microscopic observation under white light showed that HEK293 cells with 0.4  $\mu\text{M}$  rSAS1738 were not intact; some cells appeared rounded up or distorted under white light (Fig 28c, 28d). The negative control, HEK293 cells treated with 1  $\mu\text{M}$  staurosporine for 2 hrs, showed fluorescence, and the cell morphology was distorted (Fig 28b). The negative control cells appeared as healthy, intact cells (Fig 28a).

**Phase contrast light microscopy**

Microscopic observation of HEK293 and HaCat keratinocytes cells treated overnight with 0.5  $\mu\text{M}$  rSAS1738 showed distorted cell morphology, cell rounding and cell detachment, indicating cell death (Fig 29e- f). HaCat cells did not proliferate to form the typical cobblestone appearance (Fig 30c-d), whereas control cells had formed typical cobblestone appearance (Fig 29a-d, 30a-b) under the incubation conditions and, gradually, confluent growth was observed.

**Guava Viacount assay using flow cytometry**

Easy fit analysis auto-adjusts the gating to determine the live and dead cells with the Guava Viacount software that was used; including the apoptotic gating will manually demarcate live and dead cells. Moderately stained cells are indicated as apoptotic cells in the analysis. The forward scatter plot (FSC) gate can be adjusted to separate the cell debris from the different cell populations. The assay adjustment is performed with positive and negative cell controls to apply apoptotic gates and adjust scatter plot.

A representative trial is explained in the images of the positive control (Fig 31), negative control (Fig 32), and HEK293 cells treated with rSAS1738 (Fig 33) which show both easy fit and apoptotic analysis plots.

The positive control HEK293 cells shown in Fig 31a and Fig 31b were analyzed using the “easy fit” feature, which differentiates only live and dead cells. Red clusters are live cells whereas black indicates dead cells. The Viacount viability marker in Table 12 is used for Viacount live/dead analysis. The same samples were analysed applying the apoptotic gate in the Guava Viacount software as in Fig 32c and Fig 32d. The same apoptotic gate markers are used for all samples to analyze apoptotic cells (Table 13). The apoptotic gate is marked based on comparing the positive and negative cell controls so we can group the live and dead cell populations. The cells with lower intensity of staining would indicate apoptotic cells, and they are seen in between live and dead cell fractions. The same analysis is applied for negative control (Fig 32) and test samples (Fig 33) to analyze the cell death and apoptosis in HEK293 treated with rSAS1738. The percentage of cells from the triplicate samples were averaged, and the standard deviation was used to customize the error bars (Table13).

The graphical analysis of scatter plots and apoptotic gating data indicates HEK293 positive control cells had 87% live cells, 4% apoptosis and 8.7% cell death (Fig 34). Negative control HEK293 cells treated with staurosporine (1  $\mu\text{M}$ /2hr) showed 46.5% of live cells, 11.7% dead cells and 42% of apoptotic cells (Fig 35). Test samples of HEK293 cells treated with 0.2  $\mu\text{M}$  to 0.6  $\mu\text{M}$  rSAS1738 showed cell death increased from 4% to 12%. Apoptotic cells ranged from 8.9% to 38% in 0.2  $\mu\text{M}$  to 0.6  $\mu\text{M}$  rSAS1738, respectively (Fig 34,35).

### **Guava nexin annexin V binding assay by flow cytometry**

Nexin gating coordinates are adjusted using the positive and negative cell controls (Table 15 and 16). Many trials were performed to standardize the Guava Nexin assay. Once standardized, the Guava Nexin assay was performed with the rSAS1738, keeping positive and negative controls for the gating adjustment. The two best representative scatter plots are included in this report for understanding the gating. However, all percentages presented here are the cumulative data of triplicate trials performing duplicate samples (Table 17).

The positive control had a major live population of cells clustered in the bottom left of the plot (Fig 36a, 37a). This clustering in bottom left is due to the lesser staining with both Annexin V and 7-AAD. The late apoptotic or dead cells appeared in top right side of the plot due to higher staining with 7-AAD but not with Annexin V (Fig 36b, 37b). The early apoptotic cells were observed at the bottom right side of the plot being stained by Annexin V (Fig 36b, 37b).

The percentages of live, dead and apoptotic cells are automatically analyzed along with scatter plots once the samples are acquired in Guava Nexin assay on Guava 2.2.2 software. The control HEK293 cells had 26.5% live cell, 7% dead cells and 1% apoptotic cells. Analysis of the test samples showed that HEK293 cell death was 18% and early apoptotic cells were 5% when treated with 0.2  $\mu\text{M}$  rSAS1738. Cell death was 23% in presence of 0.4  $\mu\text{M}$  rSAS1738, which is higher compared to cell death of 17% in 0.6  $\mu\text{M}$  rSAS1738. However, there was an increase in early apoptosis from 14% to 35% in the presence of 0.4  $\mu\text{M}$  and 0.6  $\mu\text{M}$  rSAS1738, respectively (Table 17, Fig 39).

### **Invasion assay**

Attachment and invasion assay of *S.aureus* into HMEC cells indicated that  $2 \times 10^6$  cfu/ml of MRSA252 attached and  $10^4$  cfu/ml internalized. When the experiment was repeated using lab

strains of *S. aureus* and *S. epidermidis*,  $10^5$  cfu/ml attached in both strains; internalization into *S. aureus* was  $10^4$  cfu/ml, while *S. epidermidis* did not internalize. Treatment with rSAS1738 did not improve internalization with *S. aureus* or *S. epidermidis*. In several trials, internalization of bacteria was, in fact, 1-log less for attached and internalized bacteria in the case of *S. aureus*. HMEC cells treated with purified rSAS1738 did not change the rate of internalization of bacteria compared to control cells (Table 18). Even at the lower concentrations (0.1  $\mu$ M or 0.2  $\mu$ M) of rSAS1738 treatment, HMEC cell morphology looked unhealthy during the experiment. This experiment has been repeated thrice with duplicate samples.

### **Griess assay**

Raw cells, naive and activated, controls and treated with rSAS1738, were checked for nitrite production by Griess assay. The OD<sub>450</sub> read in an ELISA reader was recorded (Table 19) and further compared with the standard curve of sodium nitrite (Table 20). Raw cells treated with rSAS1738 generated  $<0.75$   $\mu$ M nitrite at all time points tested: 8, 20, 25 and 30 hrs. The Raw cell controls consisted of cells activated with LPS and/or IFN. Raw cells activated with both LPS (10  $\mu$ g/ml) and IFN (5 units) generated 12.5  $\mu$ M nitrite by the 30 hr time point. Similar results were seen with activated macrophages treated with 0.2  $\mu$ M rSAS1738. Raw cells activated only with LPS generated  $\sim 5$   $\mu$ M nitrite by the 30 hr time point. But naive macrophages treated with 0.2  $\mu$ M rSAS1738 generated  $<0.75$   $\mu$ M nitrite at all time points from 8 to 30 hrs (Table 20).

## Reverse transcriptase PCR amplification of SAS1738 from cDNA of MSSA476

Reverse transcriptase PCR of SAS1738 showed the amplification of SAS1738 mRNA from stationary phase MSSA476 cells. The negative control with no DNA template and RNA as template did not show any mRNA amplification. This indicates that the template RNA used for cDNA preparation did not have any DNA contamination. Hence, mRNA amplified from cDNA indicated that SAS1738 transcription from the stationary culture of MSSA476 (Fig 40).

---

```
>sas:SAS1738 hypothetical protein
MNTKFLGKTLVASALVLTTLGTGLHSSYLGLDTNKVVKTAKAEKMTDGLWKKVRDSLHSDIILSNEY
ETINVTYLLSNGYSSVSAPGNDGGHLTQSIDFKGLKQIDLTKENVYDDFNKKLDAKNTWNSLTEKLGKL
GLLQNGQKVSIIYSSDSSSPVSGKVGEGVTSGGENTLTKRFINKITID
```

---

(18a)

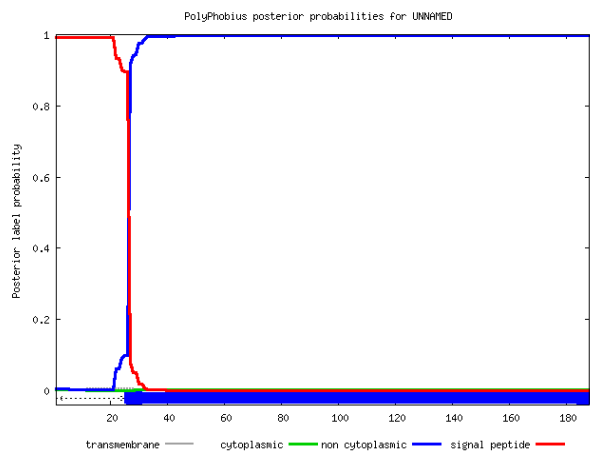


Figure 18: SAS1738 sequence data. (18a) Amino acid sequence of SAS1738; (18b) Signal peptide prediction of SAS1738 by Polyphobius.

Table 8: Signal peptide prediction of SAS1738 using Polyphobius

---

ID	UNNAMED			
FT	SIGNAL	1	26	
FT	REGION	1	9	N-REGION.
FT	REGION	10	21	H-REGION.
FT	REGION	22	26	C-REGION.
FT	TOPO_DOM	27	188	NON CYTOPLASMIC

---

---

SAS1738 protein sequence plus Polylinker in pDEST42 vector

---

MNTKFLGKTLVASALVLTTLGTGLHSSYLGLDTNKVVKTAKAEKMTDQQLWKKVRDSLHSDIILSNEY  
ETINVTYLLSNGYSSVSAPGNDDGGHLTQSIDFKGLKQIDLTKENVYDDFNKKLDAKNTWNSLTEKLGKGL  
GLLQNGQKVSIIYSSDSSSPVSGKVGEGVTSGGENTLTKRFINKITIDPAFLYKVVINSKLEGKPIPPLLGLDS  
TRTGHHHHHH

---

Red highlight indicates C-terminal V5 epitope and 6XHis-tag.

Figure 19: Sequence data of SAS1738 plus His-tag and epitope after expression from Gateway pDEST42 vector.

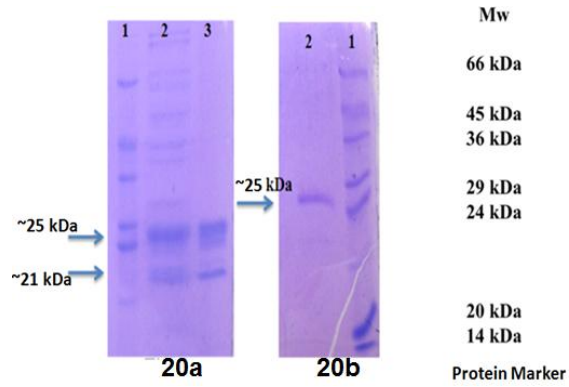


Figure 20: SDS analysis of His-tag column purified rSAS1738 expressed in *E.coli*.

(20a) Protein induced at 37°C. Bands at 25 kDa and 21 kDa; (20b) Protein induced at 30°C band at ~25 kDa.

Lane 1            Protein molecular weight marker (14 kDa - 66 kDa)  
 Lane 2, 3        rSAS1738 column purified protein



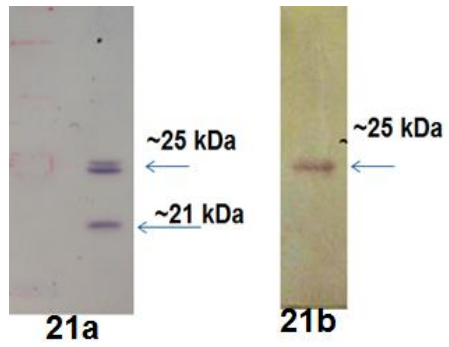


Figure 21: Western blot of rSAS1738 purified protein.

(21a) Induced at 37°C. Bands detected at 25 and 21 kDa; (21b) Induced at 30°C. Band detected at 25 kDa.

Table 9: Cytotoxicity of rSAS1738 on HEK293 cells by WST-1 assay (OD<sub>450</sub> values).

<b>WST-1 assay</b>	<b>HEK293 cells</b>	<b>0.45 <math>\mu</math>M rSAS1738</b>	<b>0.9 <math>\mu</math>M rSAS1738</b>	<b>1.8 <math>\mu</math>M rSAS1738</b>	<b>HEK293 + BSA</b>
<b>Well 1</b>	0.92	0.78	0.62	0.43	0.9
<b>Well 2</b>	0.93	0.72	0.63	0.5	0.91
<b>Well 3</b>	0.96	0.75	0.67	0.4	0.95
<b>Avg OD<sub>450</sub></b>	0.93	0.75	0.64	0.44	0.92
<b>STDEV</b>	0.02	0.03	0.03	0.05	0.03
<b>Percentage</b>	100	80.64	68.8	47.7	99

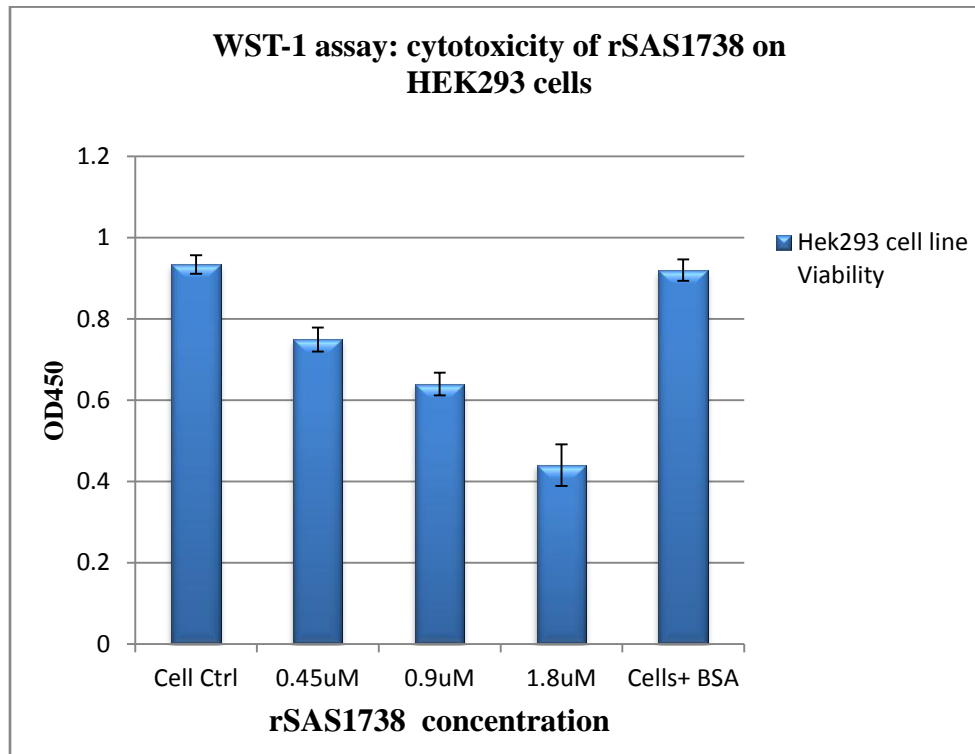


Figure 22: Bar graph of cytotoxicity of rSAS1738 on HEK293 cells by WST-1 assay (OD<sub>450</sub>).

Table 10: Cytotoxicity of rSAS1738 on HMEC endothelial cells by WST-1 assay (OD<sub>450</sub> values).

<b>WST-1/OD<sub>450</sub></b>	<b>HMEC Ctrl</b>	<b>0.45 <math>\mu</math>M rSAS1738</b>	<b>0.9 <math>\mu</math>M rSAS1738</b>	<b>1.8 <math>\mu</math>M rSAS1738</b>
<b>Well 1</b>	1	0.9	0.87	0.58
<b>Well 2</b>	1.02	0.96	0.73	0.63
<b>Well 3</b>	0.98	0.89	0.76	0.5
<b>STDE<sub>v</sub></b>	0.02	0.04	0.08	0.07
<b>Avg OD<sub>450</sub></b>	1	0.92	0.79	0.57
<b>Percentage</b>	100	92	79	57

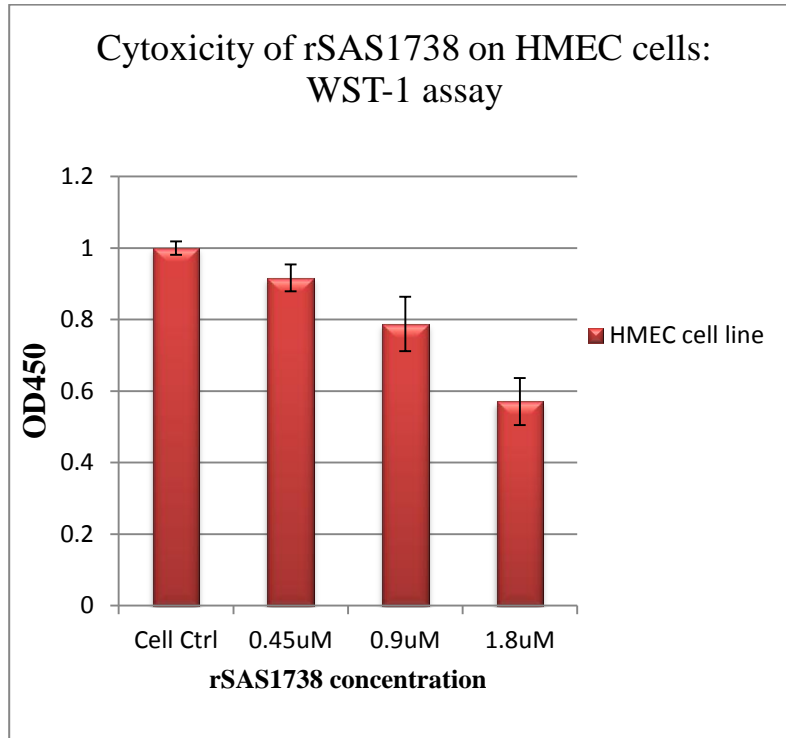


Figure 23: Bar graph of cytotoxicity of rSAS1738 on HMEC endothelial cells by WST-1 assay (OD<sub>450</sub>).

Table 11: Cytotoxicity of rSAS1738 on SVEC endothelial cells by WST-1 assay (OD<sub>450</sub>).

<b>WST-1/ OD<sub>450</sub></b>	<b>SVEC Cell Ctrl</b>	<b>0.45 <math>\mu</math>M rSAS1738</b>	<b>0.9 <math>\mu</math>M rSAS1738</b>	<b>1.8 <math>\mu</math>M rSAS1738</b>
<b>Well 1</b>	1.06	0.9	0.86	0.95
<b>Well 2</b>	1.03	1.05	0.82	0.9
<b>Well 3</b>	0.86	1	1.07	0.81
<b>STDev</b>	0.11	0.08	0.13	0.07
<b>Avg OD<sub>450</sub></b>	0.98	0.98	0.92	0.89
<b>Percentage</b>	100	100	93.87	90.8

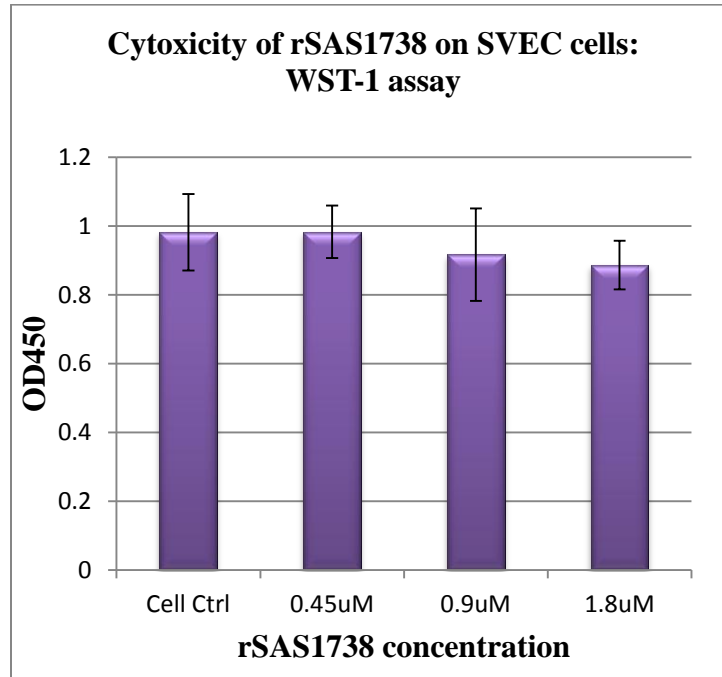


Figure 24: Bar graph of cytotoxicity of rSAS1738 on SVEC endothelial cells by WST-1 assay (OD<sub>450</sub>).

Table 12: Cytotoxicity of rSAS1738 on HaCat keratinocyte cells by WST-1 assay (OD<sub>450</sub> values).

<b>WST-1/ OD 450</b>	<b>HaCat Cell Ctrl</b>	<b>0.45 µM rSAS1738</b>	<b>0.9 µM rSAS1738</b>	<b>1.8 µM rSAS1738</b>	<b>HaCat Cells+ BSA</b>
<b>Well 1</b>	1.3	1	0.9	0.85	1.25
<b>Well 2</b>	1.26	1.1	0.85	0.79	1.33
<b>Well 3</b>	1.1	1.05	0.88	0.7	1.05
<b>Stdev</b>	0.11	0.05	0.03	0.08	0.14
<b>Avg OD<sub>450</sub></b>	1.22	1.05	0.88	0.78	1.21
<b>Percentage</b>	100	86.06	72.13	65.6	99.18



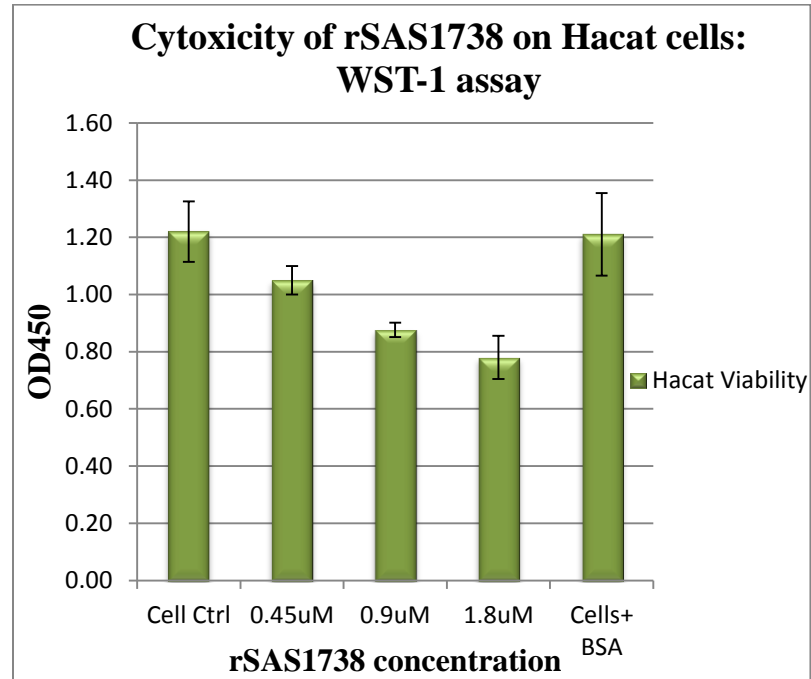


Figure 25: Bar graph of cytotoxicity of rSAS1738 on HaCat keratinocyte cells by WST-1 assay (OD<sub>450</sub>).

Table 13: Percentage of cytotoxicity of rSAS1738 on various cell lines by WST-1 assay.

<b>Cell types</b>	<b>Cell Ctrl (%)</b>	<b>0.45 <math>\mu</math>M rSAS1738</b>	<b>0.9 <math>\mu</math>M rSAS1738</b>	<b>1.8 <math>\mu</math>M rSAS1738</b>
HEK293	100	80.64	68.8	43
HMEC	100	92	79	57
HaCat	100	86.06	72.13	65.6
SVEC	100	100	93.87	90.8

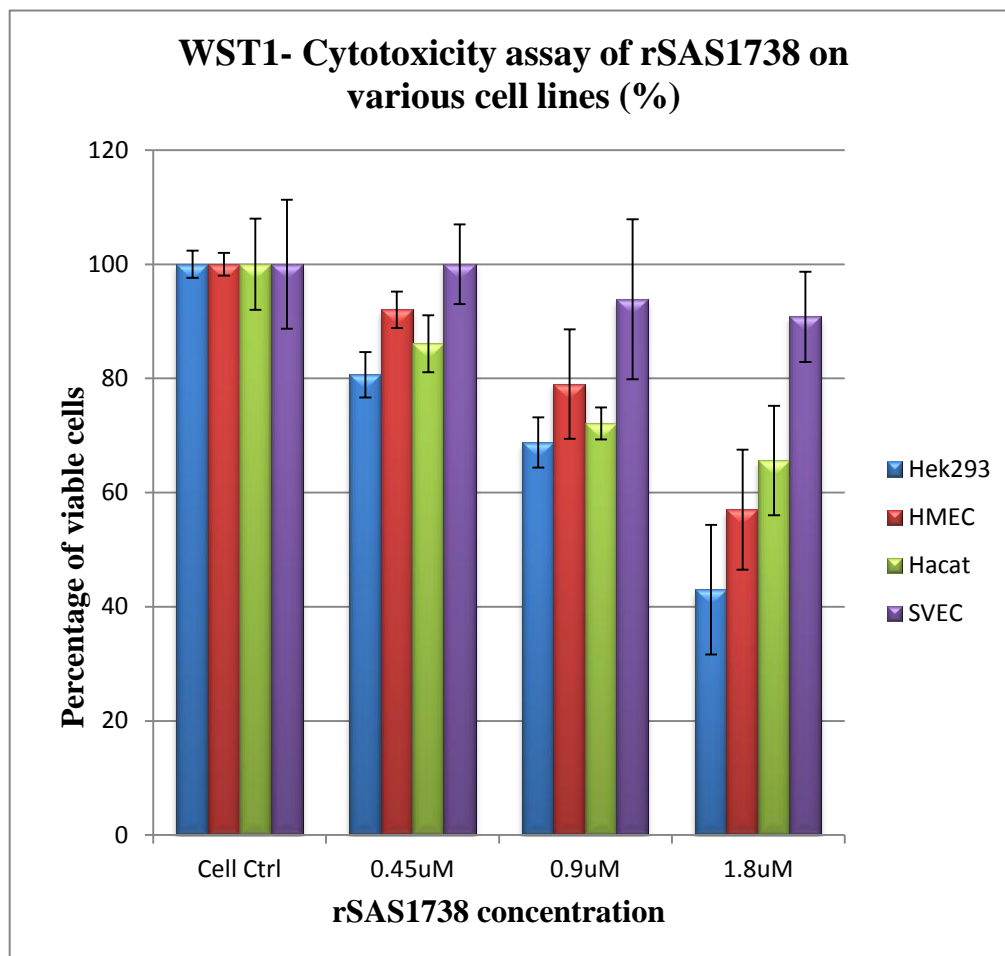


Figure 26: Bar graph of percent of reduction in viability of various cell lines treated with rSAS1738; WST-1 assay.

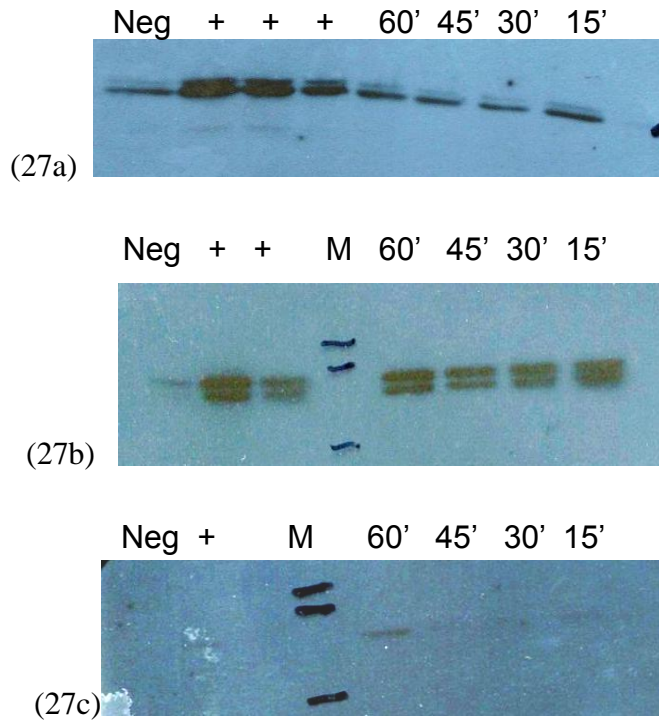


Figure 27: Detection of p38 and erk kinase activation by immunoblotting.

(27a) Activation of phospho-erk checked by probing with phospho-erk antibody;

(27b) Control: total erk kinase activation; (27c) Probed with phospho p38 antibody.

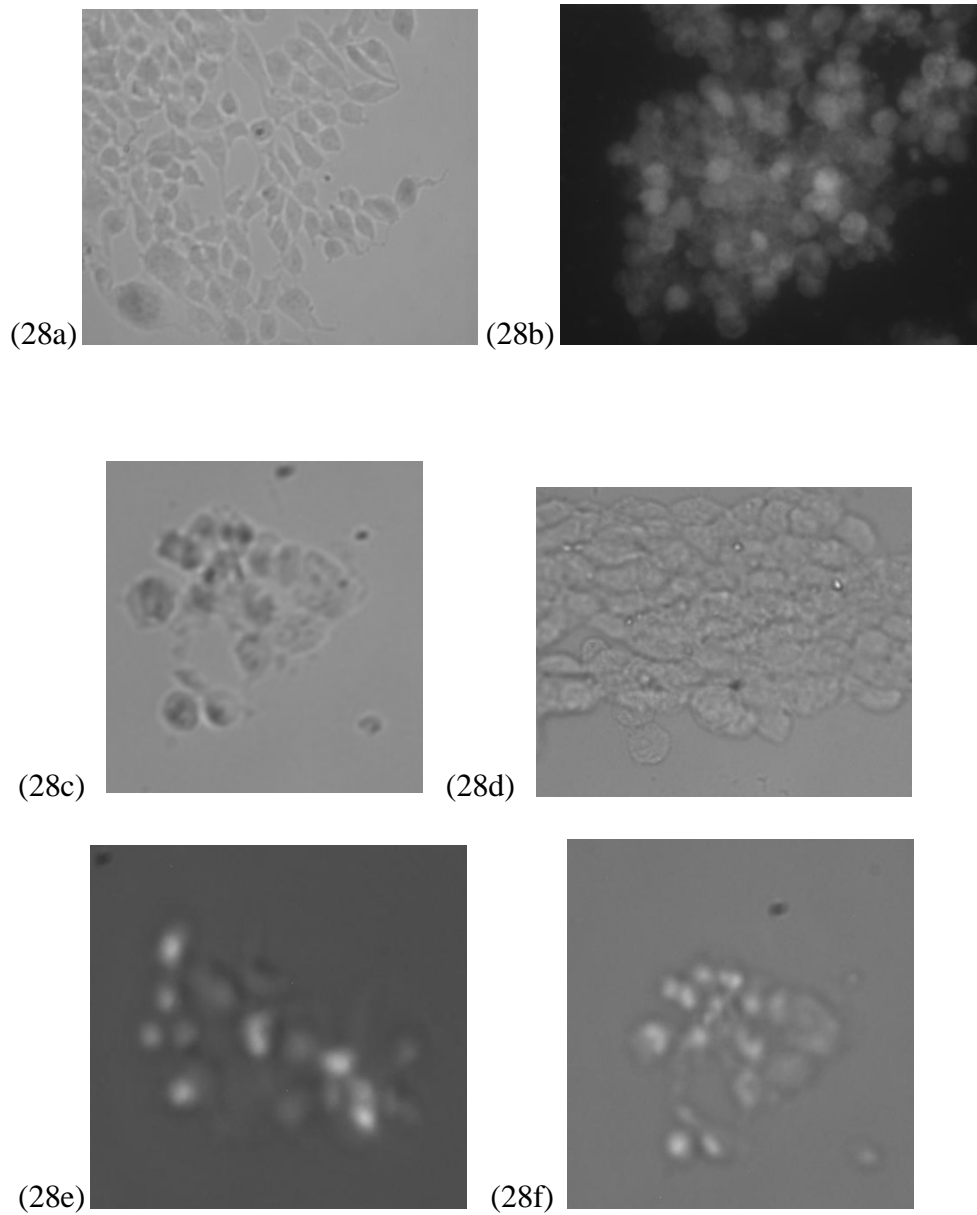


Figure 28: Effect of rSAS1738 on HEK293 cell line by fluorescent microscopy (PI staining).

(28a) Positive control; (28b) Negative control HEK293 cells treated with staurosporine;

(28c, d) HEK293 cells plus rSAS1738 (DAPI stain); (28e, f) HEK293 cells plus rSAS1738 (PI stain).

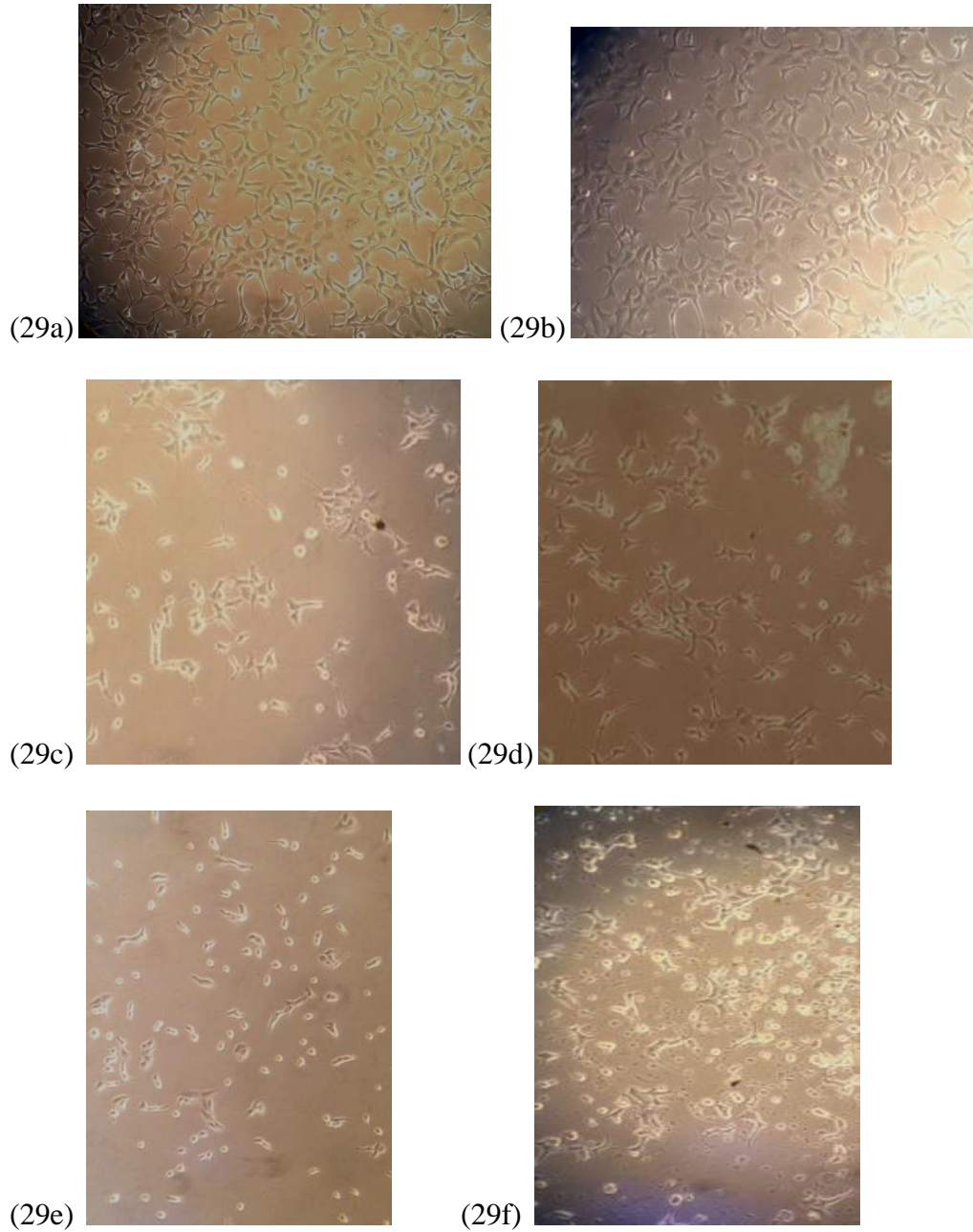


Figure 29: Effect of rSAS1738 on HEK293 cells by phase contrast microscopy (unstained).  
 (29a, d) HEK293 cells confluent; (29c, d) HEK293 cells semi-confluent; (29e) HEK293 cells  
 (semi confluent) plus rSAS1738. Cells circled and no cell clustering; (29f) HEK293 cells  
 (confluent) plus rSAS1738. Cell circling and floating.

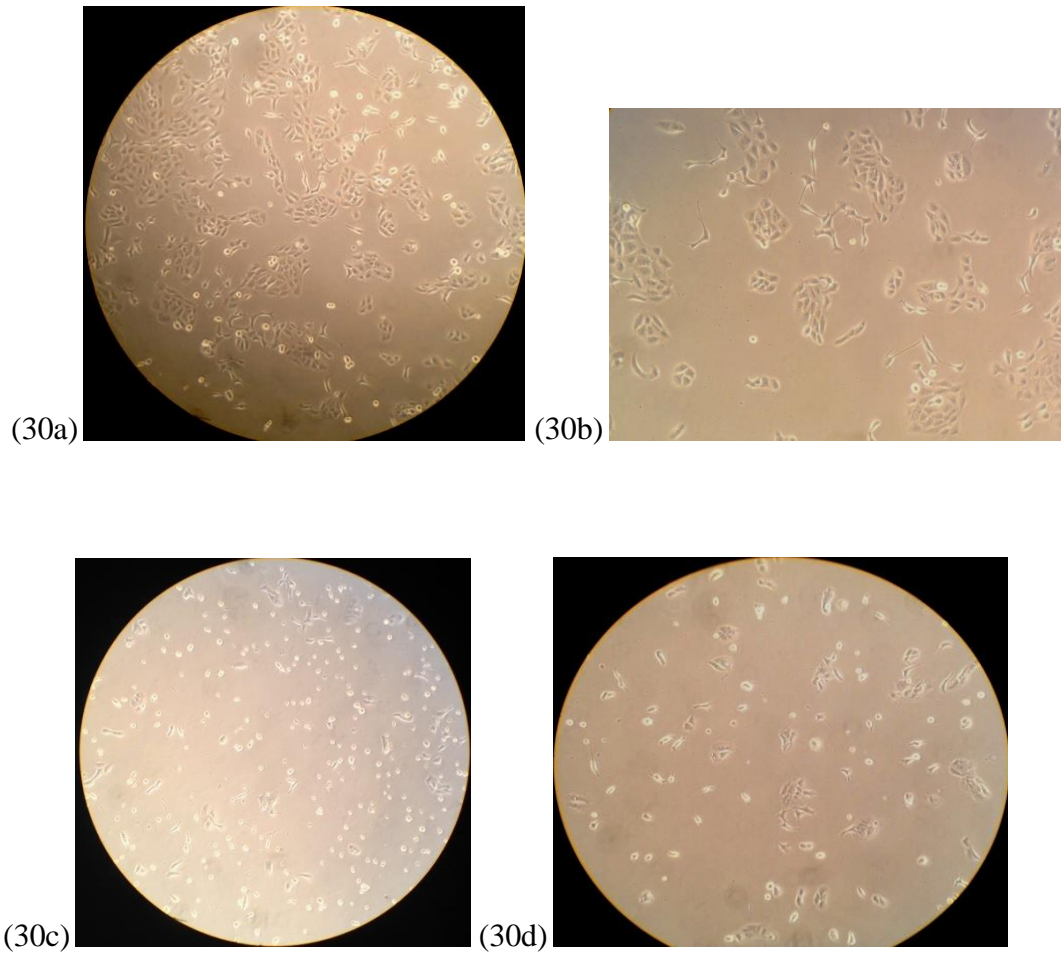


Figure 30: Effect of rSAS1738 on HaCat keratinocyte cells by phase contrast microscopy.

(30a, b) HaCat control cells; (30c, d) HaCat cells treated with rSAS1738.

Table 14: Guava ViaCount assay: ViaCount viability markers and apoptotic gate markers.

<b>Guava ViaCount Viability marker (easy fit)</b>	<b>Samples</b>
X int	2.04
Angle	10.5
<b>Guava Vicaount Apoptosis gate marker</b>	
X int	11.05
Angle	9.9



Table 15: Percentage of cell death analysis of HEK293 cells treated with 0.2 to 0.6  $\mu\text{M}$  rSAS1738 by Guava ViaCount assay.

<b>ViaCount assay</b>	<b>Positive</b>	<b>Negative</b>	<b>0.2 <math>\mu\text{M}</math> rSAS1738</b>	<b>0.4 <math>\mu\text{M}</math> rSAS1738</b>	<b>0.6 <math>\mu\text{M}</math> rSAS1738</b>
Live (%)	87.135	46.42	85.4	79.5	58
Apoptotic (%)	4.05	41.95	8.9	10.7	38
Dead (%)	8.7	11.7	4.1	11.5	12
<b>STDev of above data</b>					
Live (%)	2.18	1.2	2.2	2.24	1.42
Apoptotic (%)	1.18	3	0.8	2.29	4.15
Dead (%)	1.09	2.63	1.3	4.14	1.57

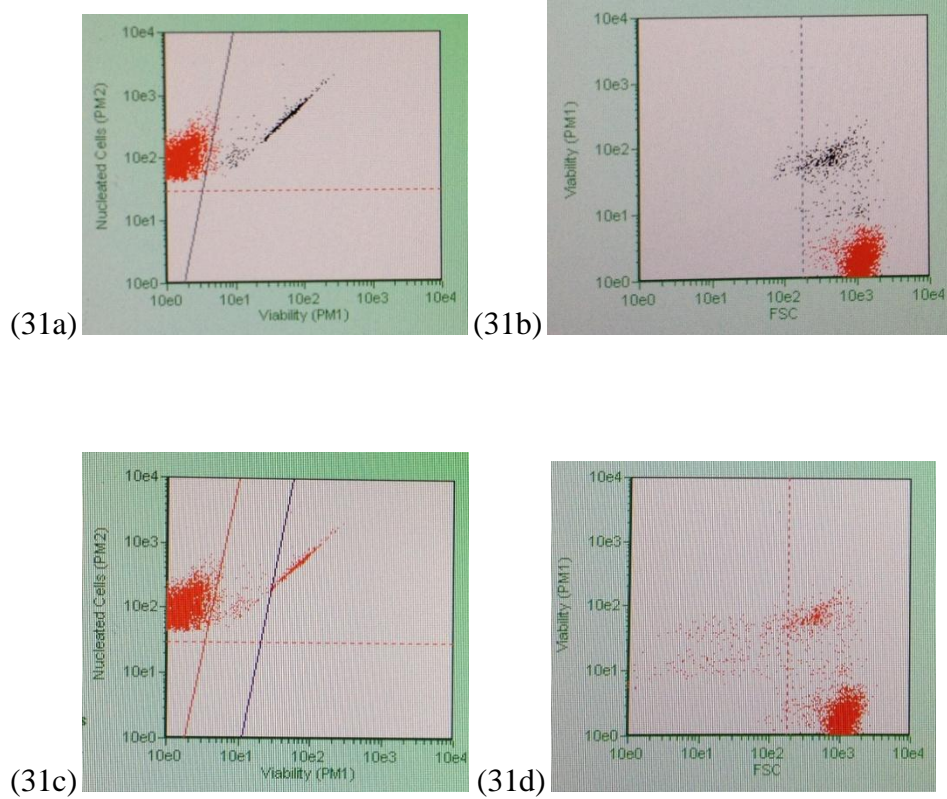


Figure 31: Guava ViaCount assay: positive control (HEK293 cells).

(31a) Easy fit analysis to check live and dead cells; (31b) Forward scatter plot of fig 31a.

(31c) ViaCount with Apoptotic gate; (31d) Forward scatter plot of fig 31c.

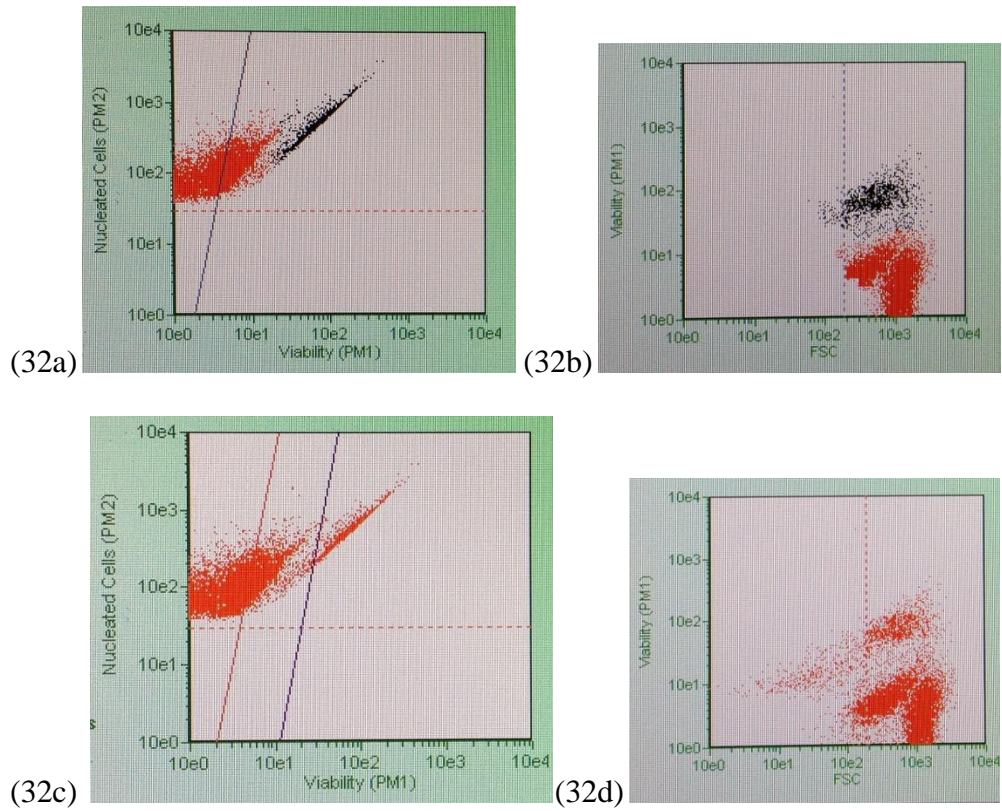


Figure 32: Guava ViaCount assay: Negative control (HEK293 plus stuarosporine 1 $\mu$ M/2hr).

(32a) Easy fit analysis to check live and dead cells; (32b) Forward scatter plot of fig 32a.

(32c) ViaCount with apoptotic gate; (32d) Forward scatter plot of fig 32c.

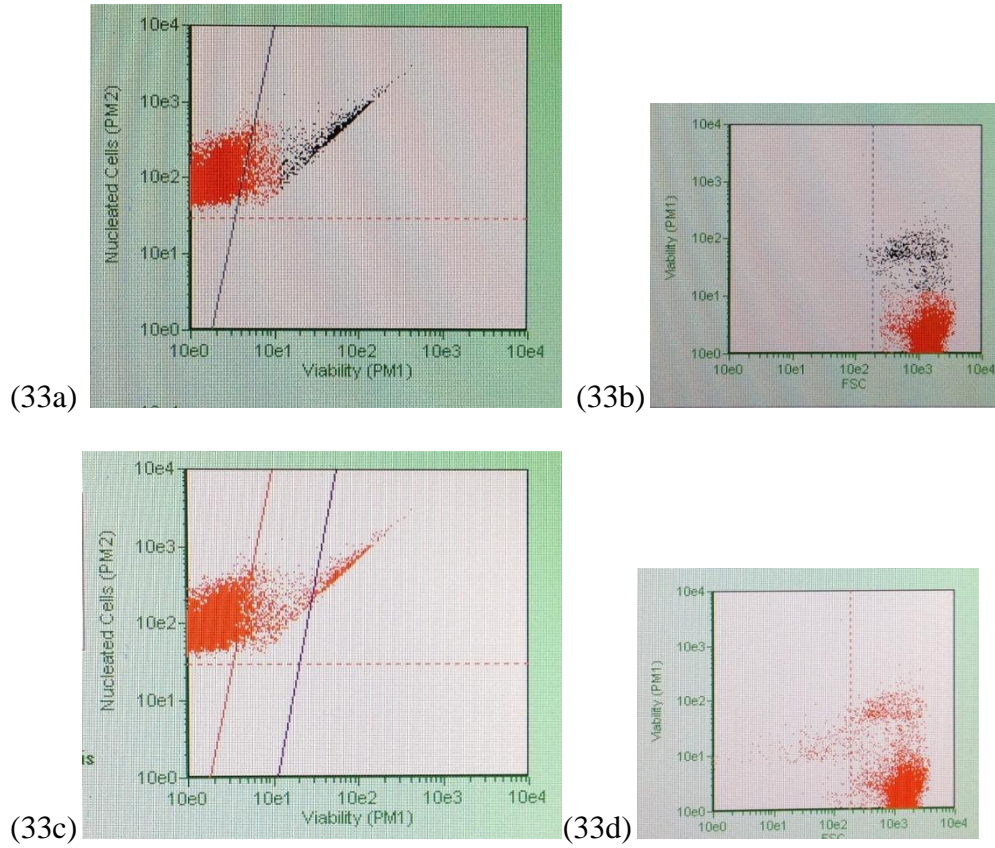


Figure 33: Guava ViaCount assay. HEK293 treated with 0.6  $\mu\text{M}$  rSAS1738.

(33a) Easy fit analysis to check live and dead cells; (33b) Forward scatter plot of fig 33a.

(33c) ViaCount with apoptotic gate; (33d) Forward scatter plot of fig 33c.

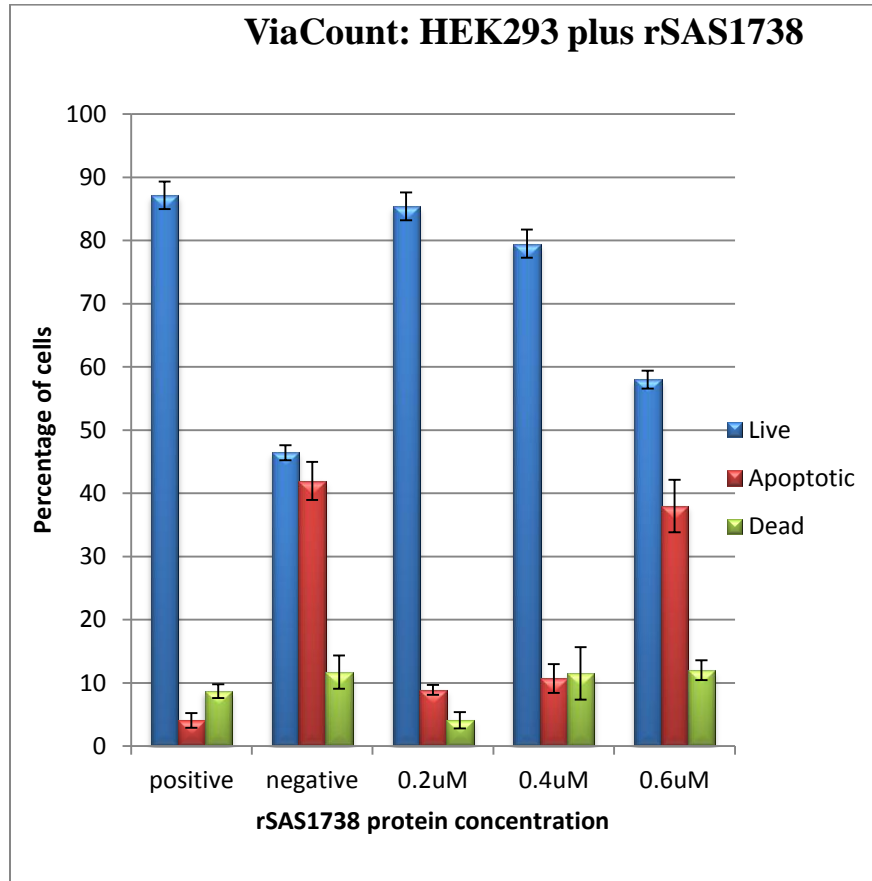


Figure 34: Bar graph of percent cell death analysis by ViaCount assay; HEK293 cells treated with rSAS1738.

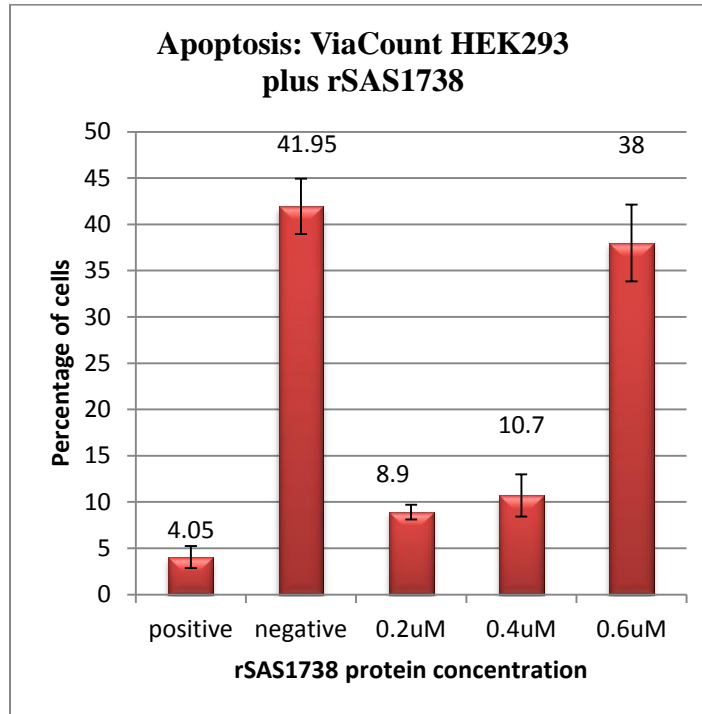


Figure 35: Bar graph of percentage apoptotic cells determined by ViaCount assay; HEK293 cells treated with rSAS1738.

Table 16: Guava nexin assay; Marker position for gate adjustments (trial 1).

<b>Nexin marker position</b>	
X	10
Y	27
X angle	-5
Y angle	13

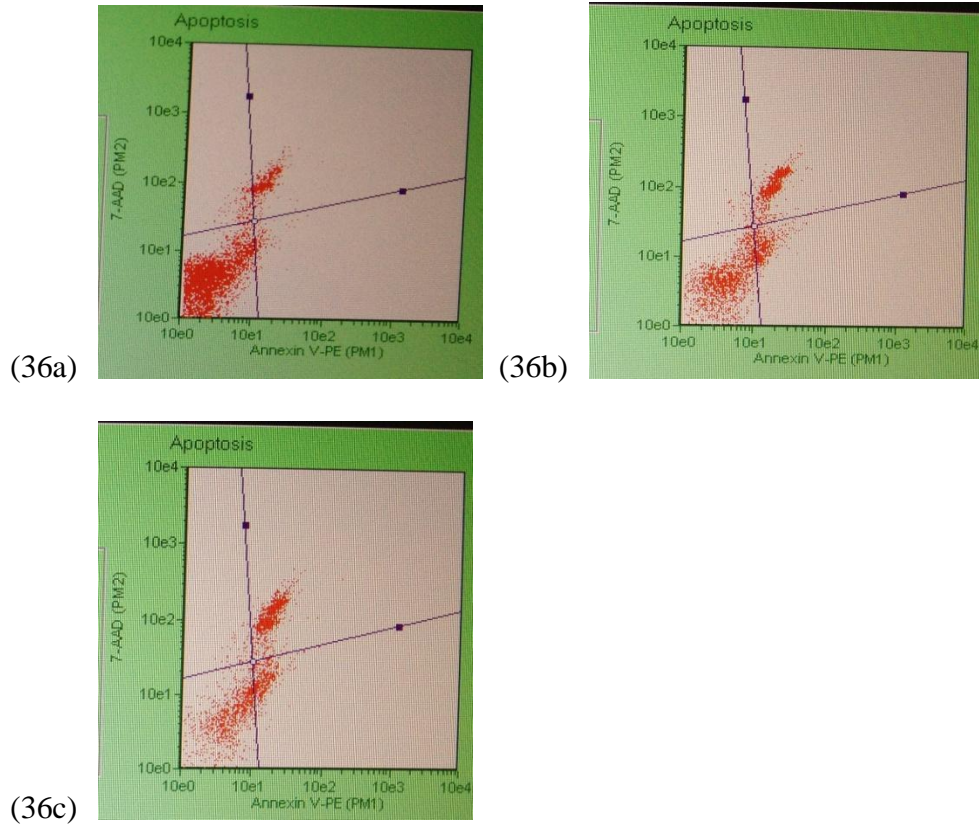


Figure 36: Guava Nexin assay (trial 1).

(36a) HEK293 cells, positive control; (36b) HEK293 plus stuarosporine (1  $\mu$ M/2hr), negative control; (36c) HEK293 cells treated with 0.6  $\mu$ M rSAS1738 (trial 1).



Table 17: Guava nexin assay; Marker position for gate adjustments(trial 2).

HEK293 cells treated with 0.4  $\mu$ M rSAS1738.

<b>Nexin marker position</b>	
X	21
Y	21
X angle	-18
Y angle	18

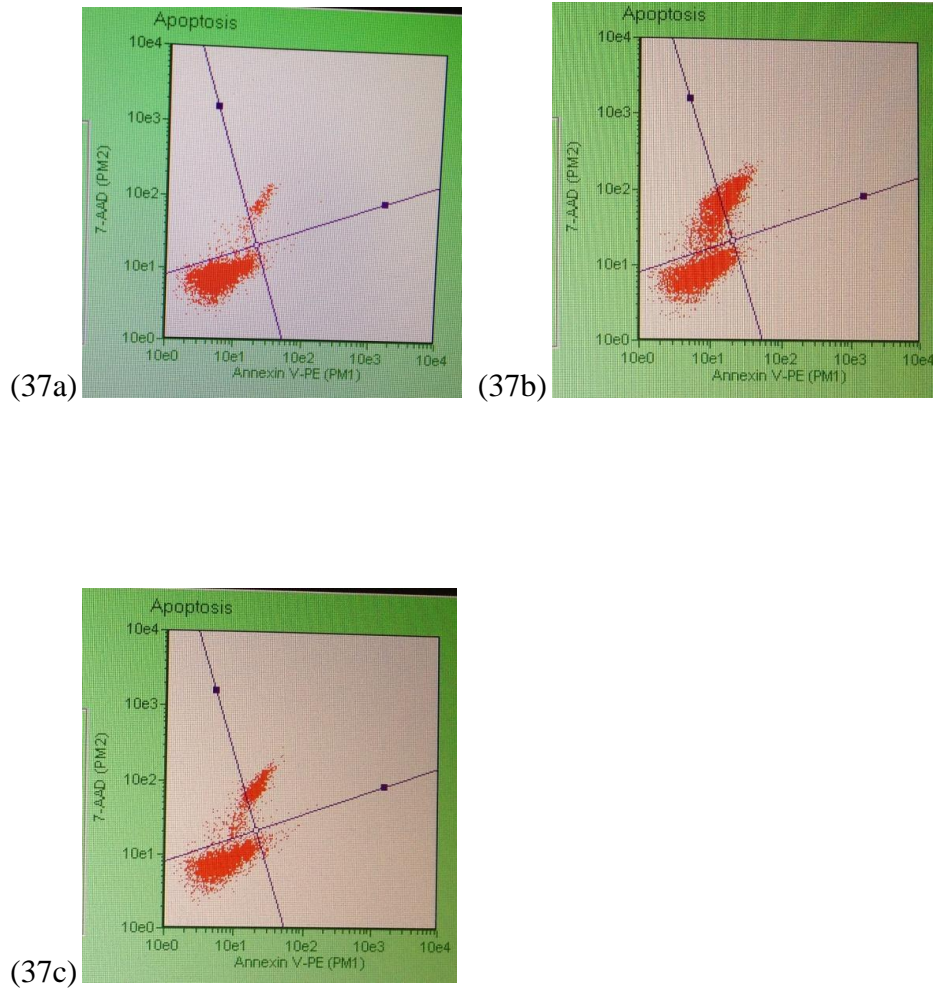


Figure 37: Guava Nexin assay (trial 2).

(37a) HEK293 cells, positive control; (37b) HEK293 plus staurosporine ( $1 \mu\text{M}/2\text{hr}$ ), negative control; (37c) HEK293 cells treated with  $0.6 \mu\text{M}$  rSAS1738 (trial 1).

Table 18: Percent cell death analysis of HEK293 cells with 0.2 to 0.6  $\mu\text{M}$  of rSAS1738 by Guava

Nexin assay.

Positive control: HEK293 cells treated with Tris-NaCl buffer

Negative control: HEK293 cells treated with staurosporine (1  $\mu\text{M}$  for 1 hr)

<b>Guava Nexin assay Cells</b>	<b>Positive control</b>	<b>0.2 <math>\mu\text{M}</math> rSAS1738</b>	<b>0.4 <math>\mu\text{M}</math> rSAS1738</b>	<b>0.6 <math>\mu\text{M}</math> rSAS1738</b>	<b>Negative Control</b>
Live (%)	86.44	71	57.85	45.85	56.2
Apoptotic (%)	1.38	5.56	13.95	35.15	5.5
Dead (%)	7.12	18.5	22.9	16.85	23.1
<b>STDev</b>					
Live (%)	3.12	0.42	2.2	4.3	6.7
Apoptotic (%)	1.3	0.21	1.2	2.75	1.4
Dead (%)	3.25	1.4	3.6	1.48	5.1

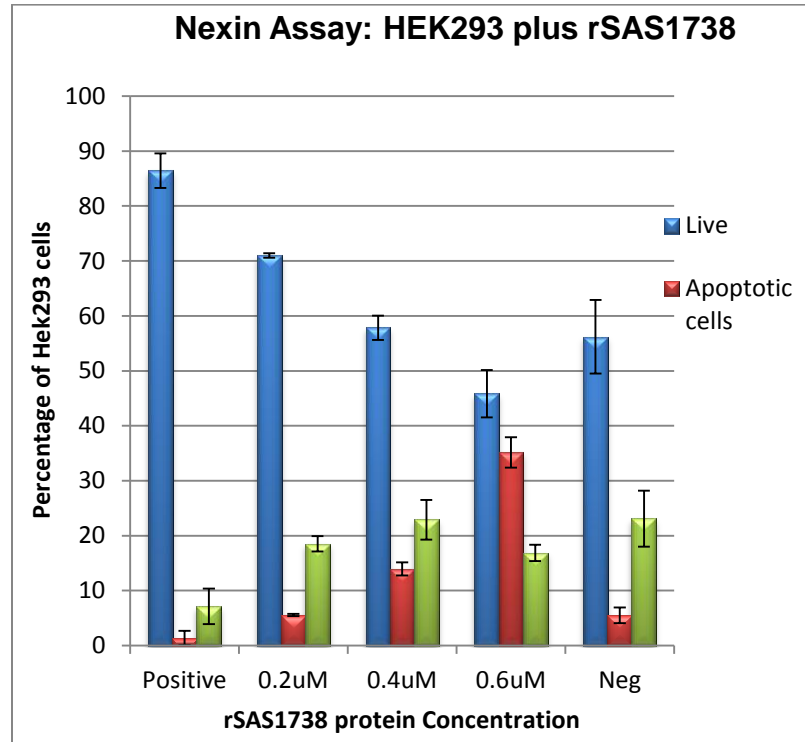


Figure 38: Percent live, dead and apoptotic cells determined by Nexin assay; HEK293 cells treated with 0.2 to 0.6  $\mu\text{M}$  of rSAS1738.

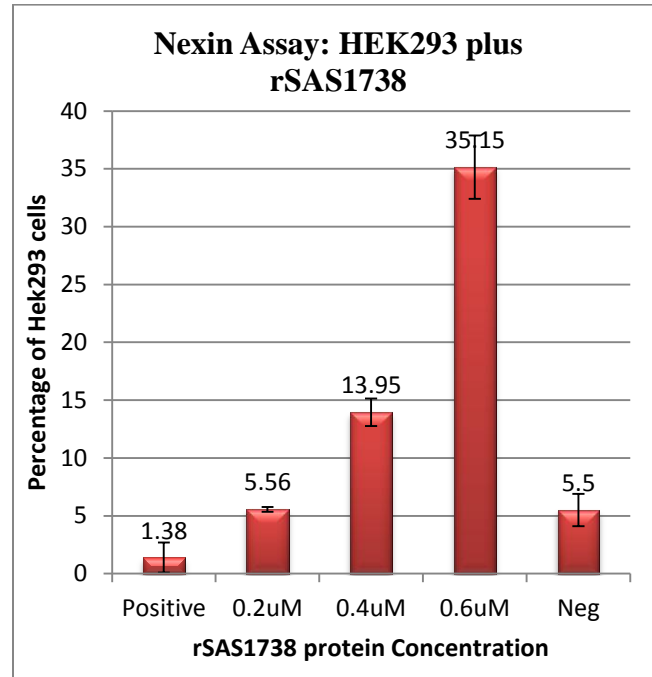


Figure 39: Percent apoptotic cells determined by Nexin assay; HEK293 cells treated with 0.2 to 0.6  $\mu\text{M}$  of SAS1738.

Table 19: Invasion assay of *S.aureus* in HMEC endothelial cells treated with 0.2  $\mu$ M rSAS1738.

<b>Bacteria</b>	<b>MRSA252</b>	<b><i>S.aureus</i> lab strain</b>	<b><i>S.epidermidis</i> lab strain</b>
Attached + internalized cell count in HMEC	$2 \times 10^6$ cfu/ml	$5 \times 10^5$ cfu/ml	$5 \times 10^5$ cfu/ml
Internalized cell count in HMEC	$4 \times 10^4$ cfu/ml	$4 \times 10^4$ cells/ml	Nil
Internalized bacterial cell count in HMEC treated with 0.2 $\mu$ M rSAS1738	$3 \times 10^4$ cfu/ml	$7 \times 10^4$ cells/ml	Nil

Table 20: Nitrite production by activated Raw 264.7 macrophages by Griess assay (OD<sub>550</sub>).

<b>Time point</b>	<b>Raw 264.7 cells positive control</b>	<b>Raw cells +LPS</b>	<b>Raw cells + BSA</b>	<b>Raw cells LPS+ IFN</b>	<b>Raw cells + LPS + IFN + 0.2 uM rSAS1738</b>	<b>Raw cells + rSAS1738</b>
<b>8 hr</b>	0.042	0.039	0.0425	0.044	0.044	0.0455
<b>20 hr</b>	0.038	0.04	0.043	0.08	0.078	0.084
<b>25 hr</b>	0.041	0.044	0.051	0.092	0.089	0.094
<b>30 hr</b>	0.041	0.047	0.061	0.12	0.094	0.1

Table 21: Determination of nitrite ( $\mu\text{M}$ ) concentration compared to sodium nitrite standard curve by Griess assay.

<b>Time point</b>	<b>Raw264.7 (ctrl)</b>	<b>Raw Cells+ LPS+ IFN</b>	<b>LPS, IFN, + rSAS1738 (0.2 <math>\mu\text{M}</math>)</b>	<b>Raw cells with BSA</b>	<b>Raw cells + LPS + IFN + 0.2 <math>\mu\text{M}</math> rSAS1738</b>	<b>Raw cells +LPS</b>
<b>8 hrs</b>	<0.75 $\mu\text{M}$	<0.75 $\mu\text{M}$	<0.75 $\mu\text{M}$	<0.75 $\mu\text{M}$	<0.75 $\mu\text{M}$	<0.75 $\mu\text{M}$
<b>20 hrs</b>	<0.75 $\mu\text{M}$	7 $\mu\text{M}$	7 $\mu\text{M}$	7 $\mu\text{M}$	<0.75 $\mu\text{M}$	<0.75 $\mu\text{M}$
<b>25 hrs</b>	<0.75 $\mu\text{M}$	11.5 $\mu\text{M}$	11 $\mu\text{M}$	12 $\mu\text{M}$	<0.75 $\mu\text{M}$	1.5 $\mu\text{M}$
<b>30 hrs</b>	<0.75 $\mu\text{M}$	12.5 $\mu\text{M}$	12 $\mu\text{M}$	12.5 $\mu\text{M}$	<0.75 $\mu\text{M}$	5 $\mu\text{M}$



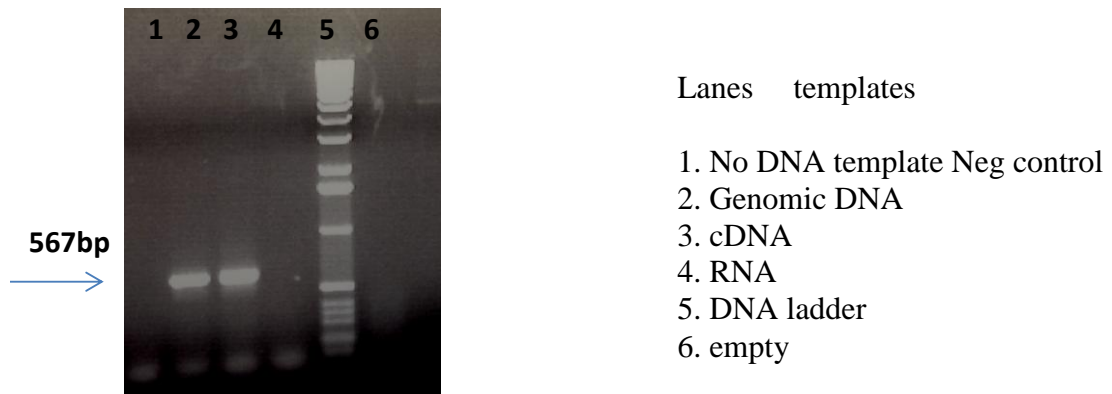


Figure 40: Reverse transcriptase PCR amplification of SAS1738 from cDNA made from MSSA476.

## Discussion

The research data suggests the lethality of the hypothetical protein, SAS1738, with various human cell lines, indicating an important role in the virulence of MSSA476. *sas1738* was cloned and expressed in the *E. coli* BL21-AI gateway expression system using the T7 promoter system. Initial expression studies showed the presence of two different sized 21 kDa and 25 kDa bands indicating proteolysis (Fig 20a, 21a). Later, protein expression was performed in buffered media called terrific broth and at a lower temperature of 30°C [206]. Modifying the expression conditions prevented proteolysis yielding a single band of ~25 kDa as expected (Fig 20b, 21b). However, the Ni-His tag column purified rSAS1738 yield was in the lower range, 350 to 500 µg/l. T7 expression systems are usually known to give 10 mg to 100 g of protein per liter. Some low expression promoters may yield protein in the range of µg to grams of protein per litre. Protein yield may vary depending on expression hosts, vectors, promoter strength, copy number or expression conditions like media and temperature [156]. Expression of rSAS1738 in our studies showed the protein accumulation in inclusion bodies, indicating that protein over-expression led to protein aggregation and formation of inclusion bodies. It may be possible to standardize the expression system to improve the yield of rSAS1738 by cloning into another promoter system. Expressing rSAS1738 without signal peptide may reduce any undesirable secretion of protein, thus minimizing any exposure to host proteases. Using codon plus *E. coli* or

using *Bacillus* as the expression host would also help to increase the yield of proteins due to codon optimization [156, 207].

*Staphylococcus aureus* infection occurs mainly through the skin surface and can further damage other tissues or organs. Initial interaction of the protein will involve surface keratinocytes that may later get into bloodstream and invade other cell types like endothelial cells or osteoblasts [171, 172, 204]. Hence, the effect of purified rSAS1738 was checked on various mammalian cell lines. Out of the seven cell lines used in these experiments, rSAS1738 was effective on three human cell lines. rSAS1738 showed varied levels of lethality with HEK293 cells, HMEC endothelial cells, and HaCat keratinocytes (fig 26, Table 12). There was negligible or no effect on CHO-I, SVEC, NIH3T3, or Raw macrophages.

The lethal effect of rSAS1738 specifically on human cells could indicate that *S.aureus* protein may be exhibiting host-specific activity. MSSA476, a human isolate from osteomyelitis and bacteremia (NCBI database) may be the reason for SAS1738 specificity to human cell lines. However, the extent of lethality varied between different cell types. The most susceptible cells were HEK293 followed by keratinocytes and endothelial cells.

HEK293 cell lines are human kidney embryonic cell lines but are not differentiated as one cell type and cannot be considered as a kidney model. HEK293 cells can be of any origin type (e.g., epithelial, endothelial or fibroblasts) since, they are embryonic cells. HEK293 is used for therapeutic protein expression and toxicity assays mainly due to the ease of handling the cell lines and they do not metabolise any of the external drugs or proteins. Several other researchers have used HEK293 cell line for toxicity and invasion assays [208-210]. HEK293 cells showed high susceptibility to rSAS1738 protein. The highest concentration of rSAS1738 used in WST-1 proliferation assay, 1.8  $\mu$ M, could kill ~50% of HEK293 cells, ~40% of HMEC endothelial cells

and ~30% of HaCat cells (Fig 26). It seems that a higher concentration of 1.8  $\mu\text{M}$  led to apoptotic and dead cells giving greater variability at higher concentration (Fig 26). However, 0.2 to 0.6  $\mu\text{M}$  rSAS1738 was used for the apoptotic assays. The concentration of rSAS1738 of 2.5, 5, and 10  $\mu\text{g}$  corresponds to 0.45, 0.9 and 1.8  $\mu\text{M}$ , respectively, in the WST-1 assay. It is not clear whether the high concentration of lethal protein led to shock and cell death. HEK293 and HaCat cells treated with 20  $\mu\text{g}$  of Bovine Serum Albumin (BSA) did not exhibit any significant cell death. Hence rules out the effect of high concentration of any arbitrary protein leading to the cell death of HEK293 and HaCat cells.

Apoptosis is marked by cellular changes like cytoplasmic shrinkage, DNA fragmentation, and budding or blebbing of organelles. Morphological changes in cell lines indicating cell death were observed in HEK293 and HaCat by microscopic observation of propidium iodide fluorescence and phase contrast microscopy (Fig 28, 29). Propidium iodide staining would not help us confirm apoptosis clearly since PI stain can penetrate damaged cells and dead cells. Apoptosis is observed based on lesser fluorescence compared to dead cell intensity. This fluorescence may be non-specific and less precise to confirm apoptosis. Hence, cell death analysis was performed by ViaCount and Nexin assay using a flow cytometer.

ViaCount measures the live and dead cells using nuclear stains that bind to DNA. The viable stain variably stains cells depending on cell health. The apoptotic index mainly depends on the low staining of the viability stain. The percentage of apoptotic cells also depends on gating efficiency. Hence, ViaCount should be supported by other confirmatory assays. The Nexin assay confirms the level of cell death and apoptosis.

The Nexin assay showed higher cell death in 0.4 to 0.5  $\mu\text{M}$  rSAS1738 in several trials. Early apoptotic levels were lower in this concentration, but late apoptosis or necrosis was 22%

greater than in control cells. However, cells treated with 0.6  $\mu\text{M}$  rSAS1738 showed less late apoptosis and higher early apoptosis than cells exposed to 0.4  $\mu\text{M}$  rSAS1738. The difference in late apoptosis or dead cells between 0.4  $\mu\text{M}$  and 0.6  $\mu\text{M}$  rSAS1738 was 17% and 23%, respectively. The 5% difference is marginal when considering the error bars. However, apoptosis levels increased markedly, 14% to 35%, when rSAS1738 was increased from 0.4 to 0.6  $\mu\text{M}$  (Fig 38). The results were similar to results analyzed by the ViaCount assay (Fig 34).

MAPK kinase is usually activated during cell growth and differentiation. MAPK-p38 can be activated during any type of cell stress or cell death. p38 activation in rSAS1738 by 1 hr indicates that HEK293 cells were stressed due to the presence of rSAS1738. The role of p38 kinase in *S. aureus* mediated apoptosis has already been shown by various research groups. Hence, we can also predict p38 activation in response to rSAS1738 protein to have a role in cell death and apoptosis since rSAS1738 had lethal effects on the same cell line (Fig 27). p38 activation indicates killing by activating the signaling cascade inside the cell, and we suspect that rSAS1738 action may be time-based killing, but not by bursting cells. In the future, we will need to check if the levels of apoptosis are reduced by blocking p38 to confirm the role of p38 kinase in cell death in response to rSAS1738 [198].

rSAS1738 did not aid the internalization of *S. aureus* (MRSA252 or lab strain) or *S. epidermidis* into HMEC endothelial cell lines (Table 18). There was no reproducibility in internalization of bacteria with rSAS1738 treatment, and results looked similar in varying concentrations of test proteins such as, 0.1  $\mu\text{M}$  and 0.2  $\mu\text{M}$ . rSAS1738 may be damaging the cells before or after bacterial invasion, leading to inconsistency of internalizing bacteria. Damaged cell lines may allow penetration of gentamycin, leading to death of internalized

bacteria. However, rSAS1738 did not show increased internalization of bacteria into HMEC cell line in these experiments.

Nitrite detection by Griess reagents are based on sulphanilic acids and alpha naphthalamine, which converts nitrites to form pink products and is read at OD<sub>450</sub> nm in an ELISA reader (Table 19). Inactivated Raw 264.7 macrophages treated with rSAS1738 or BSA did not increase nitrite levels during the 8 to 30 hrs assay time points. Purified 0.2 µM of rSAS1738 protein did not generate any nitrite in activated or inactivated macrophages, indicating rSAS1738 did not play a significant role in nitrite-dependent killing by Raw 264.7 mouse macrophages. Macrophages activated by only 1 µg of LPS generated 5 µM nitrite by 30 hrs incubation time, whereas 0.2 µM rSAS1738 did not generate nitrite even after 30 hours (Table 20). This also indicated that the purified 0.2 µM rSAS1738 had <1 µg LPS contamination. Considering the expression of rSAS1738 was performed in an *E.coli* system, the chances of LPS contamination were high [155]. The presence of LPS in the column purified rSAS1738 would affect the mammalian cell line assays, since LPS would have endotoxicity and kill the cells. Hence, purification of rSAS1738 protein should be performed such that the endotoxins are removed efficiently. During purification of rSAS1738, the Ni-His bind column washed with 25 to 30 volumes of wash buffer before eluting the pure protein from the column. The Griess assay indicated that rSAS1738 had no LPS contamination in the protein sample.

The reverse transcriptase PCR amplification of SAS1738 from the MSSA476 stationary culture (fig 40) indicates that SAS1738 is constitutively expressed in MSSA476 irrespective of host factors or any specific conditions. However, we do not know if there may be amplified expression of SAS1738 in presence of host factors or in synergy with other virulence factors.

The lethal concentration of rSAS1738 used was in the range of 0.5 to 2  $\mu\text{M}$  in all the assays. The nanomolar concentrations of rSAS1738 did not show any lethal effect on the cell lines in our experiments. Most toxins are known to function in picomole or nanomole range of concentrations to be considered lethal. However, every toxin differs in their lethality in terms of their effective concentration range, species, and cell specificity. They may also vary with pH, temperature and host interaction with other virulence factors [25, 39, 211, 212]. Toxin concentrations from nM to  $\mu\text{M}$  have been used by various research groups for different studies. One of the best examples is *S.aureus* alpha toxin, which is effective in nanomolar concentration for lysing rabbit blood cells, but 100-fold higher concentrations are required for a lethal effect on human cells. A 20  $\mu\text{g}$  concentration could show pores in some lipid membranes by some electron microscopic studies [211]. In another study, 2.5  $\mu\text{g}$  of diphtheria toxin is effectively lethal to mammalian cells such as HeLa and human kidney cells [212]. Assays with cholera toxin have been performed in nM concentrations, whereas research with shiga toxin are also used in 4  $\mu\text{g}$  to 25  $\mu\text{g}$  to study the toxin transportation into cytosol [213].

Some reasons can be speculated about the  $\mu\text{M}$  range of rSAS1738 required for the lethal effect, otherwise called the low specific activity, of rSAS1738 in these assays. Some reasons can be the methods of protein purification, solubilization and refolding conditions used in the laboratory. Also, the concentration of rSAS1738 required in-vitro may be different from in-vivo effect or in actual host pathogenesis. We do not know if the actual biological activity of rSAS1738 requires higher ( $\mu\text{M}$ ) concentrations or if it has any other drawbacks due to the expression in heterologous systems like *E.coli*. The expression of rSAS1738 in *E.coli* heterologous system and purification system may affect the specific activity. The purification of protein by denaturation conditions and renaturation would not assure the complete recovery of

active protein [155, 156]. The rSAS1738 was purified from solubilized inclusion bodies, nickel affinity column purified, and renatured or refolded by dialysis. We do not know if all of the protein was bio-active after recovery from inclusion bodies. Even though the effective lethal concentrations are 0.5 to 2  $\mu\text{M}$ , this protein concentration may include both active or inactive protein that together contributed to the higher concentration but less specific activity. Specific activity may work at much lower concentrations if we could standardize the protein solubilization and renaturation. rSAS1738 was solubilized using sonication and denaturation conditions provided by 6M urea and refolded by dialysis to gradually remove the urea. Some of the additives such as arginine, sugars, PEG could prevent aggregation during refolding; hence, adding them during dialysis may improve solubility, refolding, stability, and, ultimately, aid in increasing the bio-active protein concentration [214]. Pulse renaturation is another way to improve the refolding and stability of protein. Pulse renaturation involves adding some soluble folded protein to the dialysis mixture that continues the reaction to refold other protein molecules in the buffer mix [214]. Standardization of novel hypothetical proteins like rSAS1738 is always challenging since we do not know the activity assays to define specific activity. However, purification of proteins from inclusion bodies is considered to yield a more pure product and is resistant to host proteases. Thus, the purification of rSAS1738 from inclusion bodies is a good start to begin the protein characterization. In this research, rSAS1738 was cloned with the signal peptide and his-tag, may affect the level of protein activity. Assays without signal peptide or his-tag would be advantageous to ensure the accurate or increased protein activity.

The other speculation is that rSAS1738 could be more effective at lower concentrations in in-vivo infections when it acts in synergy with other virulence factors. Many studies show the



synergistic effect of different virulence factors leading to lethal effects on the host. There is also evidence of mixed infections acting synergistically to amplify the lethal effect [215, 216].

This research demonstrates the lethal effect of rSAS1738 specifically on human cell lines HEK293, HaCat and HMEC. The cell damage in HEK293 was found to occur by apoptosis as demonstrated by Guava ViaCount and Nexin assay using flow cytometry. The microscopic observation also revealed a reduction in the proliferation of cell lines. rSAS1738, being unique to MSSA476 compared to MRSA252, is particularly interesting, since this protein may be contributing to the invasive nature of community associated *S.aureus* independent of antibiotic resistance.

## CHAPTER 4

### CONCLUSION

Community associated *Staphylococcus* strains are more genetically diverse than HA MRSA strains [217], having distinct lineages. CA MRSA is susceptible to non beta-lactam antibiotics but have many genetic differences from HA MRSA, such as SCCmec, PVL, and ACME predicted to contribute to increased virulence [71, 89, 218]. However, there are no particular virulence markers or genetic elements restricted to CAMRSA that indicate the genetic exchanges between HA MRSA and CA MRSA strains. CA MRSA could evolve from HA MRSA or from any other *Staphylococcus aureus* strain. Hence, the distinction between CA MRSA and HA MRSA is not clear [219, 220]. The most predominant strain of CA MRSA is USA300 (ST8-Iva), whereas the European predominant clone is ST80-IVc, indicating a diverse clonality and evolution of the predominant strains around the world [5, 221, 222]. The genetic elements leading to its increased infections are still being studied to understand the evolution of the pathogen. Comparative genomics between MRSA strains are important to understand new virulence factors contributing to increased pathogenesis of bacteria. Comparative genomics of MRSA and MSSA strains related to USA300 indicated subtle changes only in the plasmid content and antibiotic susceptibility pattern. The overall analysis of strains related to USA300 did not have immense differences in virulence factors. This similarity indicates that even small genetic changes can contribute to increased virulence [158, 223]. Structural analysis of novel

hypothetical proteins to identify domains, motifs, active sites and docking sites are very important to start functional characterization of hypothetical proteins. These studies will help us to characterize the pathogen and pave the way to drug discovery [119, 121].

Our lab research was initially based on comparative genomics of MRSA252 and MSS476 strains [8]. The other method used was to analyze the entire genome of MSSA476 for the hypothetical secreted proteins using bioinformatics tools. This protein selection was based on our own strategy to check for signal peptides and transmembrane domains. Research presented in Chapter 2, about SAS0760, reveals the active site most likely involved in catalytic activity. As mentioned earlier, these studies would pave the way for further experimental characterization of this novel hypothetical protein [122]. However, the bioinformatics data of SAS0760 provides only the preliminary data for a novel protein and has to be supported by other lab experiments like protein expression studies, 3D structural analysis by x-ray crystallography or NMR studies. Further binding sites, catalytic domain and substrate specificity can be analyzed using bioinformatics tools [122]. SAS0760 protein expression must be tried in different vectors to achieve successful stable expression. The purified protein can then be used for biochemical characterization and to determine its role in virulence. SAS0760 can then be checked for hydrolytic activity on cell wall peptidoglycan components to determine if it is, in fact, a functional cysteine protease of NlpC/P60 family [121, 135, 140].

Hypothetical protein characterization is not just limited to biochemical characterization but should also be correlated with virulence of the pathogen [121]. The hypothetical protein, SAS1738, presented in Chapter 3, has been characterized to show a lethal effect on mammalian cell lines. The involvement of SAS1738 protein in cytotoxicity and apoptosis adds more information about the invasiveness of MSSA476 in human beings.

Further studies can be performed to characterize the apoptotic pathways using microarray or *C.elegans* models. Investigating the role of rSAS1738 in apoptosis and inflammation would be important to understand the molecular mechanisms of lethality and invasive nature of the hypothetical protein. The simplest animal model to study programmed cell death is *C.elegans*. Since, the apoptotic cells will exhibit refractivity and change in cell morphology, the embryos will appear as bean stage and raised button appearance [224, 225]. Apoptosis is not required for the viability of *C.elegans*, and several genes involved in the apoptotic regulation have been identified in *C.elegans*. These pathways include the genes that enhance and prevent apoptosis. One of these examples is *ced-9* gene in *C.elegans*; it is homologous to the human *bcl-2* gene, which inhibits apoptosis. The *bcl-2* and *ced-9* genes are important in regulating apoptosis [226]. Thus, we can decipher the role of rSAS1738 protein in different apoptotic pathways using the *C.elegans* mutants of apoptotic pathway.

Regulation of apoptosis is important since decreased apoptosis or necrotic cells will lead to inflammation, whereas continuous apoptosis may lead to tissue damage or injury. Inflammation results from the secretion of cytokines or chemokines such as tumor necrosis factor (TNF- $\alpha$ ), interleukin (IL)-1, IL-8, IL-18 and C-reactive protein [227, 228], whereas some are anti-inflammatory cytokines such as IL-4, IL-10, IL-11, and IL-13. The balance between pro-inflammatory and anti-inflammatory cytokines are important in regulation of inflammation and tissue damage [227-229].

Some bacterial toxins can induce cell death by necrosis or apoptosis, correlating cell death with inflammation levels, aiding our understanding of the levels of tissue injury. *S. aureus* PVL can induce cell death by both necrosis and apoptosis and can lead to an increase in pro-

inflammatory cytokines [230]. Such studies are included in our research with the hypothetical proteins to understand the role in tissue injury.

The other technique used to study apoptosis and inflammation is the human microarray, which shows numerous genes involved in both extrinsic and intrinsic pathways such as caspase activation, Fas, TRAIL, TNF or p53 signaling [231]. Microarray studies would give us an overall view of all genes activated in response to rSAS1738. Human microarrays would aid the study of inflammation by analyzing complete cytokine or interleukin profiles [232]. The human microarrays to characterize cell death and inflammation are commercially available from companies like SA biosciences (Oligo GEMArray® Human Common Cytokines Microarray # Cat. No: OHS-021), Allied Biotech or Ray Biotech [231, 232].

The localization studies of rSAS1738 lethal protein inside the mammalian cell will answer more about its mechanism of action. Any bacterial toxins, including streptolysins, pneumolysins, perfringiolysin O, listeriolysin, hemolysins or leucocidins can enter the mammalian cell by forming pores and causing damage to the cell membrane [233, 234]. The other mechanism of toxin entry is by receptor-mediated endocytosis (RME), whereby the toxin attaches to the membrane forming endosomes and permeates the membrane by altering the ionic gradient of the cell [234]. Some toxins, like the diphtheria toxin, can kill the cell by both forming pores and RME. Other toxins, such as cholera toxin, diphtheria toxin and pertussis toxin, bring about ADP ribosylation enzymatic activity leading to altered cAMP levels and cell injury [213, 233]. Some toxins are also antigenic and can lose toxicity over time or upon thermal treatment to form toxoids; these toxins can be ideal candidates for designing vaccines [233]. Purified rSAS1738 could be used to generate polyclonal antibody in rabbits. This antibody could be used to tag it with fluorescent dyes for observation in immunoelectron or confocal microscopy. The

rSAS1738 localization in mammalian cells could be studied by observing the toxin outside the membrane, nucleus or cytosol [235, 236].

Creation of a particular mutant would give comparative differences in the virulence of mutant and wild type strain since, virulence is the combined effect of all virulence factors involved in colonization, development, host damage and also host evasion factors. The mutant and wild type strain could be compared to check all of its virulence factors [237]. The mutants of hypothetical proteins, SAS1738 and SAS0760, could be generated by either deletion or site directed mutagenesis. The wild strain and SAS1738 gene knock out strains could be checked for lethality in animal models. Comparative analysis of cytokine levels and toxicity levels would determine the role of hypothetical proteins synergistic with all other virulence factors [122, 237].

The SAS0760 gene has predicted motifs belonging to DUF830. These motifs are related to the orthopox virus *oppC\_N* motif, which is related to the N-terminal domain of oligopeptide transport permeases that belongs to the conserved ATP binding cassette transporters (Zn finger in ubiquitin hydrolases (KEGG)). SAS0760 has a conserved domain belonging to domain superfamily C113998 and COG3863, which is an uncharacterized distant relative of cell wall associated hydrolases (NCBI). Deletion of this motif and domain would help us understand the role of each motif and domain in the protein. Creating a SAS0760 knock out construct may help us study the role in virulence even without expressing the protein. Since hydrolases have been implicated to play important roles in cell cycle and biofilm formation, a wild type MSSA476 and a SAS0760 gene knock out construct could be used to check biofilms or adherence assays and virulence factor expression [238, 239].

Some researchers have already indicated that CA MRSA and HA MRSA strains did not exhibit varied pathogenicity due to antibiotic resistance patterns but rather, due to other virulence

determinants like PVL or cytotoxins [98, 158, 218]. Research related to characterization of hypothetical proteins such as SAS1738 and SAS0760 are important to answer the increased virulence of MSSA476. Hypothetical proteins like SAS1738 can also serve as candidates for therapeutics and vaccine development if explored for antigenic properties. This research suggests the lethality of SAS1738 on mammalian cells, indicating that invasiveness can be independent of antibiotic resistance conferred by such unexplored hypothetical proteins. Our focus of research is very significant to understand the increased invasiveness and virulence of community associated MRSA, which would enable us to think about novel therapeutic approaches.

## REFERENCE

1. Enright MC, Robinson DA, Randle G, Feil EJ, Grundmann H, Spratt BG: **The evolutionary history of methicillin-resistant Staphylococcus aureus (MRSA)**. *Proc Natl Acad Sci U S A* 2002, **99**(11):7687-7692.
2. Jevons MP, Parker MT: **The Evolution of New Hospital Strains of Staphylococcus Aureus**. *J Clin Pathol* 1964, **17**:243-250.
3. Jordens JZ, Duckworth GJ, Williams RJ: **Production of "virulence factors" by "epidemic" methicillin-resistant Staphylococcus aureus in vitro**. *J Med Microbiol* 1989, **30**(4):245-252.
4. Daum RS, Ito T, Hiramatsu K, Hussain F, Mongkolrattanothai K, Jamklang M, Boyle-Vavra S: **A novel methicillin-resistance cassette in community-acquired methicillin-resistant Staphylococcus aureus isolates of diverse genetic backgrounds**. *J Infect Dis* 2002, **186**(9):1344-1347.
5. Klevens RM, Morrison MA, Nadle J, Petit S, Gershman K, Ray S, Harrison LH, Lynfield R, Dumyati G, Townes JM *et al*: **Invasive methicillin-resistant Staphylococcus aureus infections in the United States**. *JAMA* 2007, **298**(15):1763-1771.
6. Li M, Diep BA, Villaruz AE, Braughton KR, Jiang X, DeLeo FR, Chambers HF, Lu Y, Otto M: **Evolution of virulence in epidemic community-associated methicillin-resistant Staphylococcus aureus**. *Proc Natl Acad Sci U S A* 2009, **106**(14):5883-5888.
7. Eady EA, Cove JH: **Staphylococcal resistance revisited: community-acquired methicillin resistant Staphylococcus aureus--an emerging problem for the management of skin and soft tissue infections**. *Curr Opin Infect Dis* 2003, **16**(2):103-124.
8. Holden MT, Feil EJ, Lindsay JA, Peacock SJ, Day NP, Enright MC, Foster TJ, Moore CE, Hurst L, Atkin R *et al*: **Complete genomes of two clinical Staphylococcus aureus strains: evidence for the rapid evolution of virulence and drug resistance**. *Proc Natl Acad Sci U S A* 2004, **101**(26):9786-9791.
9. Elek SD: **Staphylococcus pyogenes and its relation to disease**: Edinburgh: E. & S. Livingstone; 1959.
10. Rosenbach A: **Mikro-organismen bei den wund-infections- Krankheiten des Menschen**. : Wiesbaden, J.F. Bergmann, ; 1884.
11. van Belkum A, Verkaik NJ, de Vogel CP, Boelens HA, Verveer J, Nouwen JL, Verbrugh HA, Wertheim HF: **Reclassification of Staphylococcus aureus nasal carriage types**. *J Infect Dis* 2009, **199**(12):1820-1826.
12. Kluytmans J, van Belkum A, Verbrugh H: **Nasal carriage of Staphylococcus aureus: epidemiology, underlying mechanisms, and associated risks**. *Clin Microbiol Rev* 1997, **10**(3):505-520.
13. von Eiff C, Becker K, Machka K, Stammer H, Peters G: **Nasal carriage as a source of Staphylococcus aureus bacteremia**. Study Group. *N Engl J Med* 2001, **344**(1):11-16.



14. Weinstein HJ: **The relation between the nasal-staphylococcal-carrier state and the incidence of postoperative complications.** *N Engl J Med* 1959, **260**(26):1303-1308.
15. Roberts J: **Nose and skin carriage of Staphylococcus aureus.** *Lancet* 1948, **1**(6497):387.
16. Smith JA, O'Connor JJ: **Nasal carriage of Staphylococcus aureus in diabetes mellitus.** *Lancet* 1966, **2**(7467):776-777.
17. Wertheim HF, Vos MC, Ott A, van Belkum A, Voss A, Kluytmans JA, van Keulen PH, Vandenbroucke-Grauls CM, Meester MH, Verbrugh HA: **Risk and outcome of nosocomial Staphylococcus aureus bacteraemia in nasal carriers versus non-carriers.** *Lancet* 2004, **364**(9435):703-705.
18. Ringberg H, Thoren A, Lilja B: **Metastatic complications of Staphylococcus aureus septicemia. To seek is to find.** *Infection* 2000, **28**(3):132-136.
19. Fowler VG, Jr., Miro JM, Hoen B, Cabell CH, Abrutyn E, Rubinstein E, Corey GR, Spelman D, Bradley SF, Barsic B *et al*: **Staphylococcus aureus endocarditis: a consequence of medical progress.** *JAMA* 2005, **293**(24):3012-3021.
20. Shorr AF, Tabak YP, Killian AD, Gupta V, Liu LZ, Kollef MH: **Healthcare-associated bloodstream infection: A distinct entity? Insights from a large U.S. database.** *Crit Care Med* 2006, **34**(10):2588-2595.
21. Landrum ML, Neumann C, Cook C, Chukwuma U, Ellis MW, Hospenthal DR, Murray CK: **Epidemiology of Staphylococcus aureus blood and skin and soft tissue infections in the US military health system, 2005-2010.** *JAMA* 2012, **308**(1):50-59.
22. Chambers HF: **The changing epidemiology of Staphylococcus aureus?** *Emerg Infect Dis* 2001, **7**(2):178-182.
23. Herold BC, Immergluck LC, Maranan MC, Lauderdale DS, Gaskin RE, Boyle-Vavra S, Leitch CD, Daum RS: **Community-acquired methicillin-resistant Staphylococcus aureus in children with no identified predisposing risk.** *JAMA* 1998, **279**(8):593-598.
24. Fukuta Y, Cunningham CA, Harris PL, Wagener MM, Muder RR: **Identifying the Risk Factors for Hospital-Acquired Methicillin-Resistant Staphylococcus aureus (MRSA) Infection among Patients Colonized with MRSA on Admission.** *Infect Control Hosp Epidemiol* 2012, **33**(12):1219-1225.
25. Dinges MM, Orwin PM, Schlievert PM: **Exotoxins of Staphylococcus aureus.** *Clin Microbiol Rev* 2000, **13**(1):16-34, table of contents.
26. Lowy FD: **Staphylococcus aureus infections.** *N Engl J Med* 1998, **339**(8):520-532.
27. Chavakis T, Wiechmann K, Preissner KT, Herrmann M: **Staphylococcus aureus interactions with the endothelium: the role of bacterial "secretable expanded repertoire adhesive molecules" (SERAM) in disturbing host defense systems.** *Thromb Haemost* 2005, **94**(2):278-285.
28. Tojo M, Yamashita N, Goldmann DA, Pier GB: **Isolation and characterization of a capsular polysaccharide adhesin from Staphylococcus epidermidis.** *J Infect Dis* 1988, **157**(4):713-722.
29. Corrigan RM, Miajlovic H, Foster TJ: **Surface proteins that promote adherence of Staphylococcus aureus to human desquamated nasal epithelial cells.** *BMC Microbiol* 2009, **9**:22.
30. Xu Y, Rivas JM, Brown EL, Liang X, Hook M: **Virulence potential of the staphylococcal adhesin CNA in experimental arthritis is determined by its affinity for collagen.** *J Infect Dis* 2004, **189**(12):2323-2333.

31. Ni Eidhin D, Perkins S, Francois P, Vaudaux P, Hook M, Foster TJ: **Clumping factor B (ClfB), a new surface-located fibrinogen-binding adhesin of Staphylococcus aureus.** *Mol Microbiol* 1998, **30**(2):245-257.
32. Rhem MN, Lech EM, Patti JM, McDevitt D, Hook M, Jones DB, Wilhelmus KR: **The collagen-binding adhesin is a virulence factor in Staphylococcus aureus keratitis.** *Infect Immun* 2000, **68**(6):3776-3779.
33. Sinha B, Francois PP, Nusse O, Foti M, Hartford OM, Vaudaux P, Foster TJ, Lew DP, Herrmann M, Krause KH: **Fibronectin-binding protein acts as Staphylococcus aureus invasin via fibronectin bridging to integrin alpha5beta1.** *Cell Microbiol* 1999, **1**(2):101-117.
34. Fitzgerald JR, Loughman A, Keane F, Brennan M, Knobel M, Higgins J, Visai L, Speziale P, Cox D, Foster TJ: **Fibronectin-binding proteins of Staphylococcus aureus mediate activation of human platelets via fibrinogen and fibronectin bridges to integrin GPIIb/IIIa and IgG binding to the Fc gammaRIIa receptor.** *Mol Microbiol* 2006, **59**(1):212-230.
35. Hagggar A, Hussain M, Lonnie H, Herrmann M, Norrby-Teglund A, Flock JI: **Extracellular adherence protein from Staphylococcus aureus enhances internalization into eukaryotic cells.** *Infect Immun* 2003, **71**(5):2310-2317.
36. Guggenberger C, Wolz C, Morrissey JA, Heesemann J: **Two distinct coagulase-dependent barriers protect Staphylococcus aureus from neutrophils in a three dimensional in vitro infection model.** *PLoS Pathog* 2012, **8**(1):e1002434.
37. Gross M, Cramton SE, Gotz F, Peschel A: **Key role of teichoic acid net charge in Staphylococcus aureus colonization of artificial surfaces.** *Infect Immun* 2001, **69**(5):3423-3426.
38. O'Riordan K, Lee JC: **Staphylococcus aureus capsular polysaccharides.** *Clin Microbiol Rev* 2004, **17**(1):218-234.
39. Bukowski M, Wladyka B, Dubin G: **Exfoliative Toxins of Staphylococcus aureus.** *Toxins (Basel)* 2010, **2**(5):1148-1165.
40. Berends ET, Horswill AR, Haste NM, Monestier M, Nizet V, von Kockritz-Blickwede M: **Nuclease expression by Staphylococcus aureus facilitates escape from neutrophil extracellular traps.** *J Innate Immun* 2010, **2**(6):576-586.
41. Kiedrowski MR, Kavanaugh JS, Malone CL, Mootz JM, Voyich JM, Smeltzer MS, Bayles KW, Horswill AR: **Nuclease modulates biofilm formation in community-associated methicillin-resistant Staphylococcus aureus.** *PLoS One* 2011, **6**(11):e26714.
42. Hennekinne JA, De Buyser ML, Dragacci S: **Staphylococcus aureus and its food poisoning toxins: characterization and outbreak investigation.** *FEMS Microbiol Rev* 2012, **36**(4):815-836.
43. Laarman AJ, Mijneer G, Mootz JM, van Rooijen WJ, Ruyken M, Malone CL, Heezius EC, Ward R, Milligan G, van Strijp JA *et al*: **Staphylococcus aureus Staphopain A inhibits CXCR2-dependent neutrophil activation and chemotaxis.** *EMBO J* 2012, **31**(17):3607-3619.
44. Verkaik NJ, Dauwalder O, Antri K, Boubekri I, de Vogel CP, Badiou C, Bes M, Vandenesch F, Tazir M, Hooijkaas H *et al*: **Immunogenicity of toxins during Staphylococcus aureus infection.** *Clin Infect Dis* 2010, **50**(1):61-68.

45. Rice K, Peralta R, Bast D, de Azavedo J, McGavin MJ: **Description of staphylococcus serine protease (ssp) operon in Staphylococcus aureus and nonpolar inactivation of sspA-encoded serine protease.** *Infect Immun* 2001, **69**(1):159-169.
46. Laarman AJ, Ruyken M, Malone CL, van Strijp JA, Horswill AR, Rooijackers SH: **Staphylococcus aureus metalloprotease aureolysin cleaves complement C3 to mediate immune evasion.** *J Immunol* 2011, **186**(11):6445-6453.
47. Periasamy S, Chatterjee SS, Cheung GY, Otto M: **Phenol-soluble modulins in staphylococci: What are they originally for?** *Commun Integr Biol* 2012, **5**(3):275-277.
48. Cogen AL, Yamasaki K, Muto J, Sanchez KM, Crotty Alexander L, Tanios J, Lai Y, Kim JE, Nizet V, Gallo RL: **Staphylococcus epidermidis antimicrobial delta-toxin (phenol-soluble modulin-gamma) cooperates with host antimicrobial peptides to kill group A Streptococcus.** *PLoS One* 2010, **5**(1):e8557.
49. Schlievert PM: **Cytolysins, superantigens, and pneumonia due to community-associated methicillin-resistant Staphylococcus aureus.** *J Infect Dis* 2009, **200**(5):676-678.
50. Bronner S, Monteil H, Prevost G: **Regulation of virulence determinants in Staphylococcus aureus: complexity and applications.** *FEMS Microbiol Rev* 2004, **28**(2):183-200.
51. Novick RP, Ross HF, Projan SJ, Kornblum J, Kreiswirth B, Moghazeh S: **Synthesis of staphylococcal virulence factors is controlled by a regulatory RNA molecule.** *EMBO J* 1993, **12**(10):3967-3975.
52. Bischoff M, Entenza JM, Giachino P: **Influence of a functional sigB operon on the global regulators sar and agr in Staphylococcus aureus.** *J Bacteriol* 2001, **183**(17):5171-5179.
53. Wren BW: **Microbial genome analysis: insights into virulence, host adaptation and evolution.** *Nat Rev Genet* 2000, **1**(1):30-39.
54. Ziebuhr W, Ohlsen K, Karch H, Korhonen T, Hacker J: **Evolution of bacterial pathogenesis.** *Cell Mol Life Sci* 1999, **56**(9-10):719-728.
55. Hacker J, Kaper JB: **Pathogenicity islands and the evolution of microbes.** *Annu Rev Microbiol* 2000, **54**:641-679.
56. Lindsay JA, Ruzin A, Ross HF, Kurepina N, Novick RP: **The gene for toxic shock toxin is carried by a family of mobile pathogenicity islands in Staphylococcus aureus.** *Mol Microbiol* 1998, **29**(2):527-543.
57. Glaser P, Frangeul L, Buchrieser C, Rusniok C, Amend A, Baquero F, Berche P, Bloecker H, Brandt P, Chakraborty T *et al*: **Comparative genomics of Listeria species.** *Science* 2001, **294**(5543):849-852.
58. Becker K, Bierbaum G, von Eiff C, Engelmann S, Gotz F, Hacker J, Hecker M, Peters G, Rosenstein R, Ziebuhr W: **Understanding the physiology and adaptation of staphylococci: a post-genomic approach.** *Int J Med Microbiol* 2007, **297**(7-8):483-501.
59. Takeuchi F, Watanabe S, Baba T, Yuzawa H, Ito T, Morimoto Y, Kuroda M, Cui L, Takahashi M, Ankaei A *et al*: **Whole-genome sequencing of staphylococcus haemolyticus uncovers the extreme plasticity of its genome and the evolution of human-colonizing staphylococcal species.** *J Bacteriol* 2005, **187**(21):7292-7308.

60. Lindsay JA, Moore CE, Day NP, Peacock SJ, Witney AA, Stabler RA, Husain SE, Butcher PD, Hinds J: **Microarrays reveal that each of the ten dominant lineages of *Staphylococcus aureus* has a unique combination of surface-associated and regulatory genes.** *J Bacteriol* 2006, **188**(2):669-676.
61. Burian M, Wolz C, Goerke C: **Regulatory adaptation of *Staphylococcus aureus* during nasal colonization of humans.** *PLoS One* 2010, **5**(4):e10040.
62. Schaffer AC, Solinga RM, Cocchiario J, Portoles M, Kiser KB, Risley A, Randall SM, Valtulina V, Speziale P, Walsh E *et al*: **Immunization with *Staphylococcus aureus* clumping factor B, a major determinant in nasal carriage, reduces nasal colonization in a murine model.** *Infect Immun* 2006, **74**(4):2145-2153.
63. Maiques E, Ubeda C, Campoy S, Salvador N, Lasa I, Novick RP, Barbe J, Penades JR: **beta-lactam antibiotics induce the SOS response and horizontal transfer of virulence factors in *Staphylococcus aureus*.** *J Bacteriol* 2006, **188**(7):2726-2729.
64. Moore PC, Lindsay JA: **Genetic variation among hospital isolates of methicillin-sensitive *Staphylococcus aureus*: evidence for horizontal transfer of virulence genes.** *J Clin Microbiol* 2001, **39**(8):2760-2767.
65. Goerke C, Matias y Papenberg S, Dasbach S, Dietz K, Ziebach R, Kahl BC, Wolz C: **Increased frequency of genomic alterations in *Staphylococcus aureus* during chronic infection is in part due to phage mobilization.** *J Infect Dis* 2004, **189**(4):724-734.
66. Goerke C, Koller J, Wolz C: **Ciprofloxacin and trimethoprim cause phage induction and virulence modulation in *Staphylococcus aureus*.** *Antimicrob Agents Chemother* 2006, **50**(1):171-177.
67. McCarthy AJ, Breathnach AS, Lindsay JA: **Detection of mobile-genetic-element variation between colonizing and infecting hospital-associated methicillin-resistant *Staphylococcus aureus* isolates.** *J Clin Microbiol* 2012, **50**(3):1073-1075.
68. Wirtz C, Witte W, Wolz C, Goerke C: **Transcription of the phage-encoded Panton-Valentine leukocidin of *Staphylococcus aureus* is dependent on the phage life-cycle and on the host background.** *Microbiology* 2009, **155**(Pt 11):3491-3499.
69. Belcaid M, Bergeron A, Poisson G: **Mosaic graphs and comparative genomics in phage communities.** *J Comput Biol* 2010, **17**(9):1315-1326.
70. Sung JM, Lloyd DH, Lindsay JA: ***Staphylococcus aureus* host specificity: comparative genomics of human versus animal isolates by multi-strain microarray.** *Microbiology* 2008, **154**(Pt 7):1949-1959.
71. Vandenesch F, Naimi T, Enright MC, Lina G, Nimmo GR, Heffernan H, Liassine N, Bes M, Greenland T, Reverdy ME *et al*: **Community-acquired methicillin-resistant *Staphylococcus aureus* carrying Panton-Valentine leukocidin genes: worldwide emergence.** *Emerg Infect Dis* 2003, **9**(8):978-984.
72. Novick RP, Subedi A: **The SaPIs: mobile pathogenicity islands of *Staphylococcus*.** *Chem Immunol Allergy* 2007, **93**:42-57.
73. Yarwood JM, McCormick JK, Paustian ML, Orwin PM, Kapur V, Schlievert PM: **Characterization and expression analysis of *Staphylococcus aureus* pathogenicity island 3. Implications for the evolution of staphylococcal pathogenicity islands.** *J Biol Chem* 2002, **277**(15):13138-13147.

74. Novick RP: **Mobile genetic elements and bacterial toxinoses: the superantigen-encoding pathogenicity islands of *Staphylococcus aureus***. *Plasmid* 2003, **49**(2):93-105.
75. Schwarz S, Cardoso M, Grolz-Krug S, Blobel H: **Common antibiotic resistance plasmids in *Staphylococcus aureus* and *Staphylococcus epidermidis* from human and canine infections**. *Zentralbl Bakteriol* 1990, **273**(3):369-377.
76. Yamaguchi T, Hayashi T, Takami H, Nakasone K, Ohnishi M, Nakayama K, Yamada S, Komatsuzawa H, Sugai M: **Phage conversion of exfoliative toxin A production in *Staphylococcus aureus***. *Mol Microbiol* 2000, **38**(4):694-705.
77. Yamaguchi T, Hayashi T, Takami H, Ohnishi M, Murata T, Nakayama K, Asakawa K, Ohara M, Komatsuzawa H, Sugai M: **Complete nucleotide sequence of a *Staphylococcus aureus* exfoliative toxin B plasmid and identification of a novel ADP-ribosyltransferase, EDIN-C**. *Infect Immun* 2001, **69**(12):7760-7771.
78. Khan SA: **Rolling-circle replication of bacterial plasmids**. *Microbiol Mol Biol Rev* 1997, **61**(4):442-455.
79. Novick RP: **Staphylococcal plasmids and their replication**. *Annu Rev Microbiol* 1989, **43**:537-565.
80. Byrne ME, Gillespie MT, Skurray RA: **4',4'' adenyltransferase activity on conjugative plasmids isolated from *Staphylococcus aureus* is encoded on an integrated copy of pUB110**. *Plasmid* 1991, **25**(1):70-75.
81. Phillips S, Novick RP: **Tn554--a site-specific repressor-controlled transposon in *Staphylococcus aureus***. *Nature* 1979, **278**(5703):476-478.
82. Soge OO, Beck NK, White TM, No DB, Roberts MC: **A novel transposon, Tn6009, composed of a Tn916 element linked with a *Staphylococcus aureus* mer operon**. *J Antimicrob Chemother* 2008, **62**(4):674-680.
83. Byrne ME, Rouch DA, Skurray RA: **Nucleotide sequence analysis of IS256 from the *Staphylococcus aureus* gentamicin-tobramycin-kanamycin-resistance transposon Tn4001**. *Gene* 1989, **81**(2):361-367.
84. Mahillon J, Chandler M: **Insertion sequences**. *Microbiol Mol Biol Rev* 1998, **62**(3):725-774.
85. **Classification of staphylococcal cassette chromosome mec (SCCmec): guidelines for reporting novel SCCmec elements**. *Antimicrob Agents Chemother* 2009, **53**(12):4961-4967.
86. Luong TT, Ouyang S, Bush K, Lee CY: **Type 1 capsule genes of *Staphylococcus aureus* are carried in a staphylococcal cassette chromosome genetic element**. *J Bacteriol* 2002, **184**(13):3623-3629.
87. Ma XX, Ito T, Tiensasitorn C, Jamklang M, Chongtrakool P, Boyle-Vavra S, Daum RS, Hiramatsu K: **Novel type of staphylococcal cassette chromosome mec identified in community-acquired methicillin-resistant *Staphylococcus aureus* strains**. *Antimicrob Agents Chemother* 2002, **46**(4):1147-1152.
88. Chongtrakool P, Ito T, Ma XX, Kondo Y, Trakulsomboon S, Tiensasitorn C, Jamklang M, Chavalit T, Song JH, Hiramatsu K: **Staphylococcal cassette chromosome mec (SCCmec) typing of methicillin-resistant *Staphylococcus aureus* strains isolated in 11 Asian countries: a proposal for a new nomenclature for SCCmec elements**. *Antimicrob Agents Chemother* 2006, **50**(3):1001-1012.

89. Diep BA, Stone GG, Basuino L, Graber CJ, Miller A, des Etages SA, Jones A, Palazzolo-Ballance AM, Perdreau-Remington F, Sensabaugh GF *et al*: **The arginine catabolic mobile element and staphylococcal chromosomal cassette mec linkage: convergence of virulence and resistance in the USA300 clone of methicillin-resistant *Staphylococcus aureus***. *J Infect Dis* 2008, **197**(11):1523-1530.
90. Moncada S, Higgs A: **The L-arginine-nitric oxide pathway**. *N Engl J Med* 1993, **329**(27):2002-2012.
91. Chan CX, Beiko RG, Ragan MA: **Lateral transfer of genes and gene fragments in *Staphylococcus* extends beyond mobile elements**. *J Bacteriol* 2011, **193**(15):3964-3977.
92. Young BC, Golubchik T, Batty EM, Fung R, Lerner-Svensson H, Votintseva AA, Miller RR, Godwin H, Knox K, Everitt RG *et al*: **Evolutionary dynamics of *Staphylococcus aureus* during progression from carriage to disease**. *Proc Natl Acad Sci U S A* 2012, **109**(12):4550-4555.
93. Herron-Olson L, Fitzgerald JR, Musser JM, Kapur V: **Molecular correlates of host specialization in *Staphylococcus aureus***. *PLoS One* 2007, **2**(10):e1120.
94. Richmond MH: **Purification and Properties of the Exopenicillinase from *Staphylococcus Aureus***. *Biochem J* 1963, **88**:452-459.
95. Couto I, de Lencastre H, Severina E, Kloos W, Webster JA, Hubner RJ, Sanches IS, Tomasz A: **Ubiquitous presence of a mecA homologue in natural isolates of *Staphylococcus sciuri***. *Microb Drug Resist* 1996, **2**(4):377-391.
96. Tsakris A, Pillai SK, Gold HS, Thauvin-Eliopoulos C, Venkataraman L, Wennersten C, Moellering RC, Jr., Eliopoulos GM: **Persistence of rRNA operon mutated copies and rapid re-emergence of linezolid resistance in *Staphylococcus aureus***. *J Antimicrob Chemother* 2007, **60**(3):649-651.
97. Chang S, Sievert DM, Hageman JC, Boulton ML, Tenover FC, Downes FP, Shah S, Rudrik JT, Pupp GR, Brown WJ *et al*: **Infection with vancomycin-resistant *Staphylococcus aureus* containing the vanA resistance gene**. *N Engl J Med* 2003, **348**(14):1342-1347.
98. Baba T, Takeuchi F, Kuroda M, Yuzawa H, Aoki K, Oguchi A, Nagai Y, Iwama N, Asano K, Naimi T *et al*: **Genome and virulence determinants of high virulence community-acquired MRSA**. *Lancet* 2002, **359**(9320):1819-1827.
99. Diep BA, Gill SR, Chang RF, Phan TH, Chen JH, Davidson MG, Lin F, Lin J, Carleton HA, Mongodin EF *et al*: **Complete genome sequence of USA300, an epidemic clone of community-acquired methicillin-resistant *Staphylococcus aureus***. *Lancet* 2006, **367**(9512):731-739.
100. Liu C, Bayer A, Cosgrove SE, Daum RS, Fridkin SK, Gorwitz RJ, Kaplan SL, Karchmer AW, Levine DP, Murray BE *et al*: **Clinical practice guidelines by the infectious diseases society of america for the treatment of methicillin-resistant *Staphylococcus aureus* infections in adults and children: executive summary**. *Clin Infect Dis* 2011, **52**(3):285-292.
101. Rybak MJ, Lomaestro BM, Rotschafer JC, Moellering RC, Craig WA, Billeter M, Dalovisio JR, Levine DP: **Vancomycin therapeutic guidelines: a summary of consensus recommendations from the infectious diseases Society of America, the American Society of Health-System Pharmacists, and the Society of Infectious Diseases Pharmacists**. *Clin Infect Dis* 2009, **49**(3):325-327.

102. Stevens DL, Bisno AL, Chambers HF, Everett ED, Dellinger P, Goldstein EJ, Gorbach SL, Hirschmann JV, Kaplan EL, Montoya JG *et al*: **Practice guidelines for the diagnosis and management of skin and soft-tissue infections.** *Clin Infect Dis* 2005, **41**(10):1373-1406.
103. Sperber WH: **The identification of staphylococci in clinical and food microbiology laboratories.** *CRC Crit Rev Clin Lab Sci* 1976, **7**(2):121-184.
104. Gruner BM, Han SR, Meyer HG, Wulf U, Bhakdi S, Siegel EK: **Characterization of a catalase-negative methicillin-resistant *Staphylococcus aureus* strain.** *J Clin Microbiol* 2007, **45**(8):2684-2685.
105. Sakai H, Procop GW, Kobayashi N, Togawa D, Wilson DA, Borden L, Krebs V, Bauer TW: **Simultaneous detection of *Staphylococcus aureus* and coagulase-negative staphylococci in positive blood cultures by real-time PCR with two fluorescence resonance energy transfer probe sets.** *J Clin Microbiol* 2004, **42**(12):5739-5744.
106. Shittu A, Lin J, Morrison D: **Molecular identification and characterization of mannitol-negative methicillin-resistant *Staphylococcus aureus*.** *Diagn Microbiol Infect Dis* 2007, **57**(1):93-95.
107. Kateete DP, Kimani CN, Katabazi FA, Okeng A, Okee MS, Nanteza A, Joloba ML, Najjuka FC: **Identification of *Staphylococcus aureus*: DNase and Mannitol salt agar improve the efficiency of the tube coagulase test.** *Ann Clin Microbiol Antimicrob* 2010, **9**:23.
108. Shrestha NK, Tuohy MJ, Hall GS, Isada CM, Procop GW: **Rapid identification of *Staphylococcus aureus* and the *mecA* gene from BacT/ALERT blood culture bottles by using the LightCycler system.** *J Clin Microbiol* 2002, **40**(7):2659-2661.
109. Olive DM, Bean P: **Principles and applications of methods for DNA-based typing of microbial organisms.** *J Clin Microbiol* 1999, **37**(6):1661-1669.
110. Enright MC, Day NP, Davies CE, Peacock SJ, Spratt BG: **Multilocus sequence typing for characterization of methicillin-resistant and methicillin-susceptible clones of *Staphylococcus aureus*.** *J Clin Microbiol* 2000, **38**(3):1008-1015.
111. Koreen L, Ramaswamy SV, Graviss EA, Naidich S, Musser JM, Kreiswirth BN: ***spa* typing method for discriminating among *Staphylococcus aureus* isolates: implications for use of a single marker to detect genetic micro- and macrovariation.** *J Clin Microbiol* 2004, **42**(2):792-799.
112. Coia JE, Browning L, Haines L, Birkbeck TH, Platt DJ: **Comparison of enterotoxins and haemolysins produced by methicillin-resistant (MRSA) and sensitive (MSSA) *Staphylococcus aureus*.** *J Med Microbiol* 1992, **36**(3):164-171.
113. Mizobuchi S, Minami J, Jin F, Matsushita O, Okabe A: **Comparison of the virulence of methicillin-resistant and methicillin-sensitive *Staphylococcus aureus*.** *Microbiol Immunol* 1994, **38**(8):599-605.
114. Priatkin RG, Kuz'menko OM: **[Secreted proteins of *Staphylococcus aureus*].** *Zh Mikrobiol Epidemiol Immunobiol* 2010(4):118-124.
115. Spaulding AR, Lin YC, Merriman JA, Brosnahan AJ, Peterson ML, Schlievert PM: **Immunity to *Staphylococcus aureus* secreted proteins protects rabbits from serious illnesses.** *Vaccine* 2012, **30**(34):5099-5109.

116. Becher D, Hempel K, Sievers S, Zuhlke D, Pane-Farre J, Otto A, Fuchs S, Albrecht D, Bernhardt J, Engelmann S *et al*: **A proteomic view of an important human pathogen--towards the quantification of the entire *Staphylococcus aureus* proteome.** *PLoS One* 2009, **4**(12):e8176.
117. Sibbald MJ, Ziebandt AK, Engelmann S, Hecker M, de Jong A, Harmsen HJ, Raangs GC, Stokroos I, Arends JP, Dubois JY *et al*: **Mapping the pathways to staphylococcal pathogenesis by comparative secretomics.** *Microbiol Mol Biol Rev* 2006, **70**(3):755-788.
118. Kuroda M, Ohta T, Uchiyama I, Baba T, Yuzawa H, Kobayashi I, Cui L, Oguchi A, Aoki K, Nagai Y *et al*: **Whole genome sequencing of methicillin-resistant *Staphylococcus aureus*.** *Lancet* 2001, **357**(9264):1225-1240.
119. Mohan R, Venugopal S: **Computational structural and functional analysis of hypothetical proteins of *Staphylococcus aureus*.** *Bioinformatics* 2012, **8**(15):722-728.
120. Friedberg I: **Automated protein function prediction--the genomic challenge.** *Brief Bioinform* 2006, **7**(3):225-242.
121. Wu HJ, Wang AH, Jennings MP: **Discovery of virulence factors of pathogenic bacteria.** *Curr Opin Chem Biol* 2008, **12**(1):93-101.
122. Galperin MY, Koonin EV: **'Conserved hypothetical' proteins: prioritization of targets for experimental study.** *Nucleic Acids Res* 2004, **32**(18):5452-5463.
123. Lubec G, Afjehi-Sadat L, Yang JW, John JP: **Searching for hypothetical proteins: theory and practice based upon original data and literature.** *Prog Neurobiol* 2005, **77**(1-2):90-127.
124. Malachowa N, Kohler PL, Schlievert PM, Chuang ON, Dunny GM, Kobayashi SD, Miedzobrodzki J, Bohach GA, Seo KS: **Characterization of a *Staphylococcus aureus* surface virulence factor that promotes resistance to oxidative killing and infectious endocarditis.** *Infect Immun* 2011, **79**(1):342-352.
125. Anantharaman V, Aravind L: **Evolutionary history, structural features and biochemical diversity of the NlpC/P60 superfamily of enzymes.** *Genome Biol* 2003, **4**(2):R11.
126. Senkevich TG, Wyatt LS, Weisberg AS, Koonin EV, Moss B: **A conserved poxvirus NlpC/P60 superfamily protein contributes to vaccinia virus virulence in mice but not to replication in cell culture.** *Virology* 2008, **374**(2):506-514.
127. Ratts R, Trujillo C, Bharti A, vanderSpek J, Harrison R, Murphy JR: **A conserved motif in transmembrane helix 1 of diphtheria toxin mediates catalytic domain delivery to the cytosol.** *Proc Natl Acad Sci U S A* 2005, **102**(43):15635-15640.
128. Tamayo AG, Bharti A, Trujillo C, Harrison R, Murphy JR: **COPI coatomer complex proteins facilitate the translocation of anthrax lethal factor across vesicular membranes in vitro.** *Proc Natl Acad Sci U S A* 2008, **105**(13):5254-5259.
129. Marchler-Bauer A, Anderson JB, Chitsaz F, Derbyshire MK, DeWeese-Scott C, Fong JH, Geer LY, Geer RC, Gonzales NR, Gwadz M *et al*: **CDD: specific functional annotation with the Conserved Domain Database.** *Nucleic Acids Res* 2009, **37**(Database issue):D205-210.
130. Firczuk M, Bochtler M: **Folds and activities of peptidoglycan amidases.** *FEMS Microbiol Rev* 2007, **31**(6):676-691.



131. Bernstein FC, Koetzle TF, Williams GJ, Meyer EF, Jr., Brice MD, Rodgers JR, Kennard O, Shimanouchi T, Tasumi M: **The Protein Data Bank: a computer-based archival file for macromolecular structures.** *J Mol Biol* 1977, **112**(3):535-542.
132. Biswas R, Voggu L, Simon UK, Hentschel P, Thumm G, Gotz F: **Activity of the major staphylococcal autolysin Atl.** *FEMS Microbiol Lett* 2006, **259**(2):260-268.
133. Heilmann C, Hartleib J, Hussain MS, Peters G: **The multifunctional Staphylococcus aureus autolysin aaa mediates adherence to immobilized fibrinogen and fibronectin.** *Infect Immun* 2005, **73**(8):4793-4802.
134. Pasztor L, Ziebandt AK, Nega M, Schlag M, Haase S, Franz-Wachtel M, Madlung J, Nordheim A, Heinrichs DE, Gotz F: **Staphylococcal major autolysin (Atl) is involved in excretion of cytoplasmic proteins.** *J Biol Chem* 2010, **285**(47):36794-36803.
135. Zoll S, Patzold B, Schlag M, Gotz F, Kalbacher H, Stehle T: **Structural basis of cell wall cleavage by a staphylococcal autolysin.** *PLoS Pathog* 2010, **6**(3):e1000807.
136. Tsuge Y, Ogino H, Teramoto H, Inui M, Yukawa H: **Deletion of cgR\_1596 and cgR\_2070, encoding NlpC/P60 proteins, causes a defect in cell separation in Corynebacterium glutamicum R.** *J Bacteriol* 2008, **190**(24):8204-8214.
137. Fukushima T, Afkham A, Kurosawa S, Tanabe T, Yamamoto H, Sekiguchi J: **A new D,L-endopeptidase gene product, YojL (renamed CwIS), plays a role in cell separation with LytE and LytF in Bacillus subtilis.** *J Bacteriol* 2006, **188**(15):5541-5550.
138. Smith TJ, Blackman, S. A. & Foster, S. J. : **Autolysins of Bacillus subtilis: multiple enzymes with multiple functions** *Microbiology* 2000, **146**:249-262.
139. Qingping Xu PA, Tamara Astakhova, Herbert L. Axelrod et al.,: **Structure of the  $\gamma$ -D-glutamyl-L-diamino acid endopeptidase YkfC from Bacillus cereus in complex with L-Ala- $\gamma$ -D-Glu: insights into substrate recognition by NlpC/P60 Cysteine peptidases.** *Acta Crystallogr Sect F Struct Biol Cryst Commun* 2010, **66**(10):1354-1364. .
140. Tatiana G Senkevicha LSW, Andrea S. Weisberga, Eugene V. Kooninb and Bernard Mossa, : **A conserved poxvirus NlpC/P60 superfamily protein contributes to vaccinia virus virulence in mice but not to replication in cell culture.** *Virology* 2008, **374**,(2):506-514
141. Lauderdale KJ BB, Cheung AL, Horswill AR.: **Interconnections between Sigma B, agr, and proteolytic activity in Staphylococcus aureus biofilm maturation.** . *Infect Immun* 2009, **77**((4)):1623-1635.
142. Stein L: **Genome annotation: from sequence to biology.** *Nat Rev Genet* 2001, **2**(7):493-503.
143. Weiner J, 3rd, Moore AD, Bornberg-Bauer E: **Just how versatile are domains?***BMC Evol Biol* 2008, **8**:285.
144. Wilson D, Pethica R, Zhou Y, Talbot C, Vogel C, Madera M, Chothia C, Gough J: **SUPERFAMILY--sophisticated comparative genomics, data mining, visualization and phylogeny.** *Nucleic Acids Res* 2009, **37**(Database issue):D380-386.
145. Kall L, Krogh A, Sonnhammer EL: **A combined transmembrane topology and signal peptide prediction method.** *J Mol Biol* 2004, **338**(5):1027-1036.
146. Cole C, Barber JD, Barton GJ: **The Jpred 3 secondary structure prediction server.** *Nucleic Acids Res* 2008, **36**(Web Server issue):W197-201.

147. Raghava GPS: **APSSP2 : A combination method for protein secondary structure prediction based on neural network and example based learning.** In., vol. CASP5. A-132.
148. Larkin MA, Blackshields G, Brown NP, Chenna R, McGettigan PA, McWilliam H, Valentin F, Wallace IM, Wilm A, Lopez R *et al*: **Clustal W and Clustal X version 2.0.** *Bioinformatics* 2007, **23**(21):2947-2948.
149. Kelley LA, Sternberg MJ: **Protein structure prediction on the Web: a case study using the Phyre server.** *Nat Protoc* 2009, **4**(3):363-371.
150. Buchan DW, Ward SM, Lobley AE, Nugent TC, Bryson K, Jones DT: **Protein annotation and modelling servers at University College London.** *Nucleic Acids Res* 2010, **38**(Web Server issue):W563-568.
151. McGuffin LJ, Jones DT: **Improvement of the GenTHREADER method for genomic fold recognition.** *Bioinformatics* 2003, **19**(7):874-881.
152. Jahn CE, Charkowski AO, Willis DK: **Evaluation of isolation methods and RNA integrity for bacterial RNA quantitation.** *J Microbiol Methods* 2008, **75**(2):318-324.
153. Brown WC, Fraser DK, Young FE: **Problems in purification of a Bacillus subtilis autolytic enzyme caused by association with teichoic acid.** *Biochim Biophys Acta* 1970, **198**(2):308-315.
154. Nickerson NN, Joag V, McGavin MJ: **Rapid autocatalytic activation of the M4 metalloprotease aureolysin is controlled by a conserved N-terminal fungolysin-thermolysin-propeptide domain.** *Mol Microbiol* 2008, **69**(6):1530-1543.
155. Kurland C, Gallant J: **Errors of heterologous protein expression.** *Curr Opin Biotechnol* 1996, **7**(5):489-493.
156. Sivashanmugam A, Murray V, Cui C, Zhang Y, Wang J, Li Q: **Practical protocols for production of very high yields of recombinant proteins using Escherichia coli.** *Protein Sci* 2009, **18**(5):936-948.
157. Waddington C: **Changing behavior: evidence based practice supporting hair removal with clippers.** *ORL Head Neck Nurs* 2008, **26**(4):8-12.
158. Baba T, Bae T, Schneewind O, Takeuchi F, Hiramatsu K: **Genome sequence of Staphylococcus aureus strain Newman and comparative analysis of staphylococcal genomes: polymorphism and evolution of two major pathogenicity islands.** *J Bacteriol* 2008, **190**(1):300-310.
159. Holden MT FE, Lindsay JA *et al.*,: **Complete genomes of two clinical Staphylococcus aureus strains: evidence for the rapid evolution of virulence and drug resistance.** *Proc Natl Acad Sci U S A* 2004, **29**(101(26)):9786-9791.
160. McGrath JAE, R.A.; Pope, F.M.: **Rook's Textbook of Dermatology (7th ed.):** Blackwell Publishing; (2004).
161. Rennie RP, Jones RN, Mutnick AH: **Occurrence and antimicrobial susceptibility patterns of pathogens isolated from skin and soft tissue infections: report from the SENTRY Antimicrobial Surveillance Program (United States and Canada, 2000).** *Diagn Microbiol Infect Dis* 2003, **45**(4):287-293.
162. **The bacterial flora of humans**
163. Frazee BW, Lynn J, Charlebois ED, Lambert L, Lowery D, Perdreau-Remington F: **High prevalence of methicillin-resistant Staphylococcus aureus in emergency department skin and soft tissue infections.** *Ann Emerg Med* 2005, **45**(3):311-320.

164. del Rio A, Cervera C, Moreno A, Moreillon P, Miro JM: **Patients at risk of complications of Staphylococcus aureus bloodstream infection.** *Clin Infect Dis* 2009, **48 Suppl 4**:S246-253.
165. Braff MH, Zaiou M, Fierer J, Nizet V, Gallo RL: **Keratinocyte production of cathelicidin provides direct activity against bacterial skin pathogens.** *Infect Immun* 2005, **73**(10):6771-6781.
166. Mongodin E, Bajolet O, Cutrona J, Bonnet N, Dupuit F, Puchelle E, de Bentzmann S: **Fibronectin-binding proteins of Staphylococcus aureus are involved in adherence to human airway epithelium.** *Infect Immun* 2002, **70**(2):620-630.
167. Aly R, Levit S: **Adherence of Staphylococcus aureus to squamous epithelium: role of fibronectin and teichoic acid.** *Rev Infect Dis* 1987, **9 Suppl 4**:S341-350.
168. Roche FM, Meehan M, Foster TJ: **The Staphylococcus aureus surface protein SasG and its homologues promote bacterial adherence to human desquamated nasal epithelial cells.** *Microbiology* 2003, **149**(Pt 10):2759-2767.
169. Mempel M, Schmidt T, Weidinger S, Schnopp C, Foster T, Ring J, Abeck D: **Role of Staphylococcus aureus surface-associated proteins in the attachment to cultured HaCaT keratinocytes in a new adhesion assay.** *J Invest Dermatol* 1998, **111**(3):452-456.
170. Genestier AL, Michallet MC, Prevost G, Bellot G, Chalabreysse L, Peyrol S, Thivolet F, Etienne J, Lina G, Vallette FM *et al*: **Staphylococcus aureus Panton-Valentine leukocidin directly targets mitochondria and induces Bax-independent apoptosis of human neutrophils.** *J Clin Invest* 2005, **115**(11):3117-3127.
171. Hauck CR, Ohlsen K: **Sticky connections: extracellular matrix protein recognition and integrin-mediated cellular invasion by Staphylococcus aureus.** *Curr Opin Microbiol* 2006, **9**(1):5-11.
172. Sinha B, Fraunholz M: **Staphylococcus aureus host cell invasion and post-invasion events.** *Int J Med Microbiol* 2010, **300**(2-3):170-175.
173. Stuehr DJ, Marletta MA: **Synthesis of nitrite and nitrate in murine macrophage cell lines.** *Cancer Res* 1987, **47**(21):5590-5594.
174. Koziel J, Maciag-Gudowska A, Mikolajczyk T, Bzowska M, Sturdevant DE, Whitney AR, Shaw LN, DeLeo FR, Potempa J: **Phagocytosis of Staphylococcus aureus by macrophages exerts cytoprotective effects manifested by the upregulation of antiapoptotic factors.** *PLoS One* 2009, **4**(4):e5210.
175. Kubica M, Guzik K, Koziel J, Zarebski M, Richter W, Gajkowska B, Golda A, Maciag-Gudowska A, Brix K, Shaw L *et al*: **A potential new pathway for Staphylococcus aureus dissemination: the silent survival of S. aureus phagocytosed by human monocyte-derived macrophages.** *PLoS One* 2008, **3**(1):e1409.
176. Bayles KW, Wesson CA, Liou LE, Fox LK, Bohach GA, Trumble WR: **Intracellular Staphylococcus aureus escapes the endosome and induces apoptosis in epithelial cells.** *Infect Immun* 1998, **66**(1):336-342.
177. Fraunholz M, Sinha B: **Intracellular staphylococcus aureus: Live-in and let die.** *Front Cell Infect Microbiol* 2012, **2**:43.
178. Qazi SN, Harrison SE, Self T, Williams P, Hill PJ: **Real-time monitoring of intracellular Staphylococcus aureus replication.** *J Bacteriol* 2004, **186**(4):1065-1077.
179. Durrbach A, Louvard D, Coudrier E: **Actin filaments facilitate two steps of endocytosis.** *J Cell Sci* 1996, **109** ( Pt 2):457-465.

180. Jevon M, Guo C, Ma B, Mordan N, Nair SP, Harris M, Henderson B, Bentley G, Meghji S: **Mechanisms of internalization of Staphylococcus aureus by cultured human osteoblasts.** *Infect Immun* 1999, **67**(5):2677-2681.
181. Edwards AM, Potter U, Meenan NA, Potts JR, Massey RC: **Staphylococcus aureus keratinocyte invasion is dependent upon multiple high-affinity fibronectin-binding repeats within FnBPA.** *PLoS One* 2011, **6**(4):e18899.
182. Schroder A, Schroder B, Roppenser B, Linder S, Sinha B, Fassler R, Aepfelbacher M: **Staphylococcus aureus fibronectin binding protein-A induces motile attachment sites and complex actin remodeling in living endothelial cells.** *Mol Biol Cell* 2006, **17**(12):5198-5210.
183. Tuchscher L, Medina E, Hussain M, Volker W, Heitmann V, Niemann S, Holzinger D, Roth J, Proctor RA, Becker K *et al*: **Staphylococcus aureus phenotype switching: an effective bacterial strategy to escape host immune response and establish a chronic infection.** *EMBO Mol Med* 2011, **3**(3):129-141.
184. Hirsch T, Marchetti P, Susin SA, Dallaporta B, Zamzami N, Marzo I, Geuskens M, Kroemer G: **The apoptosis-necrosis paradox. Apoptogenic proteases activated after mitochondrial permeability transition determine the mode of cell death.** *Oncogene* 1997, **15**(13):1573-1581.
185. Norbury CJ, Hickson ID: **Cellular responses to DNA damage.** *Annu Rev Pharmacol Toxicol* 2001, **41**:367-401.
186. Majno G, Joris I: **Apoptosis, oncosis, and necrosis. An overview of cell death.** *Am J Pathol* 1995, **146**(1):3-15.
187. Menzies BE, Kourteva I: **Internalization of Staphylococcus aureus by endothelial cells induces apoptosis.** *Infect Immun* 1998, **66**(12):5994-5998.
188. Essmann F, Bantel H, Totzke G, Engels IH, Sinha B, Schulze-Osthoff K, Janicke RU: **Staphylococcus aureus alpha-toxin-induced cell death: predominant necrosis despite apoptotic caspase activation.** *Cell Death Differ* 2003, **10**(11):1260-1272.
189. Elmore S: **Apoptosis: a review of programmed cell death.** *Toxicol Pathol* 2007, **35**(4):495-516.
190. Soong G, Chun J, Parker D, Prince A: **Staphylococcus aureus activation of caspase 1/calpain signaling mediates invasion through human keratinocytes.** *J Infect Dis* 2012, **205**(10):1571-1579.
191. Ziegler U, Groscurth P: **Morphological features of cell death.** *News Physiol Sci* 2004, **19**:124-128.
192. Cummings BS, Schnellmann RG: **Measurement of cell death in mammalian cells.** *Curr Protoc Pharmacol* 2004, **Chapter 12**:Unit 12 18.
193. Collins AR: **The comet assay for DNA damage and repair: principles, applications, and limitations.** *Mol Biotechnol* 2004, **26**(3):249-261.
194. Koopman G, Reutelingsperger CP, Kuijten GA, Keehnen RM, Pals ST, van Oers MH: **Annexin V for flow cytometric detection of phosphatidylserine expression on B cells undergoing apoptosis.** *Blood* 1994, **84**(5):1415-1420.
195. van Engeland M, Nieland LJ, Ramaekers FC, Schutte B, Reutelingsperger CP: **Annexin V-affinity assay: a review on an apoptosis detection system based on phosphatidylserine exposure.** *Cytometry* 1998, **31**(1):1-9.

196. Kyriakis JM, Avruch J: **Sounding the alarm: protein kinase cascades activated by stress and inflammation.** *J Biol Chem* 1996, **271**(40):24313-24316.
97. Raingeaud J, Gupta S, Rogers JS, Dickens M, Han J, Ulevitch RJ, Davis RJ: **Pro-inflammatory cytokines and environmental stress cause p38 mitogen-activated protein kinase activation by dual phosphorylation on tyrosine and threonine.** *J Biol Chem* 1995, **270**(13):7420-7426.
198. Lundqvist-Gustafsson H, Norrman S, Nilsson J, Wilsson A: **Involvement of p38-mitogen-activated protein kinase in Staphylococcus aureus-induced neutrophil apoptosis.** *J Leukoc Biol* 2001, **70**(4):642-648.
199. Jia-He Wang\* H-YN, Meng Zhang, Ping He, Yi Zhang and Liang Kan: **Apoptosis induced by Staphylococcus aureus in human monocytic U937 cells involves Akt and mitogen-activated protein (MAPK) phosphorylation.** *African Journal of Biotechnology* May, 2011, **Vol. 10 (21)**,:pp. 4478-4483.
200. Below S, Konkel A, Zeeck C, Muller C, Kohler C, Engelmann S, Hildebrandt JP: **Virulence factors of Staphylococcus aureus induce Erk-MAP kinase activation and c-Fos expression in S9 and 16HBE14o- human airway epithelial cells.** *Am J Physiol Lung Cell Mol Physiol* 2009, **296**(3):L470-479.
201. Ellington JK, Elhofy A, Bost KL, Hudson MC: **Involvement of mitogen-activated protein kinase pathways in Staphylococcus aureus invasion of normal osteoblasts.** *Infect Immun* 2001, **69**(9):5235-5242.
202. Xia Z, Dickens M, Raingeaud J, Davis RJ, Greenberg ME: **Opposing effects of ERK and JNK-p38 MAP kinases on apoptosis.** *Science* 1995, **270**(5240):1326-1331.
203. Herzlieb W, Kohler KM, Ewald A, Hofmann N, Gbureck U: **Antimicrobial and physicochemical properties of experimental light curing composites with alkali-substituted calcium phosphate fillers.** *Dent Mater* 2012, **28**(6):597-603.
204. Edwards AM, Potts JR, Josefsson E, Massey RC: **Staphylococcus aureus host cell invasion and virulence in sepsis is facilitated by the multiple repeats within FnBPA.** *PLoS Pathog* 2010, **6**(6):e1000964.
205. Giustarini D, Rossi R, Milzani A, Dalle-Donne I: **Nitrite and nitrate measurement by Griess reagent in human plasma: evaluation of interferences and standardization.** *Methods Enzymol* 2008, **440**:361-380.
206. Galloway CA, Sowden MP, Smith HC: **Increasing the yield of soluble recombinant protein expressed in E. coli by induction during late log phase.** *Biotechniques* 2003, **34**(3):524-526, 528, 530.
207. Jana S, Deb JK: **Strategies for efficient production of heterologous proteins in Escherichia coli.** *Appl Microbiol Biotechnol* 2005, **67**(3):289-298.
208. Mesnage R, Clair E, Gress S, Then C, Szekacs A, Seralini GE: **Cytotoxicity on human cells of Cry1Ab and Cry1Ac Bt insecticidal toxins alone or with a glyphosate-based herbicide.** *J Appl Toxicol* 2012.
209. Pomati F, Orlandi C, Clerici M, Luciani F, Zuccato E: **Effects and interactions in an environmentally relevant mixture of pharmaceuticals.** *Toxicol Sci* 2008, **102**(1):129-137.
210. Qasim M, Rahman H, Oellerich M, Asif AR: **Differential proteome analysis of human embryonic kidney cell line (HEK-293) following mycophenolic acid treatment.** *Proteome Sci* 2011, **9**:57.

211. Bhakdi S, Muhly M, Mannhardt U, Hugo F, Klapettek K, Mueller-Eckhardt C, Roka L: **Staphylococcal alpha toxin promotes blood coagulation via attack on human platelets.** *J Exp Med* 1988, **168**(2):527-542.
212. wao Kato and A. M. Pappenheimer J: **An early effect of Diphtheria toxin on the metabolism of mammalian cells growing in culture** *J Exp Med* 1960, **112**(2): 329–349.
213. Hehnly H, Sheff D, Starnes M: **Shiga toxin facilitates its retrograde transport by modifying microtubule dynamics.** *Mol Biol Cell* 2006, **17**(10):4379-4389.
214. Singh SM, Panda AK: **Solubilization and refolding of bacterial inclusion body proteins.** *J Biosci Bioeng* 2005, **99**(4):303-310.
215. Drucker DB, Aluyi HS, Morris JA, Telford DR, Gibbs A: **Lethal synergistic action of toxins of bacteria isolated from sudden infant death syndrome.** *J Clin Pathol* 1992, **45**(9):799-801.
216. Smith RJ, Schlievert PM, Himelright IM, Baddour LM: **Dual infections with Staphylococcus aureus and Streptococcus pyogenes causing toxic shock syndrome. Possible synergistic effects of toxic shock syndrome toxin 1 and streptococcal pyrogenic exotoxin C.** *Diagn Microbiol Infect Dis* 1994, **19**(4):245-247.
217. Okuma K, Iwakawa K, Turnidge JD, Grubb WB, Bell JM, O'Brien FG, Coombs GW, Pearman JW, Tenover FC, Kapi M *et al*: **Dissemination of new methicillin-resistant Staphylococcus aureus clones in the community.** *J Clin Microbiol* 2002, **40**(11):4289-4294.
218. DeLeo FR, Otto M, Kreiswirth BN, Chambers HF: **Community-associated methicillin-resistant Staphylococcus aureus.** *Lancet* 2010, **375**(9725):1557-1568.
219. Diep BA, Carleton HA, Chang RF, Sensabaugh GF, Perdreau-Remington F: **Roles of 34 virulence genes in the evolution of hospital- and community-associated strains of methicillin-resistant Staphylococcus aureus.** *J Infect Dis* 2006, **193** (11):1495-1503.
220. Seybold U, Kourbatova EV, Johnson JG, Halvosa SJ, Wang YF, King MD, Ray SM, Blumberg HM: **Emergence of community-associated methicillin-resistant Staphylococcus aureus USA300 genotype as a major cause of health care-associated blood stream infections.** *Clin Infect Dis* 2006, **42**(5):647-656.
221. Rivero-Perez B, Alcoba-Florez J, Mendez-Alvarez S: **Genetic diversity of community-associated methicillin-resistant Staphylococcus aureus isolated from Tenerife Island, Spain.** *Infect Genet Evol* 2012, **12**(3):586-590.
222. Rolo J, Miragaia M, Turlej-Rogacka A, Empel J, Bouchami O, Faria NA, Tavares A, Hryniewicz W, Fluit AC, de Lencastre H: **High genetic diversity among community-associated Staphylococcus aureus in Europe: results from a multicenter study.** *PLoS One* 2012, **7**(4):e34768.
223. Highlander SK, Hulten KG, Qin X, Jiang H, Yerrapragada S, Mason EO, Jr., Shang Y, Williams TM, Fortunov RM, Liu Y *et al*: **Subtle genetic changes enhance virulence of methicillin resistant and sensitive Staphylococcus aureus.** *BMC Microbiol* 2007, **7**:99.
224. Horvitz HR, Shaham S, Hengartner MO: **The genetics of programmed cell death in the nematode Caenorhabditis elegans.** *Cold Spring Harb Symp Quant Biol* 1994, **59**:377-385.
225. Wu YC, Tsai MC, Cheng LC, Chou CJ, Weng NY: **C. elegans CED-12 acts in the conserved crkII/DOCK180/Rac pathway to control cell migration and cell corpse engulfment.** *Dev Cell* 2001, **1**(4):491-502.

226. Hengartner MO, Horvitz HR: **C. elegans cell survival gene ced-9 encodes a functional homolog of the mammalian proto-oncogene bcl-2.** *Cell* 1994, **76**(4):665-676.
227. Elenkov IJ, Iezzoni DG, Daly A, Harris AG, Chrousos GP: **Cytokine dysregulation, inflammation and well-being.** *Neuroimmunomodulation* 2005, **12**(5):255-269.
228. Kuwano K, Hara N: **Signal transduction pathways of apoptosis and inflammation induced by the tumor necrosis factor receptor family.** *Am J Respir Cell Mol Biol* 2000, **22**(2):147-149.
229. Opal SM, DePalo VA: **Anti-inflammatory cytokines.** *Chest* 2000, **117**(4):1162-1172.
230. Ma X, Chang W, Zhang C, Zhou X, Yu F: **Staphylococcal Panton-Valentine leukocidin induces pro-inflammatory cytokine production and nuclear factor-kappa B activation in neutrophils.** *PLoS One* 2012, **7**(4):e34970.
231. Moreilhon C, Gras D, Hologne C, Bajolet O, Cottrez F, Magnone V, Merten M, Groux H, Puchelle E, Barbry P: **Live Staphylococcus aureus and bacterial soluble factors induce different transcriptional responses in human airway cells.** *Physiol Genomics* 2005, **20**(3):244-255.
232. Hashida N, Ohguro N, Nakai K, Kobashi-Hashida M, Hashimoto S, Matsushima K, Tano Y: **Microarray analysis of cytokine and chemokine gene expression after prednisolone treatment in murine experimental autoimmune uveoretinitis.** *Invest Ophthalmol Vis Sci* 2005, **46**(11):4224-4234.
233. Kenneth T: **Todar's Online Textbook of Bacteriology.** In: *Bacterial Protein Toxins.*
234. Middlebrook JL, Dorland RB: **Bacterial toxins: cellular mechanisms of action.** *Microbiol Rev* 1984, **48**(3):199-221.
235. Molinari G, Rohde M, Wilde C, Just I, Aktories K, Chhatwal GS: **Localization of the C3-Like ADP-ribosyltransferase from Staphylococcus aureus during bacterial invasion of mammalian cells.** *Infect Immun* 2006, **74**(6):3673-3677.
236. Valaitis AP: **Localization of Bacillus thuringiensis Cry1A toxin-binding molecules in gypsy moth larval gut sections using fluorescence microscopy.** *Journal of Invertebrate Pathology* 2011, **108**: 69-75.
237. Bramley AJ, Patel AH, O'Reilly M, Foster R, Foster TJ: **Roles of alpha-toxin and beta-toxin in virulence of Staphylococcus aureus for the mouse mammary gland.** *Infect Immun* 1989, **57**(8):2489-2494.
238. Tamber S, Cheung AL: **SarZ promotes the expression of virulence factors and represses biofilm formation by modulating SarA and agr in Staphylococcus aureus.** *Infect Immun* 2009, **77**(1):419-428.
239. Trotonda MP, Tamber S, Memmi G, Cheung AL: **MgrA represses biofilm formation in Staphylococcus aureus.** *Infect Immun* 2008, **76**(12):5645-5654.